University of Bath

UNIVERSITY OF BATH

PHD

Interaction of alpha-melanocyte-stimulating hormone with its receptor

Erskine-Grout, Mary Beth

Award date:
1993

Awarding institution:
University of Bath

[Link to publication](#)

INTERACTION OF ALPHA-MELANOCYTE-STIMULATING HORMONE WITH ITS RECEPTOR

Submitted by Mary Beth Erskine-Grout

for the degree of

Doctor of Philosophy

of the University of Bath

1993

COPYRIGHT

UMI Number: U601882

Dissertation Publishing

UMI U601882

ProQuest LLC
789 East Eisenhower Parkway
P.O. Box 1346
Ann Arbor, MI 48106-1346

To my parents

ACKNOWLEDGEMENTS

SUMMARY

Melanoma cells are transformed melanocytes which usually retain their receptors for alpha-melanocyte-stimulating hormone (α–MSH). MSH promotes melanogenesis and melanin dispersion in pigment cells. The selective affinity of MSH for its receptor may allow site-specific delivery of probes or drugs to melanoma during its diagnosis and treatment. This thesis concerns the interaction and synthesis of such compounds with B16 murine melanoma cells.

In vitro studies with the α–MSH analogue [^{125}I-Tyr^2,Nle^4,D-Phe^7]-α–MSH (^{125}I-NLDP) identified an average of 18,040 receptors per B16 melanoma cell. Saturation binding isotherms revealed a specific affinity of the tracer for the α–MSH receptor (α–MSH-R) with a dissociation constant (Kd) of 4.76×10^{-10} M. The fluorescent label ((chlorotriazin-2-yl)amino)fluorescein (CTAF), ^{125}iodine (^{125}I), biotin (Bi), 4-(1-Azi-2,2,2,-trifluoroethyl)benzoate (ATB) labels, and methotrexate (MTX) were attached to NLDP. Targeting of these and other probes to the α–MSH-R was determined with competition assays against ^{125}I-NLDP. All melanotropin conjugates studied, except for a streptavidin-gold-Bi-^{125}I-NLDP complex, specifically interacted with the α–MSH-R of B16 melanoma cells.

Following receptor binding, receptor-mediated transport of ^{125}I-NLDP into the melanoma cytosol was observed at 37°C. This suggests the internalisation of α–MSH-R-agonist complexes during receptor activation and subsequent cellular response. All probes tested, and MTX-NLDP, were agonistic to the α–MSH-R. The probes show promise for : 1) imaging of melanoma during its diagnosis; 2) imaging of the MSH-R-ligand complex and

its intracellular pathway; 3) site-selective drug delivery during treatment against melanoma; and 4) the extraction and purification of the MSH-R from B16 melanoma plasma membranes.

In this study, α–MSH and NLDP inhibited cell growth of B16 murine melanoma cells *in vitro*. The effect was time, concentration and cell density dependent. Pulse dosing of the cells with NLDP for 30 minutes/day had no effect on cell proliferation. During treatment of melanoma, MSH has the dual advantage of: 1) targeting probes and drugs to, and possibly within, melanoma; and 2) retarding melanoma cell growth. The application of MSH analogues in therapy against melanoma can only be evaluated with further studies *in vivo*.

ABBREVIATIONS

AC	Adenylate Cyclase
ACTH	Adrenocorticotropic Hormone
ATP	Adenosine Triphosphate
BSA	Bovine Serum Albumin
bFGF	Basic Fibroblast Growth Factor
cAMP	Cyclic Adenosine Monophosphate
CCl_4	Carbon Tetrachloride
cDNA	Complementary Diribonucleic Acid
CNS	Central Nervous System
CO_2	Carbon Dioxide
DNA	Deoxyribonucleic Acid
DTAF	((Dichloro-triazinyl)amino)fluorescein
DTT	Dithiothreitol
DIC	Diisopropylcarbodi-imide
DMSO	Dimethyl Sulphoxide
EDTA	Ethylenediaminetetraacetic Acid
EGF	Epidermal Growth Factor

Equations:

[A]	Concentration Agonist or Tracer
[B]	Concentration Unlabelled Competitor
B	Tracer Bound in the Presence of Unlabelled Peptide
Bo	Tracer Bound in the Absence of Unlabelled Peptide
C	y-Axis Intercept

cpm   Counts Per Minute

     test   = Cpm Bound for Sample Point

     max   = Maximum Bound Cpm

     min   = Minimum Bound Cpm

dpm   Disintegrations Per Minute

     min   = Activity Obtained in the Absence of Agonist

     max   = Maximum Activity Obtained in the Presence of Agonist

     specific = dpm max - dpm min

Ec50   Effective Concentration for 50% Maximal Stimulation

[H]   Concentration Free Hormone

[HR]   Concentration Hormone-Receptor Complex

Ka   Rate of Association of [H] and [R]

Kd   Rate of Dissociation of [H] and [R]

M   Slope of a Line

n   Total Number of Receptors

[R]   Concentration Free Receptor

FAB-MS   Fast-Atom Bombardment- Mass Spectrometry

FCS   Fetal Calf Serum

FITC   Fluorescein Isothiocyanate

GABA   Gamma-aminobutyric Acid

GDP   Guanasine-diphosphate

GERL   Golgi Associated Endoplasmic Reticulum of the Lysosome

GTP   Guanosine-triphosphate

HCl   Hydrochloric Acid

HEPES   4-(2-hydroxyethyl)-1-piperazineethanesulphonic acid

HOBT   Hydroxybenzotriazole

HPLC   High Performance Liquid Chromatography

HSA	Human Serum Albumin
IL	Interleukin
LH	Leutenising Hormone
LPH	Lipotropin Hormone
MEM	Modified Eagles Medium
MIF	Melanocyte-Stimulating Hormone Inhibiting Factor
MGSA	Melanoma Growth Stimulatory Activity
MRF	Melanocyte-Stimulating Hormone Releasing Factor
mRNA	Messenger Ribonucleic Acid
MSH	Melanocyte-Stimulating Hormone
α–MSH	Alpha-MSH
β–MSH	Beta-MSH
γ–MSH	Gamma-MSH
MSH-R	MSH Receptor

MSH PROBES an Toxin :

ATB	4-(1-Azi-2,2,2-trifluoroethyl)benzoate
^{125}I-ATB-NLDP	[^{125}I-Tyr^2,Nle^4,D-Phe^7,ATB-Lys^{11}]-α–MSH
Bi-NLDP	Biotinylated N$^\alpha$–[Nle^4,D-Phe^7]-α–MSH
Bi-^{125}I-NLDP	Biotinylated N$^\alpha$–[^{125}I-Tyr^2,Nle^4,D-Phe^7]-α–MSH
Bi-^{125}I-ATB-NLDP	Biotinylated N$^\alpha$–[^{125}I-Tyr^2,Nle^4,D-Phe^7,ATB-Lys^{11}]-α–MSH
CTAF	((Chlorotriazin-2-yl)amino)fluorescein
CTAF-NLDP	CTAF-N$^\alpha$–[Nle^4,D-Phe^7]-α–MSH
MTX	Methotrexate
MTX-NLDP	MTX-N$^\alpha$–[Nle^4,D-Phe^7]-α–MSH
ND$_{4-11}\alpha$-MSH	Ac-[Nle^4,D-Phe^7]α-MSH$_{4-11}$NH$_2$
NLDP	[Nle^4,D-Phe^7]-α–MSH

^{125}I-NLDP	[^{125}I-Tyr^2,Nle^4,D-Phe^7]-α–MSH
(Sa)-Bi-^{125}I-NLDP	Streptavidin Bound Biotinylated N$^\alpha$–[^{125}I-Tyr^2,Nle^4,D-Phe^7]-α–MSH
(Sa-Au)-Bi-^{125}I-NLDP	Streptavidin-Gold Bound Biotinylated N$^\alpha$–[^{125}I-Tyr^2,Nle^4,D-Phe^7]-α–MSH
N	Mean Number of Cells per Haemocytometer Square
NaCl	Sodium Chloride
NaHCO$_3$	Sodium Bicarbonate
NaOH	Sodium Hydroxide
Naps	2-Nitro-4-azidophenylsulphenyl
NEAA	Non-essential Amino Acids
PB	Phosphate Buffer
PBS	Phosphate Buffer Saline
PDGF	Platelet-derived Growth Factor
PEG	Polyethylene Glycol
Pen/Strep	Penicillin/Streptomycin
PI	Pituitary Intermediate Lobe
PKA	Protein Kinase A
PKC	Protein Kinase C
POMC	Pro-opiomelanocortin
RER	Rough Endoplasmic Reticulum
rpm	Rotations Per Minute
SDS-PAGE	Sodium dodecyl sulphate-polyacrylamide gel electrophoresis
TFA	Trifluoroacetic Acid
TGF	Transforming Growth Factor

TABLE OF CONTENTS

1. INTRODUCTION

1.1. INTRODUCTION

Alpha-melanocyte-stimulating hormone (α–MSH) is best known for its promotion of melanogenesis and pigment dispersion in melanocytes and their transformed counterparts, melanoma (154). Most human melanoma express MSH receptors (53, 71, 160). The hormone stimulates melanogenesis in pigment cells via a Gs protein coupled receptor located in the cellular plasma membrane. Receptor activation sets in motion a number of co-ordinated intracellular signalling pathways related to melanin biosynthesis and migration. These intracellular mechanisms also regulate the cell morphology and proliferation of pigment cells (99, 138).

1.2. DISTRIBUTION OF MELANOTROPINS

The various physiological effects of α–MSH are well documented in the literature (52). These reports are focused mainly on the Central Nervous System (CNS) and on pigmentation in animal models. In most animals, the primary site of biosynthesis of α-MSH is the intermediate lobe of the pituitary pars intermedia (P.I.). Here, it and other melanotropic peptides are secreted by large polygonal MSH-producing type 1 cells. These cells are rich in mitochondria, contain well developed rough endoplasmic reticulum (RER), golgi apparatus and an abundance of secretory vesicles of various densities (168).

In the P.I. of mammals, α– and β–MSH immunoreactivity is present in cells which also contain corticotrophin (ACTH, 52). This is expected as all three peptides originate from a common precursor (POMC, 128). Type 1 cells are found with smaller strictly ACTH producing type 2 cells, and astrocyte-like glial cells (type 3) which form a loose meshwork in the P.I.. These type 3 cells show no signs of secretory function but display high oxidative enzyme activity (90).

Cells containing MSH are also present in the zone intermedia and in the pars distalis (P.D.) of human pituitaries (188). Human pituitaries produce pro-γ–MSH peptides (174) and (des)acetylated-α–MSH (12, 55, 180). Immuno-gold techniques against γ– and α– MSH confirmed their localisation in mature secretory vesicles of melanotrophs (169). Desacetyl-α–MSH and α–MSH are the most common melanotropins found in adult man.

Although α–MSH is unevenly distributed in the human brain, it is associated with a number of regions. Melanotropic peptides are transported from the pituitary to the hypothalamus. The highest concentration of MSH is found in the hypothalamus (4,11). They are also associated with a number of regions of the CNS. Certain neurones of the human hypothalamus also produce β–MSH (13). In man, more than a third of the α– MSH is contained within synaptosomes, less than a third is associated with sub-cellular particles, and very low amounts occur in the cytosol (135).

Specific receptors for α–MSH are widely distributed in rodents (175). A potent MSH tracer (^{125}I-NLDP) was injected into rats to determine melanotropin uptake in tissue. Binding of the tracer was found in a number of glandular organs, adipose tissues, bladder, duodenum, skin, spleen, and hypothalamus. Other studies have shown an initial high uptake of the tracer by the kidneys, liver, spleen, adrenals, and tumour after injection into mice bearing melanoma (52). Dupont, A. *et al* (47) observed a more localised distribution

of MSH. He observed a very high uptake of ^{125}I-α-MSH into the rat pineal gland relative to other organs, 5 minutes after an intrajugular injection.

1.3. REGULATION OF MELANOTROPINS

MSH release from the CNS is controlled by MSH releasing factors (MRF) and release-inhibiting factors (MIF). Some mammalian MIFs are dopamine, γ-aminobutyric acid (GABA), enkephalin, melatonin, serotonin, and somatostatin. Some MRFs are (nor)adrenaline, vasopressin and corticotrophin releasing factor (CRF), and opiates (3, 96, 199). Both gonadal steroids oestrogen and progesterone regulate MSH release via hypothalamic MIF and MRFs in female rats (182). Stress stimuli cause a 2-8 fold increase of α– and γ–MSH in rat plasma via MRF regulation (181)

The secretion of α–MSH is subject to diurnal and annual variations. Humans have elevated α–MSH levels in the afternoon and evening (72), while the highest β–MSH values are observed first thing in the morning with lowest values after retiring (173). Our basal β–MSH content is higher in the winter than in summer (189).

1.4. EFFECTS OF MELANOTROPINS

The effects of melanotropins on the CNS are well documented (52). Alpha–MSH facilitates adaptive behaviour and improves memory in man. This occurs with the increased efficiency of impulse transmission across existing synapses, and the growth and formation of new synapses. This melanotropin induced neural plasticity also affects social,

sexual and grooming behaviour, nerve regeneration, and brain development in experimental animals.

Alpha–MSH stimulates sebum secretion in the skin of rats. It also regulates prolactin, lutenizing hormone (LH), growth hormone (hGH), aldosterone, and ACTH in glandular organs. It increases heart rate, causes permeability changes in the eye, natriuresis in the kidneys, and lipolysis in fat cells (52). It also reduces inflammation and lowers high body temperature caused by stimulation of the immune system by modulating immuno- and neuroendocrine effects of interleukin-1 (41, 114, 147).

1.5. EFFECTS OF MELANOTROPINS ON PIGMENT CELLS

1.5.1. INTRODUCTION

Pigmentation of animals is very complex with regulation-effect systems varying between species. Descriptions of pigment cell responses to melanotropins will apply primarily to melanocytes and melanoma of mammals with some reference to melanophore systems.

1.5.2. THE HUMAN EPIDERMAL MELANIN UNIT

Melanotropins are best known for eliciting a morphological change in melanocytes, pigment cells of the human skin. Melanocytes are derived from the neural crest from

where they migrate as undifferentiated melanoblasts into the dermis. They later invade the epidermis and differentiate into melanocytes (145). The function of melanocytes in mammalian skin is to form and maintain dendrites, to synthesise melanosomes, and to secrete them into adjacent keratinocytes. Keratinocytes will phagocytise single or groups of melanosomes, either free or still housed in melanocyte dendrites. The melanosomes are then broken-down by lysosomes, and the encased melanin is dispersed in the keratinocytes (56). The movement of melanosomes from the perkaryon to the dendritic processes of the melanocyte is accomplished with the energy-dependent co-ordination of microtubules and filaments (106, 151). Each melanocyte together with 36 keratinocytes constitutes the epidermal melanin unit (56).

1.5.3. BIOMECHANISMS OF MELANIN SYNTHESIS

Melanin is formed in melanosomes of pigment cells following an increase of tyrosinase, the rate-limiting enzyme of melanogenesis. Tyrosinase synthesis occurs in membrane bound poly-ribosomes of the rough endoplasmic reticulum (RER) and is regulated by MSH and L-Dopa (164). Glycosylation and processing of the enzyme is carried out in Golgi associated endoplasmic reticulum of the lysosome (GERL). The tubular end portions of the GERL bud off to form coated vesicles and are transported to premelanosomes. Here melanin biosynthesis takes place to form mature melanosomes containing melanin (125).

A summary of the Raper-Mason melanin biochemical pathway is : 1) tyrosinase catalyses the hydroxylation of tyrosine to dopa and ; 2) the oxidation of dopa to dopaquinone; 3) dopaquinone undergoes non-enzymatic cyclisation; 4) oxidation; and 5) aromatisation into 5,6 dihydroxyindoles; 6) which undergo oxidative polymerisation to form melanin (170).

Pigmentation of the human skin is categorised as either constitutive (intrinsic) or facultative (inducible). Constitutive skin colour is the genetically determined level of cutaneous melanin pigmentation in the absence of direct or indirect influences. Facultative skin colour is the increase in melanin pigmentation above the constitutive level. Skin coloration is determined by : 1) the total number of melanosomes present within the epidermal melanin unit; 2) the rate of melanogenesis within the melanocytes and; 3) the rate of melanosomal transport within the keratinocyte population. Four factors determine melanocyte form and function : 1) genotype of the melanoblast; 2) genotype of the environmental cells; 3) the environmental history of the melanocyte and ; 4) the characteristics of the differentiated environmental cells. Racial differences in pigmentation are not due to differences in the number of melanocytes, but to differences in the cellular area occupied by the RER, the development of the golgi zone, and the maturation of the melanosomes (146).

1.5.4. EFFECTS OF MELANOTROPINS ON MELANOCYTES

Functional receptors for melanotropins have been identified in mouse melanocytes (44). Melanocytes can be induced to develop dendrites and form melanin by treatment with MSH, dibutyryl cyclic adenosine monophosphate (db-cAMP), or MSH in combination with theophylline (85, 91, 98). Together, theophylline and MSH caused the differentiation of melanocyte primary cultures in serum-free media (initiation of melanin synthesis in melanoblasts; 85). Although alone, α–MSH failed to induce differentiation of cultured melanocytes in the absence of keratinocytes. Alpha-MSH had no effect in serum-free organ culture models for mouse skin (86).

The effect of α–MSH on melanocyte growth is also controversial. Stimulation of human melanocyte growth in culture by α–MSH and db-cAMP has been reported (83, 98). But other researchers did not observe a change in the rate of melanocyte growth when the cells were exposed to MSH in serum or serum-free media (54, 81, 86, 198).

In vivo reports document a more consistent response of melanocytes to MSH. Melanotropins induced differentiation in the epidermis of new-born mouse skin. Both α– and β–MSH caused skin darkening in man (107). Facultative melanogenesis in human skin was observed 10 hours after intra-muscular injections of crude MSH (104). The transdermal drug delivery of MSH *in vitro* and *in vivo* had no toxic side effects on humans (45).

1.6. EFFECT OF MELANOTROPINS ON MELANOMA

1.6.1. INTRODUCTION

The effect of melanotropins on melanoma has been studied more extensively on melanoma than melanocytes. There have been several reports of MSH increasing pigmentation, cellular cAMP levels, and tyrosinase expression while inhibiting cell growth. Alpha-MSH also increased tyrosinase activity and melanogenesis in tumour-bearing mice (100). Other investigators have also observed an anti-proliferative effect of melanotropins on melanoma *in vitro* and *in vivo* (39, 130, 136, 195), while others found MSH to stimulate melanoma cell growth (27, 122).

1.6.2. INHIBITION OF MELANOMA CELL GROWTH

MSH induced inhibition of melanoma growth is usually attributed to; the build-up of toxic products from melanin biosynthesis, raised intracellular cAMP levels, or autocrine growth inhibitors (80, 108, 136, 139, 140, 141, 148).

Wick (194) suggested three groups of toxic compounds related to major metabolites in the pigment pathway, were responsible for auto-toxicity of cells during melanogenesis. These were tyrosine, levodopa, and 5,6-dihydroxyindole. Tyrosine levels were elevated sufficiently to cause toxicity in pigment producing cells relative to their non-pigmenting counterparts (136, 137). An α-MSH induced increase in intracellular tyrosine was found to correspond with a reduction of DNA in Cloudman S91 melanoma cells (79). Levodopa was also selectively toxic to pigment cells *in vitro*. It displayed anti-tumour activity in B16 melanoma (191, 192, 193). The proposed mechanism for cell auto-toxicity by these compounds is as follows : 1) quinols present in the cell are converted to quinones by MSH-induced elevated levels of tyrosinase; 2) quinones then inactivate DNA polymerase which is sensitive to oxidising conditions; 3) the lack of active DNA polymerase inhibits cell growth. Dihydroxyindole can also be cytotoxic to melanoma cells *in vitro* but possibly via a different route (139). This compound is an extremely reactive nucleophile and electrophile. Its cytotoxicity may be related to the generation of superoxide radicals. The free radicals could then cause cell death. The chronic low amounts of superoxide radicals produced during melanogenesis might explain why melanoma cells are inherently resistant to free radical chemotherapy (30).

Several investigators observed MSH related growth inhibition of melanoma to coincide with the accumulation of intracellular messengers rather than melanin synthesis. Agents

(MSH) that induced dendrite formation, raised intracellular cAMP, and increased tyrosinase activity, also inhibited cell growth without inducing melanogenesis (163). Cyclic AMP appeared to follow a pathway which reduced cell proliferation independent from melanin synthesis. Thus, cell inhibition was not caused to by melanogenic toxic by-products. Slominiski (164) claimed the α–MSH growth inhibition seen in amelanotic cells without the involvement of melanogenesis or tyrosinase expression, was due to a rapid (a few seconds) 'outburst' in cytosolic myo-inositol phosphates. The α–MSH activated second messenger, protein kinase C (PKC) has also been observed to inhibit B16 mouse melanoma cell proliferation (28, 73). Pawelek (140) suggested MSH inhibited melanoma proliferation due to raised level of both cellular cAMP and cytotoxic by products from melanin biosynthesis.

Melanoma are also suggested to regulate their own growth with autocrine growth-inhibiting compounds. Bogdahn *et al* (21) has isolated three autocrine-secreted tumour cell growth-inhibiting agents (MIA_I, MIA_{II}, and MIA_{III}) from a malignant melanoma cell line. They were observed to inhibit proliferation of melanoma and neuroectodermal tumors. Normal fibroblasts were uneffected by the MIAs. Rodeck (148) has also described the inhibition of melanoma growth by a melanoma secreted transforming growth factor (TGF-β). Bioactive TGF-β may represent a physiological growth inhibitor of melanoma.

1.6.3. STIMULATION OF MELANOMA CELL GROWTH

Alpha-MSH has been reported to stimulate melanoma growth : 1) in soft agar cultures with low or normal tyrosinase content in the medium (122); and 2) *in vitro* using mouse melanoma tumours inoculated from cultures raised in soft agar bilayers with, or without,

serum (27). Most of these authors suggest a form of melanoma self-incitement or endogenous growth hormone caused an increase in melanoma growth (8, 118). It is produced and secreted into the surrounding environment by the cells to cause a positive feedback system (205).

Several self-regulatory human melanoma growth factors have been identified by the secretion of their RNA transcripts into the cell supernatant. These were melanoma growth stimulatory activity (MGSA), basic fibroblast growth factor (bFGF), platelet-derived growth factor (PDGF-α, PDGF-β), transforming growth factor (TGF-β1, TGF-α), and interleukin (IL-1α, IL-1β; 25, 143). The two factors bFGF and MGSA contributed to autocrine growth stimulation of melanoma. These agents were also expressed by melanocytes (148). In M2R and B16-F1 mouse melanoma cells, PKC was found to stimulate cell growth rather than reduce it (67, 119).

1.7. MECHANISMS FOR THE ACTION OF MELANOTROPINS ON MELANOMA CELLS

1.7.1. INTRODUCTION

In man, MSH is cleaved from its pro-opiomelanocortin (POMC) precursor and travels from the zona intermedia and PD into the hypothalamus. It is then secreted into the blood stream where it has pleiotropic effects throughout the body. It regulates the differentiation, growth, and melanogenesis of pigment cells and their transformed counterparts, melanoma. This is accomplished by binding to specific receptors on the cell plasma membrane. Receptor occupation triggers several signal transduction mechanisms

and the possible internalisation of the ligand-receptor complex. The intracellular pathway of the ligand-receptor complex is unknown although data suggests lysosomal degradation of the ligand. It is not known if the receptor is recycled or degraded along with the ligand. Intracellular signals are terminated with the removal of the hormone from the cell surface receptors. Uncoupling of the ligand from the MSH-receptor (MSH-R) could be due to one or a combination of events, ligand internalisation, inactivation (biodegradation), or dissociation from the receptor.

1.7.2. STRUCTURE-FUNCTION ASPECTS OF MELANOTROPINS FOR THEIR RECEPTORS

Alpha-MSH was first isolated from porcine pituitary in 1955 by Lerner and Lee (105). Its primary structure was subsequently determined by Harris and Lerner (78). The identical hormone was found in ovine, equine, and macaque pituitaries (69). The complete 13 amino acid sequence of α–MSH was identical with the N-terminal tridecapeptide sequence of corticotrophin (ACTH). The seven peptide 'core' of α–MSH was also found in β– and γ–MSH (154). The amino acid sequence of β–MSH corresponds to β–lipotropin (β–LPH) at sequence 41-58 (52). The homology of these 5 peptides suggest a common pro-opiomelanocortin precursor (POMC, 128).

The 31 kDa POMC has since been isolated from man, rat, and ox (35, 46, 129). The peptides are biologically active once cleaved from the POMC by glycosylation, amidation, or acetylation. A common precursor for the melanotropins, ACTH, lipotropin, and endorphin explains the pleiotropic nature of MSH. The close genetic relationship of these peptides would cause similarities in their function and co-localisation. The pleiotropic

effects are augmented by the biotransformation of melanotropins by metabolising enzymes to other substances such as opioids, substance P, and other neuropeptides (75, 196).

```
ACTH     H-Ser-Tyr-Ser-Met-Glu-His-Phe-Arg-Trp-Gly-Lys-Pro-Val-Gly-Lys-Lys-Arg-Arg-Pro-Val-Lys-Val
                                                                                              |
a-MSH  CH₃CO-Ser-Tyr-Ser-Met-Glu-His-Phe-Arg-Trp-Gly-Lys-Pro-Val-NH₂                         Tyr
                                                                                              |
                                                                                             Pro
                                                                                              |
       HO-Phe-Glu-Leu-Pro-Phe-Ala-Glu-Ala-Ser-Glu-Asp-Glu-Ala-Gly-Asn
```

Figure 1.1. The structures of human ACTH and α-MSH showing their homology. Taken from Shizumi (154).

```
             4                                    10
a-MSH    Met-Glu-His-Phe-Arg-Trp-Gly

             7                                    13
β-MSH    Met-Glu-His-Phe-Arg-Trp-Gly

            -53                                   -47
r-MSH    Met-Gly-His-Phe-Arg-Trp-Asp
```

Figure 1.2. The structure of the ACTH-β-LPH precursor showing the homology of α-, β-, and γ-MSH. Taken from Shizumi (154).

Figure 1.3. Schematic representation of the gene, mRNA and protein structure of bovine pro-opiomelanocortin (POMC), the precursor for adrenocorticotropin (ACTH), lipotropin (LHP), melanotropins (MSHs), endorphin (EP), adrenal growth factor (AGF, pro-γ-MSH), adrenal mitogenic hormone (AMH), and joining peptide (JP). Taken from Eberle (52).

Structure-activity relationships of melanotropins and related peptides have been well studied in amphibian (Rana pipiens and Xenopus laevis tadpoles) and reptiles (Anolis carolines) melanophores. They have also been examined in the Cloudman S91 and B16 mouse melanoma cellular models. The quantitative induction of melanogenesis by MSH has been performed with B16 melanoma monolayers in melanin assays (155).

Alpha-MSH was the most potent naturally occurring peptide in these experimental systems. β–MSH was 1/20 to 1/4th as potent as α–MSH on a weight basis (69). Gamma-MSH only induced tyrosinase activity and dendrite formation in mammalian melanoma cells at very high concentrations (10μM, 165). Gamma^1-MSH displayed 0.075% the activity of α–MSH in melanophore assays (113).

Eberle (52) has found chain elongation or shortening of the natural MSH-tridecapeptide sequence decreased biological activity in all bioassays. The shortest peptide to stimulate pigment-dispersion in the frog skin was the 6-9 fragment -His^6-Phe^7-Arg^8-Trp^9-. This is regarded as the 'core' sequence for melanotropic activity. The shortest peptide sequence with measurable activity in melanoma cells was the 5-10 fragment -Glu^5-His^6-Phe^7-Arg^8-Trp^9-Gly^{10}-. Eberle (52) claimed the different responses are due to the higher sensitivity of melanophore versus melanoma assays.

Further studies (52) depicted two separate regions within the α–MSH sequence containing MSH bioactivity. Message 1 was the central sequence 4-8 -Met^4-Glu^5-His^6-Phe^7-Arg^8- which stimulated bioactivation. Message 2 was the C-terminal 10-13 -Gly^{10}-Lys^{11}-Pro^{12}-Val^{13}-NH$_2$ sequence which potentiated the effect. The -Phe^7-Arg^8- and -Lys^{11}-Pro^{12}- regions were particularly important for binding and stimulation of MSH receptors. No clear distinction could be made between the binding and biological stimulation within the MSH peptide.

13

When the size or lipophilicity of the peptide was increased, its activity generally dropped by a factor of 2-10 fold. Attachment of MSH to polyethylene glycol (PEG-5000) at its N-terminal reduced its biological activity to 1% its original value. Blockage of α–MSH at the N-terminus with bulky protecting groups reduced the activity by a factor of 400 (52). Generally, conjugates retained a high degree of biological activity when they were attached to the protein via its N-terminus. The C-terminal of α–MSH was stricter than the N-terminal. A basic side-chain at position 11 and a conformational stabilising element at position 12 were necessary for biological stimulation. The presence of a residue at position 13 was also essential for biological activity (50).

Oxidation of the Met^4 resulted in a 20-100 fold loss in activity and reduced binding to melanoma cells (158). This may represent a pathway for the inactivation of the hormone *in vivo*. Alpha-MSH labelled at its $tyrosine^2$ residue with ^{125}iodine using an equimolar chloramine T procedure, produced a monoiodinated tracer with 50% the biological activity of unlabelled α–MSH (49). Nle^4-containing MSH peptides were not oxidised at position 4, and therefore were more resistant to chloramine T oxidation during iodination and retained their biological and binding properties. Replacement of Met^4 by the isosteric residue of norleucine increased the tyrosinase activity of α–MSH by 62.5% in Cloudman melanoma assays.

In all pigment cell bioassays $[Nle^4,D-Phe^7]$-α–MSH (NLDP) was more active than α–MSH. It was 8-120 fold more potent in Cloudman melanoma cells and 12-fold more active in B16 melanoma assays. It was the most potent α–MSH derivative available other than the homologous $[Nle^4,D-Phe^7, Trp(Naps)^9]$-α–MSH photoaffinity label (52). NLDP expressed tyrosinase-stimulating activity for up to 6 days after removal from the cell medium (119). NLDP appeared to almost irreversibly bind to the MSH-R with

conformational properties which stabilised the interaction. The D-Phe residue in position 7 might protect the peptide from chemical degradation during *in vitro* and *in vivo* conditions. This would explain the higher potency observed with [D-Phe[7]]-α–MSH analogues relative to the [L-Phe[7]]-hormone (52).

Dissociation constants (Kd) for α–MSH, [Nle[4]]-α–MSH, and [Nle[4],D-Phe[7]}-α–MSH were obtained from competition binding assays on B16 mouse melanoma suspensions. They were 1.9, 1.8, and 0.32×10^{-9} M, respectively (158). The exchange of L-Phe[7] for D-Phe[7] in [Nle[4]]-α–MSH caused a 6 fold increase in the affinity of the peptide for B16 receptors. The three analogues were monoiodinated at the Tyr[2] residue and compared in binding and bioassays (53). Alpha-MSH was iodinated using the enzymobeads procedure (Immunobeads, Bio Rad Inc.). This protocol gently iodinated the peptide without oxidising the Met group and thus, preserving its biological and binding activities. All three radio-ligands displayed similar melanotropic activities to those observed with the unlabelled analogues. [Tyr $^{125}(I)^2$]-α–MSH was 0.8, {Tyr $^{125}(I)^2$, Nle[4]]-α–MSH was 0.4, and [Tyr $^{125}(I)^2$, Nle[4], D-Phe[7]]-α–MSH was 10.5 fold more potent than unlabelled α–MSH in B16 melanin dispersion assays. However in human D10 melanoma cells the [Nle[4]]-α–MSH tracer led to a high degree of non-specific binding (53). Due to its : 1) resistance to degradation, and/or dissociation from the MSH receptor; 2) strong biological activity before and after radio-labelling; and 3) low non-specific background labelling; NLDP is a suitable melanotropin for targeting of the MSH-R for studies of interactions of melanotropins with the MSH-R.

At present, there are no reports describing a potent α–MSH antagonist which binds to the MSH-R without eliciting a biological response from melanoma. Derivatives of Ac-Nle[4]-Asp[5]-His[6]-D-Phe[7]-Arg[8]-Trp[9]-Lys[10]-NH$_2$ were tested on melanophores for their potential as α–MSH antagonists. However, several modifications in the amino acid sequence of the

peptide resulted in a complete loss of antagonistic activity and a recovery of very weak agonistic action (2).

1.7.3. BINDING OF MELANOTROPINS TO SPECIFIC RECEPTORS OF MELANOMA

Specific binding of melanotropins and their analogues has been well documented for mouse and human melanoma. It has been demonstrated with murine and human cell lines *in vitro* or with tumours raised in mice. Receptor auto-radiography of α–MSH receptors is a quantitative method for assessing melanoma distribution in tissues.

Binding of ligands to the MSH-R was dependent on the concentration of extra cellular calcium (64, 116, 149). Calcium increased the binding affinity of β–MSH for its receptor by a factor of 20 (63). Calmodulin inhibitors inhibited ligand binding to the receptor indicating regulation by a calmodulin-related calcium-binding protein (66). It is not known if the calcium sensitivity of the MSH-R was mediated by a separate calcium-binding protein, or if it itself functioned as a hormone-operated calcium gate (149). Calcium ions were the most effective of a series of divalent cations in the stimulation of MSH-R activity. These results implicate calcium as a physiological regulator of the MSH-R (64). The MSH and ACTH receptors belong to a unique class of peptide hormones that specifically require calcium for their activity (68).

Alpha-MSH-receptors have been identified on a number of mouse melanoma lines. The best studied of these are the B16 and S91 Cloudman models. Out of a panel of 20 human lines, 13 expressed α–MSH receptors (71, 158). Saturation and competition binding assays have quantified binding affinities for various MSH analogues and described MSH-R

density per cell. Dissociation constants were fairly consistent regardless of experimenter or subclone. Kds of α–MSH ranged from $1.31\text{-}2.6\text{x}10^{-9}$ M in B16 and Cloudman melanoma (158, 176) with more variability in human lines at $0.92\text{-}2.2\text{x}10^{-10}$ M (38, 53). Receptors of human melanoma appeared to have a 10 fold greater affinity for α–MSH than murine lines. Iodination of the hormone increased its affinity for the receptor with a tracer Kd of $0.9\text{-}1.6\text{x}10^{-9}$ M for 3 B16 subclones (166). Iodination of α–MSH also increased its affinity (28%) for receptors on human D10 melanoma cells (158). The superagonist analogue NLDP, had a greater affinity for the α–MSH receptor than α-MSH with a Kd which ranged from 2.3 to $6.3\text{x}10^{-11}$ M in human melanoma, and $5.6\text{x}10^{-11}$ M for its tracer in a B61 line (176). These results are in agreement with others citing NLDP as having a 3.12 fold stronger affinity for its receptor than α–MSH in human D10 melanoma (158).

The association of ^{125}I-α–MSH to 205 human melanoma cells and its analogue ^{125}I-[Nle^4]-α–MSH to B16 cells were similar (157, 158). Indicating that both peptides were recognised in the same way, by similar receptors, in both species. Dissociation of the MSH tracers from their receptors was time, temperature, and concentration dependent. Non-specific binding was virtually independent of time and temperature (below 25%), but not concentration. Panasci et al (133) found both total and non-specific binding increased proportionately to the ligand concentration. At 4ºC the amount of bound tracer did not increase from 4 to 24 hours. Eberle (52) observed the association of MSH-Rs with there ligands at 37 and 25ºC to be rapid but did not reach a steady-state equilibrium. The specific binding decreased after reaching a maximum value at 30 minutes and 2 hours, respectively. Fifty percent of the bound ligand had left the cell after 35 minutes. After 4 hours all specific binding was gone. At 25ºC, 50% of the receptor-bound tracer had dissociated from the cell by 90 minutes. At 15ºC, the tracer had reached a stable association for the cells after 3-4 hours, while at 0-1ºC maximum binding was not reached until 8 hours. At 15 and 0-1ºC, 23 and 7% of the peptide was lost from the cell at 4 and 5

hours, respectively. An increase in time and incubation temperatures accelerated the loss of specific binding. This loss could be due to decomposition, dissociation, or internalisation of the tracer (52).

Siegrist *et al* (157, 158) observed degradation of an α–MSH tracer after an incubation in B16 and D10 melanoma cell supernatant at 37°C. They attributed this to proteolytic enzymes secreted by the cells, into the media, has been observed with 3 human melanoma lines (42). Peptide degradation was significantly reduced with the addition of 1 and 0.3 mM 1,10-phenanthroline to the binding buffer of D10 and B16 cells, respectively. Dissociation of the tracer was delayed from 35 minutes to 2 hours in D10 cells, and useful in establishing an equilibrium for specific binding of B16 cells. Recent experiments have shown that 1,10-phenanthroline was not necessary if the binding temperature was 15°C or below, and the chemical homogeneity of the tracer was good (52). Siegrist suggested the use of the more degradation resistant α-MSH analogue NLDP, in future MSH binding studies.

1.7.4. DEMONSTRATION OF MELANOTROPIN RECEPTORS *IN VIVO*

Melanotropin receptors have been characterised in experimental tumours *in situ* of murine melanoma. Frozen tissue sections of *in situ* tumours from mice inoculated with B16 mouse melanoma, were subject to auto-radiography with the ^{125}I-NLDP tracer (176). Specific binding was demonstrated when unlabelled melanotropins inhibited tracer binding to the tumours in a concentration dependent manner. Specific binding sites of α–MSH were distributed throughout the tumour but not associated with neighbouring non-tumour tissue or fibrovascular elements.

Siegrist *et al* (159) also observed the high affinity of melanotropins for their receptors *in vivo*. He inoculated mice with S91 Cloudman melanoma and 4 B16 mouse melanoma subclones. Receptor auto-radiography of the resulting tumours displayed higher binding capacities and affinities than isolated cultured cells. Receptor density was greater in sections with 14,700 receptors/cell compared to 10,500 sites/cell for isolated cells. The affinity of B16 sections for ^{125}I-NLDP was twice that of isolated cells with an average Kd values of 0.58 and 1.2×10^{-9} M, respectively.

1.7.5. CHARACTERISATION OF THE MELANOTROPIN RECEPTOR PATHWAY

Binding of melanotropins must occur on the extra-cellular surface in order for activation of MSH receptors. When α–MSH is applied to the outside of the cell, melanophores respond with melanin dispersion. Alpha-MSH injected intracellularly with micro-electrodes had no effect on melanogenesis (70, 89).

Varga *et al* (183, 184) incubated Cloudman mouse melanoma cells for 15 minutes at 37°C with β–MSH tracer and monitored the binding pattern of the peptide with auto-radiography. He found the label clustered over the perinuclear area of the cell surface. Further studies with an α–MSH-ferritin-fluorescein conjugate displayed a patchy binding over the cell surface, and at areas adjacent to the nucleus (43). Legros *et al* (103) also observed the distribution of α–MSH on the human melanoma plasma membrane was patchy and limited to a defined area of the cell surface. Similar results were obtained with cultured guinea-pig melanocytes (57). The FITC-β–MSH probe accumulated specifically on the Cloudman melanoma cell surface, overlying the Golgi region. It was observed 30 minutes later in Golgi vesicles (184, 185). Varga suggested internalisation of the hormone

is instrumental during induced melanogenesis because of the association of the α–MSH conjugate with Golgi regions and internal vesicles.

More recent experiments also support the hypothesis for receptor-mediated internalisation of the agonist-MSH-R complex by melanoma cells. Most of the evidence for MSH-R internalisation comes from acid treatment of melanoma cells during binding assays at metabolically active temperatures. Isotonic acid buffers are known to remove cell-surface-bound ligand, leaving only internalised α–MSH tracer behind (158). An α-MSH agonist was not observed within B16 cells following a 24 hour incubation at 4°C (133). A 37°C incubation on the other hand, demonstrated a time-dependent decrease in acid-soluble radioactivity with an initial increase, and eventual decrease, in acid resistant radio-activity. Internalisation was temperature dependent while the binding process was not. After a 4 hour incubation at 37°C, degradation products of the tracer were found in the cellular sample, but not the medium. Panasci (133) claimed the interaction between melanotropins and their receptors was similar to other polypeptide hormones and their receptors; i.e. a process involving binding, internalisation, and hormonal degradation (lysosomal), with down regulation of the receptor in the presence of saturating hormone concentrations.

Eberle (52) confirmed these findings. After 10 minutes at 37°C, mouse melanoma internalised 28% of an iodinated photo-reactive melanotropin. After 7 hours, 75% of the ligand was internalised with 25% bound to the cell surface. At temperatures of 0-15°C, internalisation of MSH peptides were considerably reduced or abolished. These results also imply down regulation of the MSH-R. Human D10 cells responded differently to α–MSH. After 30 minutes at 37°C, only 4% of the ligand was internalised. After 3 hours internalisation did not exceed 10%. Desensitisation of the MSH-receptor system has been observed in S91 melanoma tumours. Adenylate cyclase activity, an enzyme involved in MSH-receptor signalling, is much lower after stimulation by α–MSH (101).

In other receptor systems occupied receptors of the cell plasma membrane will become associated with coated pits which invaginate into the cytosol to form coated vesicles containing the agonist-receptor complex (87). Consequently, internal binding sites for MSH are associated with coated vesicles (31, 33). Orlow *et al.* (132) claimed these internal binding sites for MSH are an important criteria for cellular responsiveness to the hormone. Coated vesicles from melanoma tumours also contained MSH regulated kinase activity (23, 31, 82). The internalisation of the hormone or the hormone-receptor complex may have played a role in the physiological response of the cells via the generation of second messengers (111).

1.7.6. CHARACTERISATION OF THE MELANOTROPIN RECEPTOR

The MSH receptor has been described as a single population on both mouse and human melanoma plasma membranes with Scatchard Plot analysis of saturation binding data. Proteins bound by the monoiodinated [Nle^4,D-Phe^7,Trp(Naps)^9]-α-MSH conjugate identified similar receptors for both murine and human melanoma using SDS-PAGE techniques. A 45 kDa glycoprotein was selectively bound by α-MSH-photoaffinity labels in several B16 subclones, Cloudman mouse, and 3 human melanoma lines by 3 separate research groups (53, 152, 158, 166). The receptor was acidic with an isoelectric point of 4.5-4.9.

Other experimenters observed a doublet band of 43 and 46 kDa for B16 melanoma (1, 66). In human D10 cells a minor band was seen along side the 45 kDa protein (158). These results suggest two labelled proteins representing one class of receptor. Heterogeneity of melanotropin receptors of B16 subclones has also been demonstrated.

Solca *et al* (167) identified 3 different forms of MSH-Rs on 3 B16 subclones with varying Kds (0.9-1.6×10^{-9} M) with different molecular weights (42, 45 kDa, and a 43 and 46 kDa doublet).

The MSH-R has been further characterised by molecular cloning techniques. Cloudman mouse melanoma DNA clone (cDNA) libraries were constructed revealing a 317 amino acid protein with a molecular weight of 34.795 kDa (38, 126). It bound iodinated NLDP in a specific manner when expressed in COS-7 cells. Binding was displaced by the melanotropins α-, β-,γ-MSH and ACTH.

A cDNA library has been encoded from a human melanoma with a large number of MSH binding sites. It produced a 2.1 kb clone which selectively bound melanotropins when transfected into other human cells. The amino acid sequence of this human MSH-R was 76% and 39% identical and collinear with murine MSH-R and the human ACTH-R, respectively. This MSH-R protein might be universal for pigment cells. Several other human melanoma and two primary human melanocyte lines expressed small amounts of this MSH-R mRNA (126). An MSH-R gene 361 amino acids in length has been cloned from a human cervical cancer cell line (62). Its pharmacology characterised it as an α-MSH-R, specific to the heptapeptide core common to adrenocorticotropic hormone, α-, β-, and γ-MSH.

The murine MSH-R contained seven hydrophobic segments of amino acids which were predicted to span the cell membrane 7 times. This transmembrane topography is characteristic of a G-protein-coupled receptor. One cytoplasmic loop and its COOH-terminal contained sequences for cAMP-dependent protein kinase recognition (38, 126).

1.8. MELANOTROPIN REGULATION OF INTRACELLULAR SIGNALLING OF MELANOMA CELLS

1.8.1. INTRODUCTION

Once occupied by an agonist, the MSH-receptor transduces the hormonal message across the cell membrane to an effector which generates one or several intracellular signals. Binding and activation of intracellular messengers by the occupied MSH-R is dependent upon available calcium. In pigment cells the major pathway(s) for the signalling of MSH across the cell membrane involves: 1) the stimulation of a Guanosine-triphosphate (GTP) regulatory protein; 2) which activates adenylate cyclase (AC); 3) followed by an increase of intracellular 3',5'-cyclic adenosine monophosphate (cAMP); 4) which induces the activation of protein kinase(s) and protein phosphorylation; 5) this is succeeded by RNA synthesis; 6) protein synthesis; and 7) tyrosinase activation (52)

1.8.2. MELANOTROPIN REGULATION OF PROTEIN(S)

The GTP-binding properties of the MSH-R have been described by the amino acid sequence of the purified receptor (38, 97). Non-hydrolysable GTP analogues or cholera toxin lead to long-lasting activation of melanophores and melanoma. Thus, the stimulation of adenylate cyclase (AC) by the activated hormone-receptor complex involved a GTP-stimulatory protein (15, 110). The affinity of MSH for its receptor was reduced by GTP (64). The regulation of the MSH-R affinity for ligands by GTP and calcium (Section 1.7.3.) might occur on opposite faces of the cell plasma membrane. The negative biofeedback system between the occupied receptor and the GTP protein suggests a means for receptor desensitisation.

1.8.3. MELANOTROPIN REGULATION OF AC AND cAMP

MSH stimulated AC activity in both melanotic and amelanotic variants of Cloudman S91 mouse melanoma (16, 17). It usually led to pigment dispersion via increased levels of cAMP and tyrosinase activity (84). Adenylate cyclase activity increased with decreasing carbohydrate content in the membrane. Membrane carbohydrates may participate in the hormonal responsiveness of the cell (153).

The MSH induced rise in cellular cAMP levels of murine melanoma reached 200-fold by 5 minutes and returned almost to basal levels by 5 hours (48). Calcium was necessary for the transduction of the MSH-R signal. As with binding, AC was specifically inhibited by calmodulin inhibitors (65). Although the precise intracellular site of calcium is not known, it appears to lie functionally between the receptor, prior to AC stimulation (116).

1.8.4. MELANOTROPIN REGULATION OF PROTEIN KINASE(S) AND PROTEIN PHOSPHORYLATION

Protein kinases are known to modulate the activity of membrane transducing systems with specific phosphorylation reactions (178). Receptor phosphorylation is an important mechanism of controlling receptor desensitisation and internalisation. Activation of protein kinase A (PKA) and protein kinase C (PKC) were induced by MSH via the cAMP pathway in a dose-related manner (29). Two of three protein kinase isotypes found in melanocytes (α, β, and E) have been detected in melanoma ($\alpha-$ and $\beta-$; 203). In murine melanoma, the catalytic subunit of PKA was translocated to the nucleus after activation by

cAMP (48). Protein kinase C potentiated the effect of α–MSH but did not itself induce pigment dispersion (117). Protein kinase C is another suggested site of intracellular calcium regulation (119). The kinase is further controlled by diacylglycerols (131). Phorbol esters inhibited phosphorylation of the minor 34 kDa protein seen in S91 Cloudman cells (52). These results suggest a relationship between PKA, PKC and receptor phosphorylation with the activated MSH-R. Transmembrane signalling of MSH appears to involve cAMP activation of protein kinases(s) and protein phosphorylation (52).

1.9. SCOPE OF THESIS RESEARCH

Alpha-MSH derivatives either alone, or conjugated to a toxin or probe, are potential agents for specifically targeting melanoma during diagnosis and therapy. The MSH agonist-receptor system needs to be more thoroughly described before it can be effectively manipulated against melanoma. A panel of MSH derivatives were synthesised and tested in binding and biological activity assays to help define the MSH-receptor pathway (1). It was necessary for these ligands to maintain a high degree of specificity for the MSH-R and respond biologically in order to describe the agonist-MSH-receptor complex and its metabolic fate. An α-MSH-toxin conjugate was developed and tested for site-selective delivery to the α-MSH-R of B16 melanoma cells.

There are several reports of activated MSH-receptor (MSH-R) complexes stimulating second messenger systems which result in reduced melanoma proliferation. Alpha-MSH may also inhibit growth causing the cytotoxic accumulation of melanin by-products. Studies were performed on B16 mouse melanoma cells to clarify conflicting reports of stimulation, inhibition, or negligible effect of MSH on melanoma growth. The effects of

α–MSH and a potent analogue were examined in chronic and pulse doses on cell monolayers *in vitro*.

2. MATERIALS AND METHODS

2.1. CELL CULTURE

2.1.1. SOLUTIONS

2.1.1.1. WATER

All water used for the preparation of cell culture media and solutions was freshly double glass distilled by a bi-distillation Fistreem still (Fisons Ltd) fitted with a Fistreem pre-dionizer (Fisons Ltd).

2.1.1.2. BALANCED SALT SOLUTION

Phosphate buffered saline without calcium and magnesium (PBS) was obtained from Oxoid Ltd in tablet form. Ten tablets were dissolved in 1 litre of freshly double distilled water and divided into 125 ml Flow bottles before steam sterilisation in an autoclave (British Steriliser Co. Ltd, Swingclave Type SFT-LAB) at 121ºC for 15 minutes and stored at 4ºC. No bottles were kept past 1 month.

2.1.1.3. BASE AND ACID SOLUTIONS

Sodium bicarbonate (7.5%, NaHCO$_3$, BDH Chemicals), 1 N sodium hydroxide (NaOH, BDH Chemicals), and 1 N hydrochloric acid (HCl, BDH Chemicals) were prepared with double distilled water, steam sterilised and stored at room temperature.

2.1.1.4. ETHYLENEDIAMINETETRA ACETIC ACID

0.02% EDTA (BDH Laboratory Reagents) solution prepared in PBS was steam sterilised in 100 ml Flow bottles. Twenty ml aliquots were put into sterile universals (Sterilin Ltd) and stored at -20°C until required. No EDTA solutions were kept past 6 months.

2.1.1.5. TRYPAN BLUE

This stain was obtained from Sigma Ltd and stored at room temperature as a 0.1% solution in PBS.

2.1.1.6. GROWTH MEDIA AND ADDITIVES

RPMI 1640 (Flow and Imperial Laboratories) was obtained as 10X sterile liquid concentrates containing phenol red and no L-glutamine or sodium bicarbonate. The following media supplements were all obtained sterile from Flow or Imperial Laboratories and aseptically divided into 20 ml aliquots, L-glutamine (200 mM), an antibiotic solution (pen/strep) of penicillin (5000 IU/ml) and streptomycin (5000 mg/ml) and non-essential amino acids (NEAA). RPMI 1640 media and NEAA were stored at 4°C while L-glutamine and pen/strep were stored frozen at -20°C.

Fetal calf serum (FCS) from Flow and Gibco Laboratories was batch-tested for the support of cell growth supplemented at 10% to RPMI 1640 growth media. Maximum

growth occurred with batch numbers 9130012 (Flow) and 30A0212S (Gibco), used from 26.3.90-16.8.91 and 16.8.91-1.10.92 respectively. Serum arrived in 500 ml bottles and were allowed to thaw completely before being mixed and stored at -20ºC in 110 ml aliquots.

RPMI 1640 media was aseptically prepared from sterile components according to the following recipe, stored at 4ºC and used within two weeks. It was checked visually every day for contamination.

10X RPMI 1640 Medium	50.0 ml
Water	421.5 ml
L-Glutamine	5.0 ml
Pen/Strep	5.0 ml
NEAA	5.0 ml
$NaHCO_3$	13.5 ml
FCS	55.6 ml

Occasionally media required a small addition (c. 1 ml) of sterile 1 N NaOH or HCl to attain a final pH of 7.2-7.4.

2.1.2. PREPARATION OF REUSABLE ITEMS

All recycled items were rinsed in tap water immediately after use and then processed as follows. Glassware was soaked in a 2% solution of RBS 25 (Fisons Ltd) at approximately 40ºC for 30 minutes, then thoroughly cleaned using a nylon brush. Articles were subsequently rinsed in three changes of tap water, and left for 30 minutes in the last rinse. The process was then repeated using single distilled water. Finally, all glassware was left

to stand in a large volume of freshly collected double distilled water for no longer than 1 hour. After drying in a hot air oven (Gallenkamp), all items were capped with aluminium foil and sterilised by dry heat at 160°C (Gallenkamp Sterilising Oven) for a minimum of 1 hour.

Non-glass items, mainly tips for replicating pipettes, bottle caps and syringes were rinsed immediately after use and then cleaned by boiling in three changes of fresh distilled water. Finally, they were rinsed and left for 1 hour in a large volume of freshly double distilled water, dried, sealed in autoclave bags (DRG Hospital Supplies) and sterilised in an autoclave (Drayton Castle Laboratory Steriliser) at 121°C for 15 minutes.

2.1.3. EQUIPMENT

Sterile tissue culture polystyrene flasks (25, 75, 150, and 175 cm², Falcon, Becton Dickinson and Co.) and 24-well plates (16 mm diameter, Corning Cell) were regularly obtained from Imperial Laboratories. Clear, rigid polystyrene boxes (3.25 litres, Gallenkamp) sealed with gas tight vinyl tape (Intech Tapes Ltd) were used to house the 24-well plates. Five, 10, and 20 ml screw capped universal containers were obtained from Sterilin Ltd. Polypropylene 2 ml ampoules with screw-caps were obtained sterile from J. Bibby Sciences and used for the storage of cells in liquid nitrogen.

All manipulations requiring a sterile environment were performed in a vertical recirculating laminar flow cabinet (MDH Ltd). Other experimental protocols were performed at the bench.

All cells were stored in 2 ml ampoules, shelved in the vapour phase of a Union Carbide LR-40 liquid nitrogen refrigerator at approximately -148°C. Cells were maintained in a LEEC PF2 anhydric incubator (Laboratory and Engineering Company) with forced air circulation and thermostatic controls adjusted to give a temperature of 37°C. It was regularly checked with a digital thermometer with a thermocouple probe (Jenway Ltd) in a beaker of sterile water.

An inverted biological microscope WILD M40 (Wild Heerbrugg Ltd) was used for the examination of growing cell cultures and counting cells. A standard double grid haemocytometer (Fisons Ltd) was used to count cell density.

2.1.4. B16 CELL CULTURE METHODS

2.1.4.1. CELL LINE SUB-CULTURE

Sub-culture was undertaken weekly when the cells had reached confluence (roughly 2×10^7 cells/175 cm^2) and the growth rate had almost ceased. In this state, the cells completely covered the floor of the tissue culture flask and further growth was limited by contact-inhibition and the availability of nutrients in the media. After this point, the media pH dropped below 7.0 and there was some cell detachment.

The culture was optically examined to ensure the cells were healthy with no free-floating cellular debris or contamination in the growth medium. Aseptically, the old media was decanted off and the monolayer was rinsed two times each with 5 ml of pre-warmed

31

(37°C) sterile PBS. The flask was then incubated with 2 ml of pre-warmed 0.02% EDTA at 37°C for 10-30 minutes.

Upon removal from incubation the flask was gently agitated to dislodge the cells from the substrate, and 5-10 ml of fresh media was added. Using a sterile plugged Pasteur pipette, the cell suspension was gently aspirated until well mixed, and 0.40 ml was put into a sterile test tube to determine cell density. A new 175 cm² culture flask containing 100 ml of pre-warmed media was then inoculated with 10^6 cells and purged with 5% CO_2 in air (BOC special Gases) for 30 seconds before the cap was tightly sealed. The flask was put in an incubator and checked every day for health and contamination until the following week.

2.1.4.2. DETERMINATION OF CELL DENSITY

Subcultured cells prepared in a suspension form were thoroughly mixed and 0.1 ml of trypan blue was mixed in with 0.4 ml of the suspension for 5 minutes while being gently agitated. Viable cells excluded the dye while non-viable cells were stained dark blue. A cell density count would only include the former.

A drop of the cell-dye mixture was loaded into a haemocytometer chamber under a coverslip pressed down such that interference patterns appeared along its edges. Each chamber was divided into 9 large squares by 3 white lines, the 4 corner squares were further subdivided in 16 squares/corner, and the central square was subdivided into 25 smaller squares. A total count was made on the 4 corner and the central square of the haemocytometer grid with an inverted microscope.

If cell clumping was observed the count was abandoned and the cell suspension was further aspirated and a new sample was taken. If the cell density was greater than 150

cells/chamber then counting was impeded by overcrowding and the cell suspension was diluted before a new count was attempted. Conversely, if the cell count was below 25 cells/chamber the cell suspension was concentrated by centrifugation (1000 rpm for 5 minutes). A new cell-dye suspension was prepared if manipulations took longer than 15 minutes due to cell death from exposure to the dye.

Since each large square had an area of 1 mm^2 and a depth of 0.1 mm with the coverslip on, the total volume for each square was 10^{-4} ml. Where N is the mean of the 5 large squares, the cell density of the cell suspension was $Nx10^4$. To account for the dilution of the cell suspension with the dye, the end equation was $5(Nx10^4/4)$. Cells counted in this manner gave a standard deviation of 7.4% for 4 separate readings of a cell suspension.

2.1.4.3. CELL STORAGE

All cells were routinely stored frozen in liquid nitrogen, or its overlying vapour, after exposure to 10% of the cryoprotectant dimethyl sulphoxide (DMSO, BDH Chemicals grade 1, stored at room temperature in a dark glass container). Cell suspensions were prepared from the monolayer state during routine sub-culture, and centrifuged at 1000 rpm for 10 minutes (Jouan B3-11 bench centrifuge). The supernatant was removed and the cell pellet resuspended in a volume of filter-sterilised (0.2 μm sterile filters, Gelman Sciences) growth media containing 10% DMSO for a cell density of $2x10^6$ cells/ml. Replicate volumes of 1 ml were placed in 2 ml polypropylene ampoules with a maximum of eight placed in a Union Carbide BF6 biological freezer unit plug, in the top of a Union Carbide LR 33-10 liquid nitrogen refrigerator. Here the cells were cooled to below -70°C in nitrogen vapour at a rate of approximately 1°C/minute before being transferred to a liquid nitrogen freezer for long term storage.

33

2.1.4.4. RECOVERY OF CELLS FROM STORAGE

Immediately upon removing ampoules from storage they were placed in a 37°C water bath, ensuring that the water did not ride above the screwcap. They were swabbed with 70% ethanol (Haymans Methylated Spirits diluted with H_2O) when completely thawed and the contents were aseptically transferred into a 175 cm^2 flask containing 100 ml prewarmed media. After 4-5 days the cells formed a monolayer suitable for routine subculture.

2.1.4.5. PREPARATION OF CELLS IN 24-WELL PLATES

The cell density was determined for a cell suspension from a confluent monolayer during routine subculture before inoculation into 24-well plates. For all binding isotherms and assays, wells were seeded with 5×10^5 cells/well. Unless stated otherwise, wells for the tyrosinase assays were seeded with 3×10^4 cells/well. Wells for cell growth experiments were inoculated with 2.4×10^4-5×10^5 cells. All wells were filled (total volume 3 ml) with media and placed in a clear polystyrene box containing a 100 ml beaker of distilled water to maintain humidity. The box was then purged with 5% CO_2 for 3 minutes and sealed with gas tape. Following an overnight incubation at 37°C, the cells were ready for experimental use.

2.2. SYNTHESIS OF PEPTIDES

Samples of [Nle^4-DPhe^7]-α–MSH (NLDP) and α–MSH were obtained from Sigma Chemical Co. for reference with peptides synthesised in our laboratory. All other peptides

34

and further batches of NLDP and α–MSH were prepared by Dr. G. W. Olivier, therefore the protocol for their manufacture will not be described in full (Appendix 1). Prior to experimental use the peptides were dissolved 1 mg/ml in sterile 0.1 mM HCl and stored sterile at 4°C in a plastic screwtop-top eppendorf (Sarstead Plastics). All manipulations of peptides took place with plastic equipment due to the 'sticky' nature of α–MSH analogues.

2.3. IODINATION OF PEPTIDES

All tracers followed the same format for iodination using the equimolar chloramine T procedure (52). The photoaffinity tracers were not exposed to light during their manipulation and stored in foil-wrapped eppendorfs. They could not be monitored with UV light during collection of the fractions. Thus, a 5 ml sample of the tracer was used for HPLC analysis.

2.3.1. SOLUTIONS

2.3.1.1. STOCK SOLUTIONS

The following stock solutions were routinely prepared and stored at 4°C :

1) 0.25 M Na_2HPO_4 (FSA Laboratory Supplies) in H_2O.

2) 0.25 M NaH_2PO_4 (FSA Laboratory Supplies) in H_2O.

3) 1% TFA (trifluoroacetic acid, Aldrich Chemical Co., HPLC grade) in H_2O.

4) 50, 60, and 80% methanol (FSH Chemical Co., HPLC grade) with 1% TFA.

5) 0.1% TFA in H$_2$O (HPLC solvent A).

6) 70% acetonitrile/0.1% TFA (HPLC solvent B)

2.3.1.2. FRESHLY PREPARED SOLUTIONS

The following solutions were prepared fresh the day of each iodination :

1) 0.25 M phosphate buffer (PB), pH 7.4 (from Na$_2$HPO$_4$ and NaH$_2$PO$_4$ stock

    solutions).

2) 0.25% BSA (bovine serum albumin, Sigma Chemical Co.) in 0.05 M PB.

3) 1% Polypep (Sigma Chemical Co.) in 0.05 M PB.

4) 0.1% chloramine T (BDH Chemicals Ltd) dissolved immediately prior to use in

    H$_2$O.

2.3.2. PREPARATION OF THE COLUMN

Iodinated peptide was initially purified with a C18 reverse-phase column with Spherisorb
ODS 'Bond Elut' (Analytical International, MFG code OH53). The column was prepared
and conditioned with the following 1 ml wash routine:

1) 3x1% TFA.

2) 3x80% methanol/1% TFA.

3) 1x1% Polypep in 0.05 M PB.

4) 3x80% methanol/1% TFA.

5) 3x1% TFA.

2.3.3. IODINATION OF PEPTIDES

A 1.5 ml plastic eppendorf containing 0.02 ml of 0.25 M PB and 1.5 µl of peptide (from the 1 mg/ml stock) was transferred to a radioactive fume hood for the addition of 1.5 mCi Na-^{125}I (ICN Biomedicals, Inc). This was followed by 0.01 ml of freshly prepared 0.1% chloramine T which started the reaction. After 30 minutes 0.6 ml of 0.25% BSA in 0.25 M PB was added to halt the reaction and bind unbound ^{125}I$_2$.

2.3.4. PURIFICATION OF THE TRACER

The eppendorf contents were loaded onto the pre-conditioned C18 column. The column received the following 1 ml washes :

1) 2x0.25 M PB.
2) 4x50% methanol/1% TFA.
3) 2x60% methanol/1% TFA.

The last two sets of washes were saved (6 ml in total) and the peptide was further purified by HPLC using a C18 reverse-phase wide pore (300 A°) column, 25 cm in length and 4.6 mm in diameter. The methanolic washes were loaded onto the column which was run with an exponential gradient starting at 95% A, 5% B, reaching 40% A, and 60% B after 55 minutes before returning to the original values. A UV detector was employed at 217 nm (a HPLC trace of ^{125}I-NLDP is listed in Appendix 1). Ten 1 ml fractions were collected after 28 minutes (flow rate 1 ml/minute) and their activity was assayed on a gamma-counter.

The monoiodinated compound usually came off the column between 30-36 minutes, separating the free NLDP (usually 3 minutes earlier) and the diiodinated compound (usually 3 minutes later). The tracers were stored up to two weeks at -20ºC in HPLC buffer without signs of degradation.

2.3.5. PREPARATION OF STREPTAVIDIN TRACERS

Monoiodinated biotinylated-streptavidin-NLDP ((Sa)-Bi-^{125}I-NLDP) was freshly prepared by adding iodinated Bi-NLDP : streptavidin (Sigma Chemical Co.) diluted in sterile PBS for a 4:1-1:25 molar ratio. The mixture was gently shaken for 30 minutes at room temperature and added to an excess of Dynabeads M-280 streptavidin (100 ml : 100 mg/ml, Dynal, Merseyside) prewashed in PBS with 0.02% sodium azide (Sigma Chemical Co.) and stored at 4ºC. The solution was gently shaken at room temperature for 30 minutes to remove free Bi-^{125}I-NLDP (1). The supernatant containing streptavidin bound Bi-^{125}I-NLDP was assayed on the gamma-counter. The Dynabeads activity was assayed to measure the amount of free Bi-^{125}I-NLDP. If there was a substantial amount of unreacted Bi-^{125}I-NLDP (above 4x10^6 cpm), the amount of streptavidin was increased until very little unbound ^{125}I-NLDP was associated with the beads (99%). This was to assure that free Bi-^{125}I-NLDP did not contaminate the solution of (Sa)-Bi-^{125}I-NLDP. The mixture ratio of Bi-^{125}I-NLDP to streptavidin was kept between 4:1-1:25 to allow theoretical optimal binding of the biotin molecule for streptavidin (4:1), while keeping non-specific binding of free streptavidin to a minimum. Monoiodinated biotinylated-streptavidin-gold-NLDP ((Sa-Au)-Bi-^{125}I-NLDP) was prepared following the same protocol using 10 nm streptavidin-gold conjugates (Sigma Chemical Co.).

2.4. RADIO-IMMUNOASSAY FOR α–MSH IN FETAL CALF SERUM

All materials and methods followed the experimental format of Bowley *et al* (26).

2.4.1. SOLUTIONS

2.4.1.1. ASSAY BUFFER

The assay medium was a gelatine/phosphate buffer containing 0.05 M sodium-phosphate, pH 7.5, 0.1% gelatine (Davis), and 0.9% sodium-chloride (NaCl, BDH Chemicals).

2.4.1.2. α-MSH ANTIBODIES

Alpha-MSH antibody plasma (R6FB, 26) was stored at 4°C, and diluted 1:100 in assay buffer. This stock solution was stored for months without a loss in activity. The stock was diluted 1:150 in buffer (33 ml/5 ml) before use.

2.4.1.3. α-MSH STANDARDS

Alpha-MSH standards are prepared by dissolving 1 mg α–MSH (Sigma) in 1 ml of 0.01 M HCL and 0.25% BSA. This solution was then diluted in medium containing 0.25%

BSA for a final α-MSH concentration of 4 ng/ml. Half ml aliquots were then put into 4 ml polyethylene assay tubes (Bibby) and stored at -40°C.

2.4.1.4. CHARCOAL SOLUTION

A Charcoal/dextran solution was prepared by combining 1% Norit A charcoal (FSA Laboratory Reagents, dried for several days at 100°C) with 0.1% dextran T 70 (Sigma Chemical Co.) made up in assay medium (26). The solution was kept homogeneous by continuous stirring during the assay. All solutions and samples were kept on ice during preparation of the radio-immunoassay.

2.4.2. RADIO-IMMUNOASSAY PROCEDURE

2.4.2.1. DAY ONE

The α-MSH standard curve was prepared by the addition of 0.2 ml buffer, 0.1 ml standard α-MSH, and 0.05 ml α-MSH of the antibody solution in polyethylene LP4 tubes (Luckham Ltd LP4 gamma-counter tubes). The serum standard curve was prepared by replacing 0.1 ml of the assay buffer with 0.1 ml of FCS passed through a set-pack (conditioned as for iodination, Section 2.3.2.). Samples were tested for α-MSH by replacing the standard with 0.1 ml samples of FCS. Each tube was vortexed before the addition of 0.05 ml of ^{125}I-α-MSH (prepared by the chloramine T method, Section 2.3.) containing 2500 cpm in buffer. The solution was again vortexed and incubated at 4°C for 2 days. Ten doubling serial dilutions of the hormone standard were used for the standard

curves. All hormonal concentrations and samples were prepared in duplicate. Zero concentrations and reagent blank tubes were included in each assay.

2.4.2.2. DAY THREE

After 2 days, the separation of free from bound ^{125}I-α-MSH tracer was achieved by adding 0.5 ml of ice-cold charcoal/dextran solution to the tubes. They were vortexed and incubated at 4ºC for 10 minutes. The tubes were then centrifuged (2000 rpm) at 4ºC for 15 minutes and the supernatant was quantitatively aspirated. The pellets were counted on a gamma-counter for 5 minutes. Each assay was repeated twice.

2.4.2.3. CALCULATIONS

Counts due to non-specific binding were deducted from all values and the standard curve was plotted as %B/Bo, where:

B = tracer bound in the presence of unlabelled peptide.

Bo = tracer bound in the absence of unlabelled peptide.

non-specific = tracer bound with excess unlabelled peptide.

2.5. BINDING OF α–MSH ANALOGUES TO B16 CELLS

2.5.1. BINDING BUFFER

The buffer for binding assays was prepared fresh the day of the assay and maintained at the incubation temperature used during the assay. It consisted of a RPMI 1640 sterile

41

solution without additives, containing 25 mM 4-(2-hydroxyethyl)-1-piperazineethanesulphonic acid (HEPES, BDH Biochemicals), 0.2% BSA, and 10^{-9}-10^{-10} M ^{125}I-NLDP. In some cases, a synthetic collagenase inhibitor and 1,10-phenanthroline were added to the binding buffer for final concentrations of 10^{-10}-10^{-7} M and 0.3 mM respectively.

The following stock solutions were :

    1) 0.25 M HEPES buffer pH 7.2-7.4.

    2) 2% BSA.

    3) 10^{-2} M synthetic collagenase inhibitor (molecular weight 379, SmithKline and

        Beecham).

    4) 1 M 1,10-phenanthroline (Sigma Chemical Co.).

The HEPES and BSA stock solutions were made-up in RPMI 1640 media and stored in 5 ml aliquots at -20ºC. The stock buffers were good for 6 months. The synthetic collagenase inhibitor and 1,10-phenanthroline were stored in ethanolic solutions, also at -20ºC.

2.5.2. BINDING ASSAYS OF ^{125}I-NLDP AT 0-4ºC

Media from wells seeded overnight with 5×10^5 cells/well was removed and the number of cells in 4 sample wells were counted. This cell density produced a confluent monolayer of cell on the well floor. Cells were not used unless they were confluent. Other wells were washed twice with 3 ml of sterile RPMI 1640 media without FCS, NEAA, Pen/Strep, or glutamine, which had been cooled to 4ºC. The last wash was left in the wells and the 24-well plates were put on ice at 4ºC for 30 minutes. In this way the cells were brought down to 1.5-4ºC (as measured by a thermocouple probe). The second wash was removed from

the wells and replaced with 0.5 ml of ice-cold binding buffer. The 24-well plates were put on ice in a a plastic box sealed with gas tape, with an atmosphere of 5% CO_2, and incubated at $4^\circ C$ for 1 minute to 24 hours. After the incubation, the cells were washed twice with 3 ml of ice-cold serum free media and detached from the wells in 0.5 ml 1 M NaOH, and put into LP4 tubes where their activity was counted on a LKB Wallac 1277 Gammamaster. Non-specific binding was assessed by adding an excess (10^{-6} M) unlabelled NLDP to the binding buffer.

External-cell-surface binding to α–MSH receptors was evaluated by determining the dissociation of bound tracer after a 5 minute acid wash in 0.5 ml of ice-cold PBS pH. 2.0. The pH of the PBS was compared with an acid solution of a known pH of 2.0 (Documenta Geigy). The solution consisted of 2 ml 0.2 N KCl (potassium-chloride, FSH laboratory supplies) and 5.9 ml 0.2 N HCl. Cellular internalisation of the tracer was estimated by subtracting non-specific binding from wells treated with the acid wash.

2.5.3. BINDING ASSAYS OF ^{125}I-NLDP AT 15 AND $37^\circ C$

Binding assays were also performed at 15 and $37^\circ C$. They followed the same procedure as the $4^\circ C$ isotherm except for the pre-incubation and incubation temperatures. The cells were washed, pre-incubated, and incubated in buffers at 15 or $37^\circ C$, respectively. The cells were incubated in a Grant Instruments water bath at $15^\circ C$ or in an incubator at $37^\circ C$.

2.5.4. COMPETITION BINDING ASSAYS

The dissociation (Kd) and association constants (Ka) for α-MSH derivatives were determined using competition binding assays. The protocol was similar to the 4ºC binding assays with an incubation time of eight hours. A concentration series of a competitive unlabelled analogue was added to the binding buffer. The tracer concentration in the binding buffer was roughly 10^{-10} M. In all cases, the radio-tracer used was ^{125}I -NLDP with a known dissociation constant (Kd, determined with 4ºC saturation binding isotherms and Scatchard Plot analysis, Section 2.5.6.1.). The Kd of NLDP was estimated by competition with ^{125}I-NLDP (Section 2.5.6.2.). The binding affinity of the other radio-iodinated analogues was determined by competing these tracers with serial dilutions of unlabelled NLDP. Maximum binding and complete inhibition of the tracers was established with, respectively none, or an excess of (10^{-6} M), cold competitor to the binding buffer.

2.5.5. CALCULATION OF TRACER CONCENTRATIONS

The maximum specific activity of ^{125}INa is 80.5×10^{12} Bq/matom. Assuming maximum specific activity of ^{125}INa and a 1:1 ratio of ^{125}I : NLDP; and since :

1 matom ^{125}I $\equiv 10^{-3}$ moles ^{125}I-NLDP

1 mole ^{125}I-NLDP $\equiv 80.5 \times 10^{12} \times 10^{3}$ Bq.

Since 1 Bq equals 1 decay/sec :

1 mole ^{125}I-NLDP $\equiv 80.5 \times 10^{12} \times 10^{3} \times 60$ dpm.

Since our gamma-counter has 70% counting efficiency :

$$1 \text{ mole } ^{125}\text{I-NLDP} \equiv \frac{80.5 \times 10^{12} \times 10^{3} \times 60 \times 70 \text{ cpm}}{100}$$

$$\equiv 3.38 \times 10^{18} \text{ cpm.}$$

The number of counts per minute equivalent to 0.5 ml 1M ^{125}I-NLDP is given by :

$$\equiv 1.69 \times 10^{15} \text{ cpm.}$$

The same calculations were performed for tracers of other α-MSH analogues.

2.5.6. RADIO-LIGAND–α–MSH RECEPTOR BINDING ANALYSIS

2.5.6.1. SCATCHARD PLOT ANALYSIS OF SATURATION BINDING ISOTHERMS AT 0-4°C

Ligand-receptor interactions were analysed with MINSQ non-linear regression analysis with a weight of 1, and Equation 2.5.6.1. using data transformed from Scatchard Plots (22, 112). According to the Law of Mass Action :

[H] = the concentration of free hormone.

[R] = the concentration of free receptor.

[HR] = the concentration of the hormone-receptor complex.

Ka = the rate constant of [HR] association

= [HR]/[H][R].

Kd = 1/Ka

= rate constant of [H][R] disassociation.

$$\text{at equilibrium } [H][R] \underset{\text{Kd}}{\overset{\text{Ka}}{\rightleftharpoons}} [HR] .$$

n = total number of receptors

= [HR] + [R].

[R] = n - [HR].

$$Ka = \frac{[HR]}{[H](n-[HR]).}$$

Equation 2.5.6.1. : $Ka(n)-Ka[HR] = [HR]/[H]$.

These calculations give an equation for a straight line where :

y axis = $[HR]/[H]$.

x axis = $[HR]$.

slope = $-Ka$.

x-intercept (where $y = 0$) = n.

a straight line = one population of receptors.

a curvilinear line = a mixture of receptors.

During binding assays :

% receptor-specific bound = $\frac{(\text{total bound} - \text{nonspecifc bound}) \times 100\%.}{\text{total bound}}$

2.5.6.2. ASSUMPTIONS OF SCATCHARD PLOT ANALYSIS

During a Scatchard Plot analysis certain assumptions are made (22):

1) the labelled hormone is biologically identical to the native hormone.

2) the labelled hormone is homogeneous.

3) the receptor is homogeneous.

4) the receptor acts independently.

5) the receptor is unoccupied.

6) the reaction is at equilibrium.

7) there is no non-receptor binding.

46

2.5.6.3.ANALYSIS OF COMPETITION ASSAYS

During competition binding assays the following Equation 2.5.6.2. was used to calculate dissociation constants for unlabelled α-MSH analogues competed against a tracer :

$$\text{cpm test} = \frac{((\text{cpm max} - \text{cpm min}) [A])}{[A] + (KdA)([B]/KdB)} + \text{cpm min.}$$

Where :

cpm test = cpm bound for sample point.

cpm max = maximum bound cpm.

cpm min = minimum bound cpm (non-specific).

receptor specific cpm = cpm max - cpm min.

A = tracer.

B = unlabelled competitor.

the relative % maximum binding of the tracer [A] is :

$$\% \text{ max binding} = \frac{\text{cpm test} - \text{cpm min}}{\text{cpm max} - \text{cpm min}}$$

the curve is fitted as :

$$\% \text{ max binding} = \frac{[A]}{[A] + (KdA) [B]/KdB.}$$

For most competition assays, unlabelled α–MSH analogues were competed against the ^{125}I-NLDP tracer with a known Kd (determined by 0-4°C saturation binding isotherms and Scatchard Plot analysis). The Kd of unlabelled NLDP was determined by competition with 125I-NLDP. The Kds of other tracers of α-MSH analogues were then calculated by competition with unlabelled NLDP. To avoid a loss of more than 10% of the [HR] due to dissociation of [H] and [R], the allowable separation times of free [H] from bound [H] was 10 seconds-2.9 hours for a [H] with a Kd of 10^{-9}-10^{-11} M, respectively (112).

2.6. TYROSINASE ACTIVITY ASSAYS

2.6.1. SOLUTIONS

2.6.1.1. ASSAY MEDIUM

The medium used during the tyrosinase assay was RPMI 1640 media containing additives and [3',5'-^{3}H]-L-tyrosine (>50 Ci/mM, Amersham Co.) at 0.2 μCi/ml. The media also contained fresh serial dilutions of α–MSH peptides. Alpha–MSH or its analogues were not added to control wells. The [3',5'-^{3}H]-L-tyrosine stock 1 Cui/ml was stored at 4°C for 6 months. The media was aseptically prepared in plastic vessels the day of the assay.

2.6.1.2. CHARCOAL SOLUTION

A solution containing 10% dried charcoal in sterile PBS was used to separate [3',5'-^{3}H]-L-tyrosine from ^{3}H$_2$O (144). The solution was prepared fresh and kept in an ice cold homogeneous state.

2.6.2. ^3H_2O STANDARD CURVE

To measure ^3H_2O production during tyrosinase assays a quench curve was established on the LKB Wallac 1215 Rackbeta liquid scintillation counter using ^3H-O internal standards from Pharmacia (Internal standard kit for liquid scintillation counting ^3H_2O for organic solvents ^3H-O, 0.0909 mCi or 3.36 kBq activity/capsule, Appendix 1).

The protocol for the standard curve was as follows :

1) 8 ml organic scintillation fluid (OpitiPhase 'Safe', LKB Scintillation Products) was added to 10 x 10 ml Beta-counter vials (polyethylene, Packard Chemicals and Supplies) with an internal standard capsule/vial.

2) 1 ml of distilled water was added to each vial after the standard had dissolved in the scintillation fluid.

3) 0, 10, 20, 30, 40, 50, 60, 70, 80, or 100 ml of the quenching agent carbontetrachloride (CCl_4, Sigma Chemical Co.) was added to the vials.

4) the vials were vortexed and allowed to equilibrated for one hour at $4^{\circ}C$ before the curve was programmed into the Beta-counter.

2.6.3. TYROSINASE ASSAY PROCEDURE

B16 mouse melanoma cells were seeded in 24-well plates overnight (Section 2.1.4.5.). One ml of fresh assay media was added to the wells replacing the overnight growth media.

The cells were placed in pre-gassed air-tight boxes and incubated at 37°C for 1-3 days. After incubation, 0.90 ml of the supernatant was removed and put into 1.5 ml plastic eppendorfs (with air-tight lids) containing 0.4 ml of charcoal solution. The eppendorfs and plates were placed on ice to minimise ^3H_2O evaporation during manipulations. The eppendorfs were then vortexed and shaken for 15 minutes per hour at 4°C. They were revortexed and centrifuged at 800 rpm for 15 minutes. The clear supernatant (0.9 ml/eppendorf) was transferred into Beta-counter vials containing 8 ml of scintillation fluid. They were vortexed again and equilibrated for 1 hour at 4°C, in the dark, before they were read by a Rack Beta Counter.

2.6.4. CALCULATIONS FOR Ec50 VALUES

The half-maximal biological activation of tyrosinase was measured by the water by-product. Values were calculated with dose/response curves using INSTAT linear regression analysis. The equation for a straight line is y = mx + c where :

 y = response in dpm.

 x = concentration dose.

 M = the slope of the line.

Where :

 C = y axis-intercept.

 x = log concentration agonist.

  = log[A]

 dpm = M log [A] + C.

 log [A] = $\dfrac{(dpm - C)}{M}$

50

The values for M and C were obtained from the linear portion of a dose/response curve.

These values enabled the Ec50s (half-maximal biological stimulation) to be calculated. The

Ec50 takes place where :

50% maximum increase in activity = dpm min + 1/2 x dpm specific.

Equation 2.6.4. :

Ec50 = antilog (dpm min + (1/2 x dpm specific - C)/M).

dpm min is the activity obtained in the absence of agonist

dpm max is the maximum activity associated with the agonist

dpm specific is dpm max - dpm min.

2.7. GROWTH INHIBITION OF B16 CELLS BY α–MSH AND NLDP

2.7.1. CHRONIC DOSING WITH α-MSH AND NLDP

B16 mouse melanoma cells were seeded ($2.5x10^4$-$5x10^5$) into 24-well plates overnight.

The seeding media was replaced with 3 ml of pre-warmed RPM1 growth media containing

10^{-11}-10^{-7} M NLDP or 10^{-9} M α–MSH. Control wells contained hormone-free media. The

cells were incubated at 37°C for 24 hours, the hormone-media was removed and the cells

were washed twice in 3 ml of sterile PBS before the process would be repeated daily for

1-6 days. After incubation, the cells were counted on a haemocytometer and their

morphology, melanin production, cell growth characteristics, and media condition were

assessed.

2.7.2. PULSE DOSING WITH NLDP

Cells (seeded 5×10^4 c/well) were exposed to a daily 10^{-9} M pulse of NLDP over 4 days. The cells were exposed to the hormone-media for 30 minutes at 37°C before the media was removed and the cells were washed twice in 3 ml of PBS. Three ml of hormone-free media was added to each well and the plates were incubated at 37°C until treatment the next day.

Growth inhibition of B16 cells was calculated with Equation 2.7. :

% growth inhibition = [1-(mean no. of treated cells/mean no. of untreated cells)]x100%.

3. RESULTS

3.1. DETERMINATION OF ENDOGENOUS α-MSH IN CULTURE MEDIA

It was necessary to determine the amount of endogenous alpha-melanocyte-stimulating hormone (α-MSH) in the cell culture media to accurately assess the response of the B16 mouse melanoma cells to hormonal binding and stimulation (Section 2.4., 26). Figure 3.1. shows the standard curves of an α–MSH radio-immunoassay. One curve contained hormone free fetal calf serum. Samples of fetal calf serum used in cell culture work were compared to the serum standard curve to evaluate the presence of α–MSH. Alpha-MSH was not detected in any sample (data not shown). These results were confirmed in replicate assays. It is deduced that all hormonal effects observed with α–MSH and its analogues were due solely to experimentally added ligand.

3.2. BINDING OF α-MSH ANALOGUES TO B16 CELLS

3.2.1. INTRODUCTION

Studies of the binding of ligands to the α-MSH-R and the fate of the ligand-α–MSH receptor complex, are a primary concern in understanding the hormonal influence of α–MSH on the cell. This work can be advanced with melanotropin probes specific for

the α-MSH-R. Specific binding of α-MSH analogues also provide the basis for future cancer therapy studies using α-MSH-toxin conjugates to specifically deliver drugs to melanoma. Internalisation of the α-MSH-receptor complex may be necessary to achieve melanoma cytotoxicity with chemotheraputic agents selectively delivered via the α-MSH receptor (α-MSH-R). Scatchard plot analysis of saturation binding isotherms with the ^{125}I-NLDP tracer provide an estimation of : 1) the number of receptors/cell; 2) the level of receptor heterogeneity within the cell plasma membrane; and 3) the affinity of the α-MSH analogue for its receptor.

Competition of an agonist with another with a known affinity constant (Kd), allows the Kd of the former ligand to be determined. This information allows for the characterisation of the hormonal binding sequence of α-MSH and its receptor. It enables researchers to design new α-MSH analogues with strong affinities for the α-MSH-R. These compounds might serve as tools in further receptor research, or as targeting agents to cells expressing the α-MSH receptor.

3.2.2. BINDING OF ^{125}I-NLDP TO B16 CELLS AT 37°C

A modification of Eberle's binding assay (52) was developed with the α-MSH analogue [Nle^4,D-Phe^7]-α-MSH (NLDP) to establish specific binding of α-MSH to receptors of B16 cells. Details of the procedure are described in Section 2.5.

3.2.2.1. EFFECTS OF MULTIPLE WASHES ON BINDING

After incubation in a binding buffer containing approximately 1.18×10^{-10} M ^{125}I-NLDP, the cells were rinsed 1-4 times in 3 mls of RPMI 1640 medium. There was a rapid

initial rise in binding, reaching a plateau after 2 hours (Figure 3.2.1.). One to two washes gave the highest level of binding with the lowest amount of intrasample variability as displayed by their smaller standard deviations. The data from 3 and 4 washes was twice as scattered from their means than data obtained from 1 and 2 rinses. Washing the cells more than 2 times often dislodged cells from the monolayer. This is the likely cause for the greater variability observed with more than two washes.

3.2.2.2. EFFECTS OF INCUBATION MEDIUM AND BSA ON BINDING ASSAYS

The suitability of RPMI 1640 (Flow Inc.), Modified Eagles Medium with Earles Salts (MEM, Gibco) and phosphate buffered saline (PBS) binding buffers were tested in binding experiments. The ^{125}I-NLDP binding assay employed by Siegrist et al. (157) contained 0.2% BSA to reduce non-specific binding. It was possible that this large protein might inhibit specific binding in these assays. Hence, RPMI 1640, MEM and PBS binding buffers in the presence and absence of 0.2% BSA were examined for specific and non-specific binding of the tracer to the cells (Figure 3.2.3.), and the polystyrene well plates (Figure 3.2.2.).

Cells incubated in the RPMI and MEM buffers (Figures 3.2.2. and 3.2.3.) showed binding profiles similar to the one observed in Figure 3.2.1.. Maximum specific binding was reached at 1 hour, followed by the loss of tracer from the cells until a plateau was reached after 2 hours. Binding of ^{125}I-NLDP in the PBS binding buffer on the other hand, did not have this binding pattern. The PBS buffer displayed a reduction in bound ligand after 0.5 hours with a plateau after 1-2 hours (Figure 3.2.2.). Specific cellular binding was lower in MEM or PBS media than in the RPMI buffer (Figures 3.2.2. and 3.2.3.).

Non-specific binding of the tracer to wells of the assay plates in either RPMI or PBS buffers, in the absence of cells, with or without 0.2% BSA, were comparable at 1 and 2 hours (Figure 3.2.2.). Non-specific binding to the cells was determined with the addition of 10^{-6} M cold NLDP to the binding buffer (Section 2.5.). Percent non-specific binding was calculated as the non-specific bound / total bound, times 100%. It was higher in the MEM buffer (33%) than the RPMI recipe (23.5%, Figure 3.2.3.). This resulted in greater specific binding of the tracer in the RPMI binding buffer.

The RPMI buffer containing 0.2% BSA maintained the highest level of cell-associated binding for the longest period, with the lowest background binding to the wells (Figure 3.2.2.). BSA did not interfere with the binding of ^{125}I-NLDP to the cells. Neither the maximum cellular cpm, specific binding, or the rate of the ligand-receptor reaction time, were altered with the addition of 0.2% BSA. BSA continued to be used in the binding buffer to safeguard against non-specific binding during longer assay incubations. The RPMI based binding buffer containing 0.2% BSA was used in future experiments.

3.2.2.3. EFFECTS OF 1,10-PHENANTHROLINE ON BINDING ASSAYS

Protein endopeptidases are secreted by melanoma cells (42). These might prolong the time necessary for a ligand to reach equilibrium by continually degrading the tracer during binding incubations. Siegrist *et al.* (157) found 1,10-phenanthroline stabilised [Nle⁴]-α–MSH over 2 hours at 37°C in the presence of mouse B16 or human D10 melanoma. He observed 1 and 0.3 mM 1,10-phenanthroline were the best concentrations for inhibiting tracer degradation and non-specific binding (less than 25%) for D10 and B16 cells, respectively. Non-specific binding was measured in the presence of excess unlabelled ligand. Contradictory information (14) suggested such high levels of this metallo-protease inhibitor would be cytotoxic to the cell and reduce

ligand-receptor activity. Thus, binding assays were performed with and without, 0.3 mM 1,10-phenanthroline on B16 melanoma at 37°C.

Experiments performed in binding buffers containing 1.03×10^{-10} M ^{125}I-NLDP displayed maximum binding at 1 hour which dropped to a plateau after 2 hours (Figure 3.2.4.). The binding profile of the buffer containing 1,10-phenanthroline was similar to the one without (Figure 3.2.4.). Although, the amount of specifically bound tracer was reduced (35.5%) with the addition of 1,10-phenanthroline. These results were confirmed in repeated assays. The protease inhibitor was not included in future binding buffers.

3.2.2.4. POSSIBLE INTERNALISATION OF ^{125}I-NLDP

Internalisation of specifically-bound tracer at 37°C is partially established with acid stripping. Panasci $et\ al.$ (133) used 0.2 M acetic acid pH 2.5 to remove surface-bound $(^{3}H)ND_{4-11}\alpha$–MSH from B16 F1 cells. This technique exposed B16 cells to a low pH which effectively degraded the ligand and altered the receptor binding conformation. Thus, removing specifically receptor-bound ligand from the cell external plasma membrane. The freed ligand was washed away leaving any internalised ligand intact. Details of this procedure are described in Section 2.5.2..

Figure 3.2.5. shows the total amount of acid resistant tracer bound by B16 mouse melanoma cells at 37°C over 4 hours in 1.18×10^{-10} M ^{125}I-NLDP. Only 4.7% of the tracer was acid resistant after 1 minute, 15.8% after 0.5 hours, with maximum acid resistance plateauing after one hour (26.0-33.2%). Non-specific binding was minimal (3.3%). This pattern of results was observed in replicate assays.

57

3.2.3. BINDING OF ^{125}I-NLDP TO B16 CELLS AT 15°C

Binding assays were performed at 15°C over 25 hours, with 1.08×10^{-10} M ^{125}I-NLDP. These assays followed the same experimental format as described earlier, except the B16 when cells were incubated at 15°C instead of 37°C. Figure 3.2.6. shows the relatively rapid occupation of extracellular sites over 6 hours. After this time, there was a slow accumulation in the number of external binding sites. This increase did not appear to reach a plateau after 6 hours. It is difficult to assess the equilibrium time necessary for the ligand-binding equilibrium, due to lack of data points between 6 and 25 hours. There was no reduction of the externally bound ligand with time as witnessed at 37°C. Conversely, intracellular radioactivity steadily rose over the incubation period, reaching a maximum of 42.1% after 25 hours. Non-specific binding was consistently 2-4% after 1 hour.

3.2.4. BINDING OF ^{125}I-NLDP TO B16 CELLS AT 0-4°C

3.2.4.1. EFFECTS OF ACID WASHES ON BINDING ASSAYS

Binding assays performed at 0-4°C followed the same protocol as previous assays. The cells and all reagents were chilled in an ice-cold water bath to 0-4°C. When the cells were treated with an acid wash, bound radioactivity (6-8%) was less than non-specific values (8-12%) after a 6 hour binding incubation in ^{125}I-NLDP (Figure 3.2.7.). Thus, all specific activity was removed from the cells after 6 hours with an acid wash. Hence, the tracer was restricted to the cell external-cell surface at 0-4°C.

3.2.4.2. EFFECTS OF INCUBATION TIMES ON BINDING ASSAYS I

Twenty-four well plates were seeded overnight with 5, 4, 3, 2, and 10^5 cells/well. They were then incubated with 1.18×10^{-10} M ^{125}I-NLDP for 0.5 and 2 hours (Figure 3.2.8.). Cells bound an average of 2.44 times more tracer at 2 hours than at 0.5 hours. Non-specific binding on the other hand, was higher at 0.5 than at 2 hours. Non-specific binding was 14-78.9% of the total bound cpms at 30 minutes, compared to 10.3-15.2% at 2 hours. At 2 hours the combined higher specific activity and lower non-specific binding resulted in a higher specific binding than was observed at 0.5 hours.

3.2.4.3. EFFECTS OF CELL DENSITY ON BINDING ASSAYS

Specific binding increased steadily with both incubation times and cell density at both 0.5 and 2 hours (Figure 3.2.9.).

Binding assays with over 5×10^5 cells/well (cell confluence) were not performed. The proportionate increase in receptor activity would be counteracted by a decrease in cell surface area available for ligand-receptor interaction due to cell clumping. Future work was done with 5×10^5 cells/well. The minimum tracer incubation period was 2 hours.

3.2.4.4. EFFECTS OF PROTEASE INHIBITORS ON BINDING ASSAYS

The effect of 0.3 mM 1,10-phenanthroline on the binding of ^{125}I-NLDP to B16 plasma membranes was examined. Two binding assays containing 1.24×10^{-10} M ^{125}I-NLDP were run in parallel on B16 over 8 hours (Figure 3.2.10.). One assay contained 0.3 mM in the binding buffer. The binding profiles were similar. Both binding curves gradually rose over time until a maximum binding plateau was reached at 6 hours. 1,10-phenanthroline was not included in future work as it was not advantageous to binding specificity or association times of the free ligand for cell surface binding sites.

A synthetic collagenase inhibitor (a gift from SmithKline and Beecham) was also studied under these binding conditions. Serial dilutions of 10^{-5}, 10^{-6}, and 10^{-7} M were added to a binding buffer of 2×10^{-10} M ^{125}I-NLDP. B16 cells were incubated in the buffer for 8 hours (Figure 3.2.11.). Except for an early plateau (4 hours), the binding curves were similar to Figure 3.2.10.. Differences in the amount of bound tracer was not consistently altered by inhibitor concentration. The collagenase inhibitor was not included in further studies.

3.2.4.5. EFFECTS OF INCUBATION TIMES ON BINDING ASSAYS II

All binding assays up to this point had used approximately 1.18×10^{-10} M tracer (157). Different concentrations of ^{125}I-NLDP were tested during 0-4ºC binding assays on 5×10^5 cells/well to determine the optimal tracer dilution and incubation time at this cell density (Figures 3.2.12. and 3.2.13.).

Figure 3.2.12. displays the binding data for wells simultaneously incubated in 2.7×10^{-11} and 1.08×10^{-10} M ^{125}I-NLDP over 20 hours. Both tracer concentrations gave the 0-4ºC binding profile observed previously. There was a rapid increase in bound tracer with a small accumulation after 6 hours. Non-specific binding decreased with time at both tracer concentrations. It went from 43.7-83.6% at 0.5 hours, to 12.8-11.7% at 22 hours, for 1.08×10^{-10} M and 2.7×10^{-11} M tracer, respectively. In all assays, the percentage of non-specific binding decreased over time. Optimal results were obtained with a binding buffer incubation over 6 hours.

3.2.4.6. EFFECTS OF ^{125}I-NLDP CONCENTRATION ON BINDING ASSAYS

Tracer dilution did not alter the percentage of non-specific binding at maximum values of total binding. The amount of specific binding was proportional to the dilution of the

agonist. Four times as much ligand specifically bound 3.2 fold more sites during maximum binding.

This trend was not observed when comparing assays performed 3 weeks apart using 3 different cell passage numbers (A and B, Figure 3.2.13.). During independent binding assays, 3.94 fold more specific activity was observed using a binding buffer containing 1.42 fold more ligand (5.9×10^{-11} M and 8.38×10^{-11} M).

A higher tracer concentration shortened binding equilibrium times when assays were run simultaneously (Figures 3.2.12. and 3.2.13., A and B assays). A higher tracer concentration resulted in more agonist bound when assays were performed simultaneously over 6 hours. The specific radioactivity at 6 hours was 64.2 and 59.3%, for 1.08×10^{-10} and 2.7×10^{-11} M, respectively. These results are in agreement with the Law of Mass Action. An increase in available ligand decreases the time it takes free and bound ligand to reach an equilibrium.

This trend was not repeatable when comparing assays performed over a 3 week period (Figure 3.2.13., A and B assays). Here a more dilute tracer concentration bound more of the total specific activity after 6 hours (5.9×10^{-11} M, 70%; 8.38×10^{-10} M, 57%). Cell detachment from the well plates was often observed after 8 hours. Technical limitations of tracer production did not make routine assays with tracer concentrations above 1.18×10^{-10} M feasible. Thus, future work continued to use a binding buffer incubation times of 8 hours in approximately 1.18×10^{-10} M ^{125}I-NLDP. Occasionally, the binding equilibrium was not completely established (the continued accumulation of bound ligand after 8 hours at 0-4°C) under these conditions.

3.2.4.7. SATURATION BINDING ISOTHERMS OF ^{125}I-NLDP

B16 murine melanoma were incubated for 8 hours in a ^{125}I-NLDP dilution series of $10^3-2 \times 10^6$ cpm/well. Figure 3.2.14. presents an example saturation binding isotherm. Values of bound versus free radio-ligand in a Scatchard Plot allow for the calculations of the Ka, Kd, n, and analysis of the receptor population. Figure 3.2.15. displays the Scatchard Plot for the raw data in Figure 3.2.14. The 95% regression confidence limits are displayed as dotted lines, while its R^2 is 0.962 (R^2 is the square of the correlation coefficient for the regression points). The data was linear confirming the existence of one major population of receptors. The points not included in the confidence limits were not evaluated as data obtained at these very dilute ligand concentrations are highly susceptible to experimental error. Assuming one population of receptors, the specific binding isotherm can be described by Equation 2.5.6.1. $[HR]/[H] = Ka(n)-Ka[HR]$ (Section 2.5.6.). Estimates of Ka (the slope of the line) and n (the y axis intercept/slope) are obtained by fitting the data to Equation 2.5.6.1. using non-linear least squares regression analysis. The Kd is calculated as the inverse of Ka. Table 3.2.1. lists the estimates obtained from five replicate saturation binding isotherms.

The values of Ka were in good agreement with standard errors of 10-20%. There was more variation in the number of receptors per B16 cell with a mean of 18,022 (±13,040). This change in receptor number was not surprising considering the 2 year period in which these assays were performed. Inherent changes in cellular activity with time are frequent. A mean Kd of 4.76×10^{-10} M for ^{125}I-NLDP was used during calculations of binding affinities of other ligands in competition assays.

Table 3.2.1. The Ka (SD), Kd (SD), n(SD)s for five replicate saturation binding isotherms of ^{125}I-NLDP on B16 cells, and their means. The binding (Figure 3.2.14.) and Scatchard plots (Figure 3.2.15.) are derived from binding isotherm 2*. All data are listed in Appendix 2.

BINDING ISOTHERM	Ka (10^9 M^{-1})	Kd (10^{-9} M)	n
1	2.09 (±0.19)	0.478 (±0.043)	28,000 (±1400)
2 *	1.70 (±0.11)	0.588 (±0.038)	10,100 (±400)
3	1.88 (±0.38)	0.532 (±0.108)	5,900 (±700)
4	2.53 (±0.32)	0.395 (±0.050)	35,700 (±2,500)
5	2.31 (±0.40)	0.433 (±0.075)	10,500 (±1000)
MEAN	2.10 (±0.33)	0.476 (±0.076)	18,040 (±13,022)

3.2.4.8. COMPETITION ASSAYS

Routine determination of binding affinities for other α–MSH derivatives was conducted using competitive binding techniques. A radio-labelled ligand with a known binding affinity (^{125}I-NLDP) was incubated for 8 hours at 0-4°C with 5×10^5 B16 cells/well in the presence of various concentrations of unlabelled competitor. Assuming the ligands compete for the same receptor (as indicated by the Scatchard Plot), the level of non-specific binding is identical for the radio-ligand and its competitor, and there is little depletion of ligands in the binding medium, experimental results can be described by Equation 2.5.6.2. (Section 2.5.6.2.):

$$\text{cpm test} = \frac{((\text{cpm max} - \text{cpm min}) [A])}{[A] + (KdA) ([B]/KdB)} + \text{cpm min.}$$

Ten replicate experiments were performed with cold (unlabelled) NLDP in competition with ^{125}I-NLDP (Table 3.2.2.). The mean dissociation constant for NLDP was 2.225×10^{-9} M (SD ± 0.505×10^{-9} M, Table 3.2.3.). This value was used to calculate the dissociation constants for radio-ligands other than ^{125}I-NLDP.

Figure 3.2.16. compares the binding affinities of three separate samples of NLDP. One sample was obtained from Sigma Chemical Co.. Another was synthesised by G. Olivier in our laboratory. Both preparations were freshly reconstituted in 1 mM HCl. The third sample was taken from the second sample but stored in solution for 29 weeks prior to use. The relative dissociation constants were 2.13, 2.82, and 2.36×10^{-9} M. There was little difference between samples stored for 29 weeks in 1 mM HCl, those newly reconstituted, or those obtained from Sigma Chemical Co. All peptide preparations were used within 6 months of reconstitution.

Table 3.2.2. lists the dissociation constants (Kd) obtained from individual assays together with their standard deviations, at a 95% confidence level, calculated with MINSQ non-linear analysis (Section 2.5.6.). A summary for each analogue is presented in Table 3.2.3.. This table lists the number of replicate experiments, the mean Kds, standard deviations of the means, and the affinities for the α–MSH receptor relative to acetylated α–MSH. Figures 3.2.16.-3.2.25. plot an example competition assay/α–MSH analogue (data for all assays are listed in Appendix 2).

All probes except for the (Sa-Au)-Bi-^{125}I-NLDP tracer selectively competed with NLDP for the α–MSH receptor. The value obtained for the dissociation constant for α–MSH was 6.46×10^{-9} M. The value of its NLDP analogue was 2.92 fold less (2.22×10^{-9} M). Since Kd = 1/Ka, NLDP had a 2.92 fold greater affinity for the α–MSH-R than α-MSH. The difference of the means of α–MSH and NLDP was <0.01 significant, at 95% confidence, using the two-sided Students unpaired T-test. The CTAF-NLDP complex was the only probe with a Kd higher than α–MSH. It displayed a 7.19 fold loss in receptor affinity at a <0.01 significance level. The addition of methotrexate to NLDP resulted in a small decrease in the Kd relative to NLDP (1.14 fold, <0.05 significance). Biotinylation of the NLDP N-terminus increased the peptides binding affinity 6.31 fold (<0.01). The affinities of ^{125}I-NLDP (0.287 significance) or Bi-^{125}I-NLDP (0.952 significance) compounds were unaffected when bound with the

photoaffinity molecule. The addition of streptavidin (Sa) to Bi-NLDP had no observed effect on binding affinity (0.376 significance), but caused high non-specific binding (data not shown). Conversely, incorporation of the gold-streptavidin complex (Sa-Au) to Bi-^{125}I-NLDP removed the ability of the Bi-^{125}I-NLDP to compete with NLDP for the α–MSH receptor. Iodination of the NLDP N-terminus resulted in a 4.65 fold increase (<0.01 significance) in the ligands affinity for the receptor. Iodination of biotinylated NLDP on the other hand, had no effect on ligand affinity (0.397 significance).
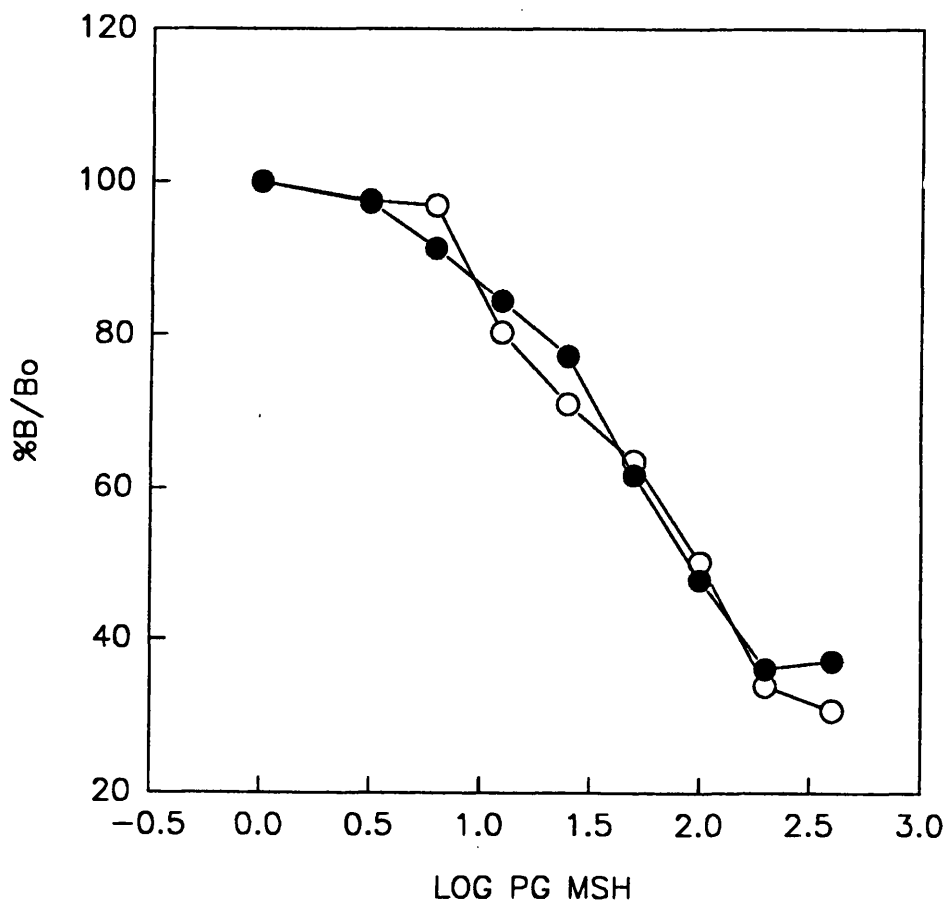
Figure 3.1. Typical standard curves of α–MSH radio-immunoassays with log pg α–MSH/tube plotted against % bound ^{125}I-α–MSH in the presence of unlabelled α–MSH/^{125}I-α–MSH bound in the absence of unlabelled α–MSH. Each assay point was determined in the presence ● and absence ○ of plasma. Points represent the means of two sample wells.
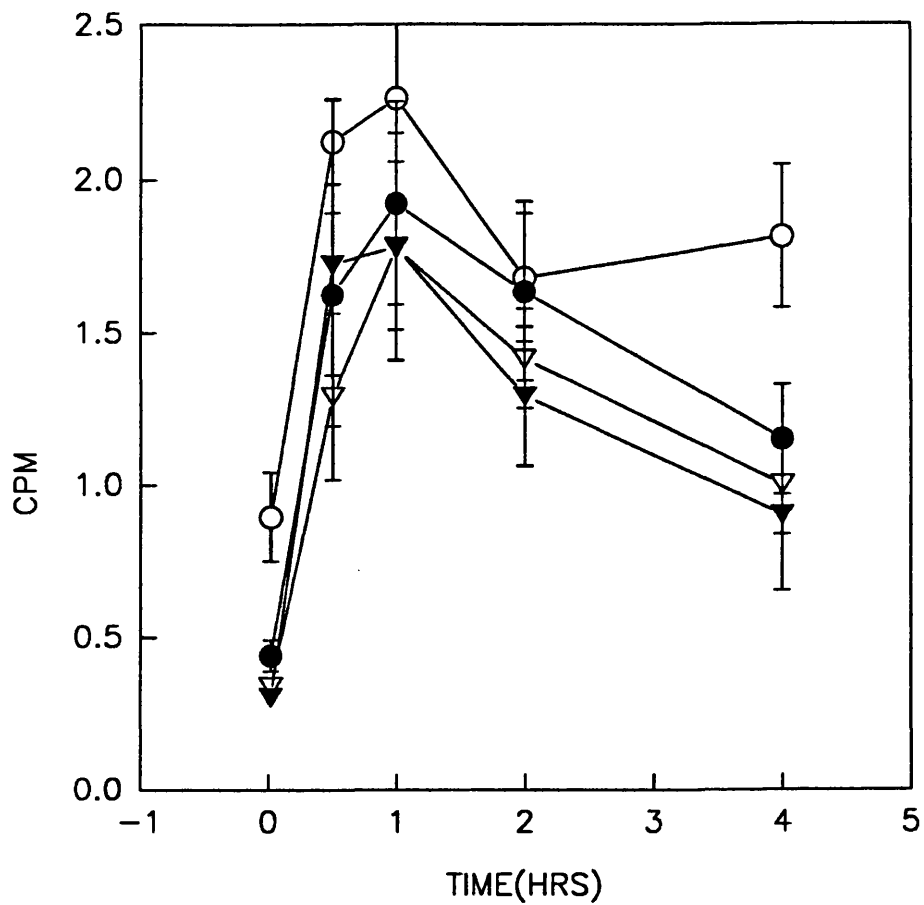
Figure 3.2.1. Total binding/10,000 of ^{125}I-NLDP to B16 cells at 37°C using 1 ○ ;

2 ● ; 3 ▽ ; and 4 ▼ washes after binding vrs time. Bars indicate SD values

of 4 sample wells.
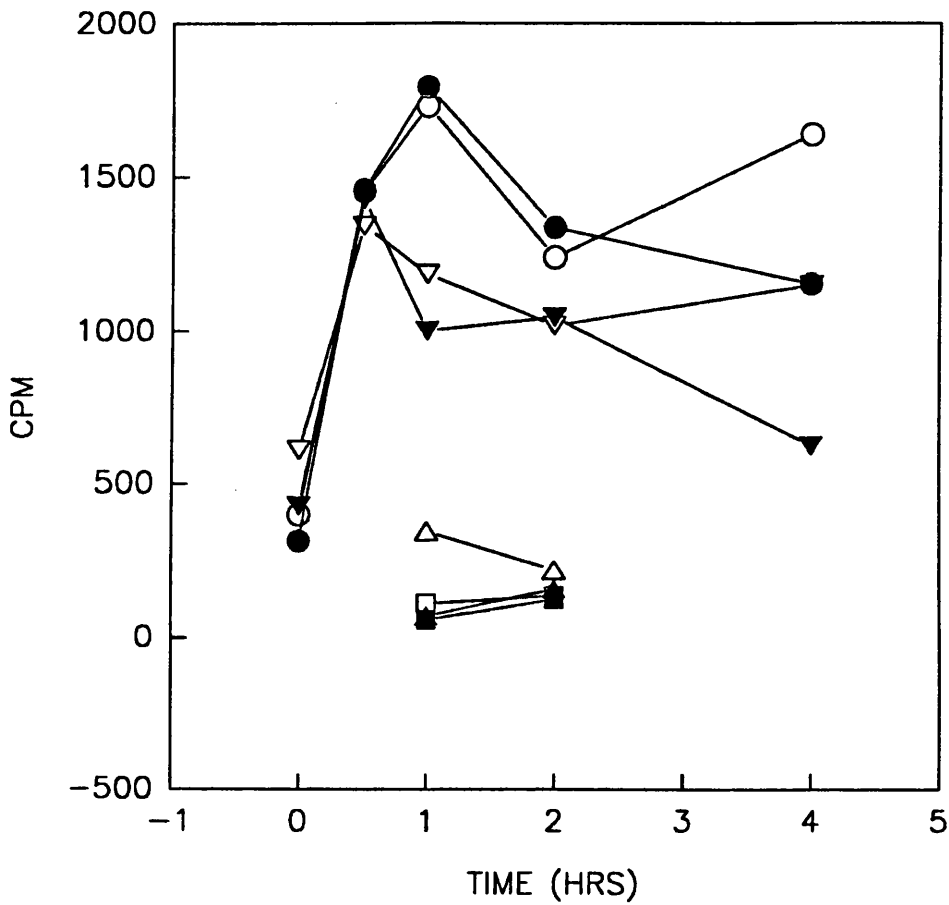
Figure 3.2.2. Binding of ^{125}I-NLDP to B16 cells at 37°C in RPMI or PBS buffers with, or without, 0.2% BSA vrs time. Binding in RPMI ● ; RPMI with BSA ○ ; PBS ▼ ; PBS with BSA ▽ ; non-specific binding to the wells in RPMI ▲ ; RPMI with BSA ■ ; PBS △ ; PBS with BSA □ . Points represent the means of 4 sample wells.
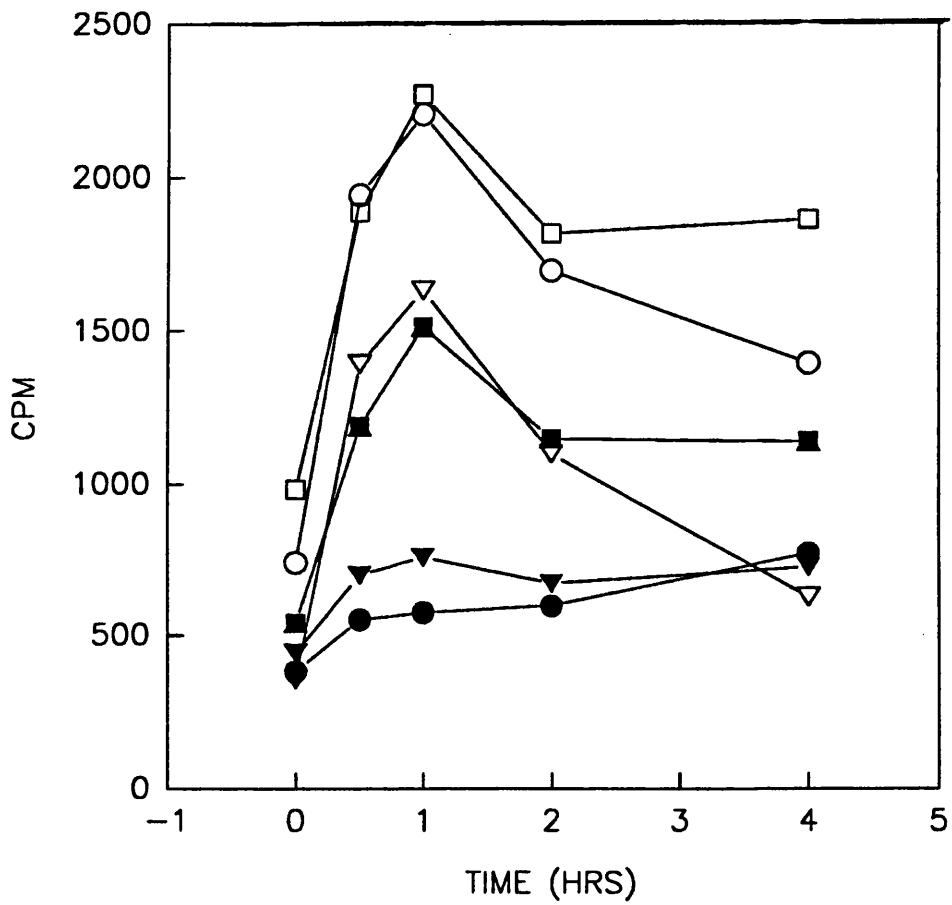
Figure 3.2.3. Binding of ^{125}I-NLDP to B16 cells at 37°C in RPMI or MEM media vrs time. Total binding in RPMI $\square$; non-specific binding in RPMI $\blacktriangledown$; specific binding in RPMI $\blacksquare$; total binding in MEM $\bigcirc$; non-specific binding in MEM $\bullet$; and specific binding in MEM $\triangledown$. Points represent the means of 4 sample wells.

69
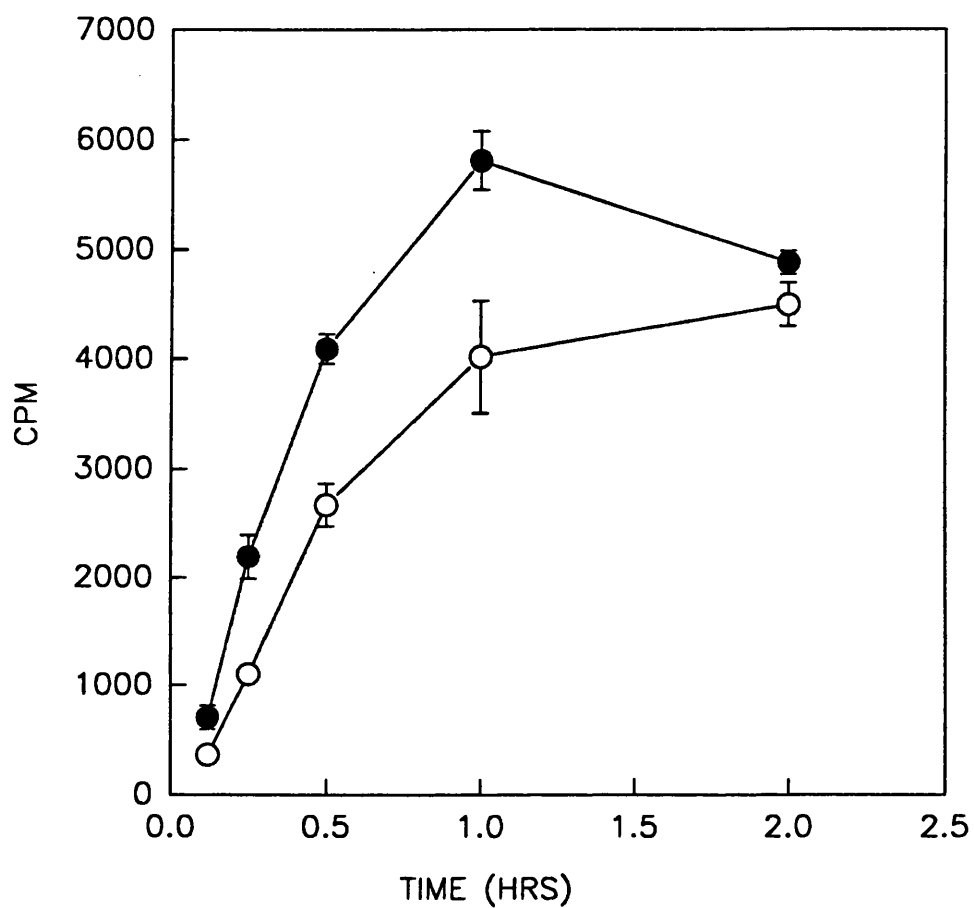
Figure 3.2.4. Binding of ^{125}I-NLDP to B16 cells at 37°C in RPMI with ○ ; and without ● 0.3 mM 1,10-phenanthroline vrs time. Bars indicate SD values of 4 sample wells.
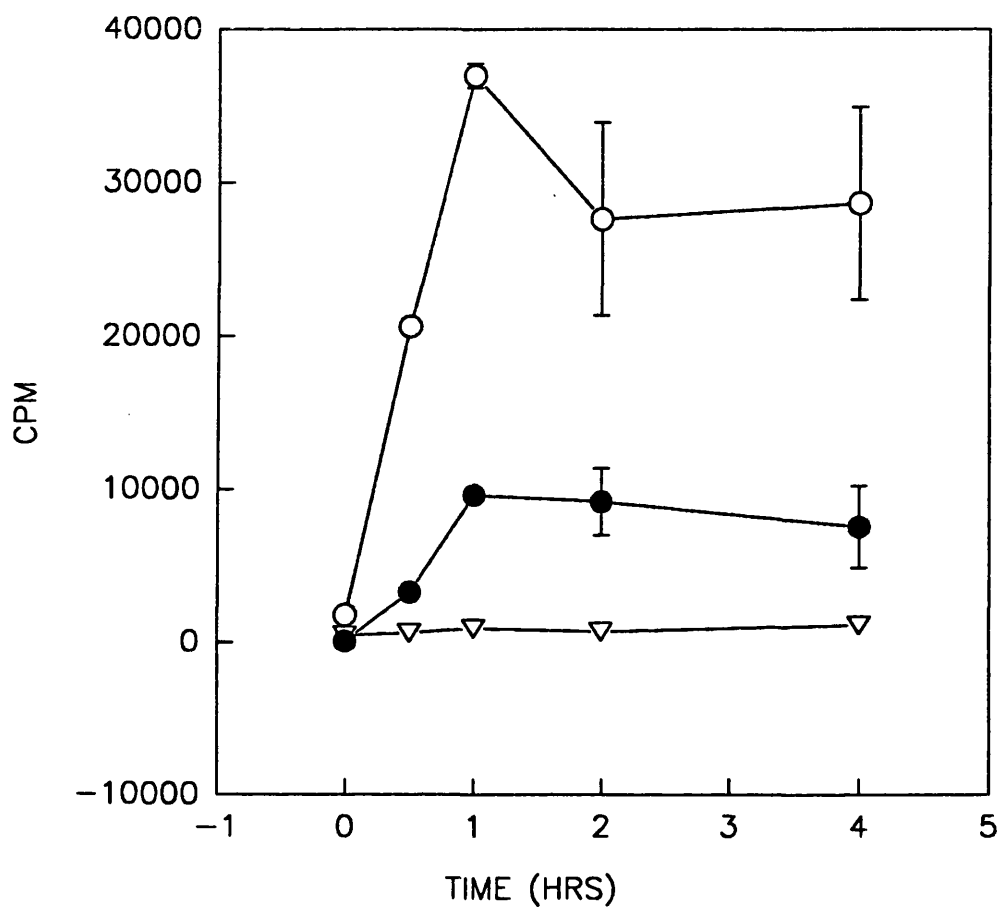
Figure 3.2.5. Total O ; non-specific ∇ ; and acid stripped ● ; ^{125}I-NLDP bound to B16 cells at 37°C vrs time . Bars indicate SD values of 4 sample wells.
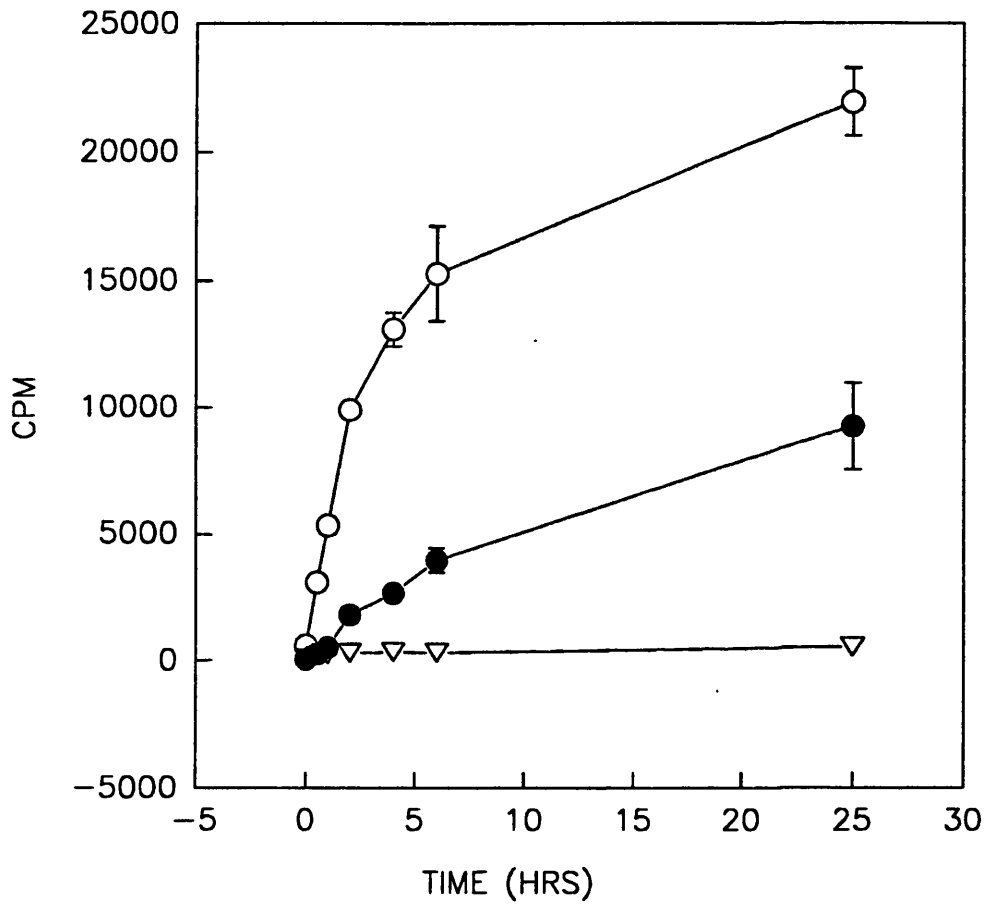
Figure 3.2.6. Total $\bigcirc$; non-specific $\triangledown$; and acid stripped $\bullet$; ^{125}I-NLDP bound to B16 cells at 15°C vrs time. Bars indicate SD values of 4 sample wells.
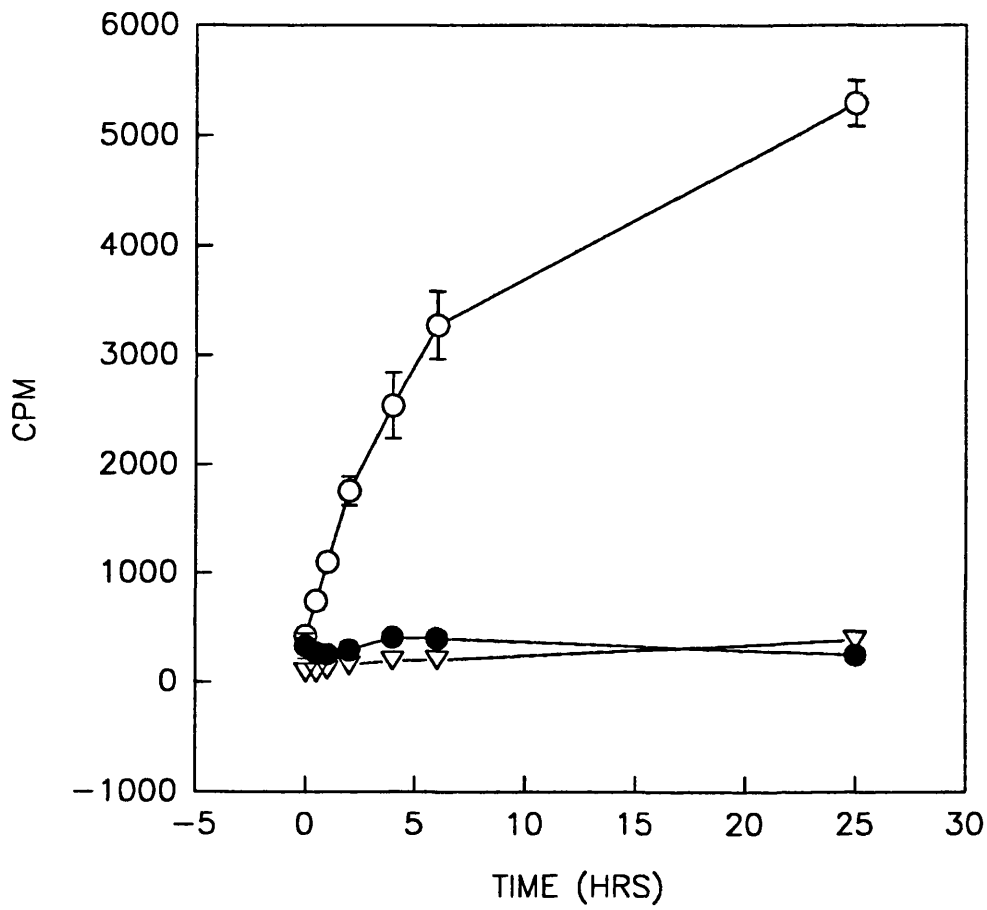
Figure 3.2.7. Total O ; non-specific ● ; and acid stripped ▽ ; ^{125}I-NLDP

bound to B16 cells at 0-4ºC vrs time. Bars indicate SD values of 4 sample wells.
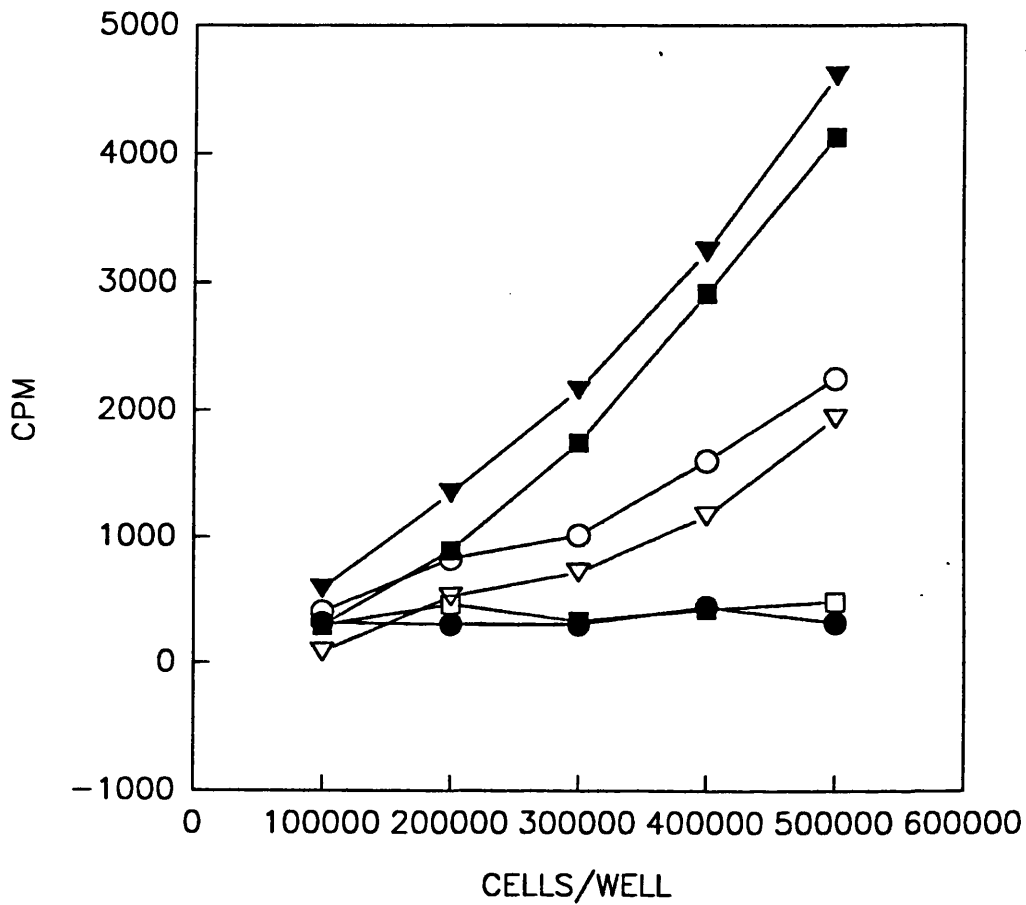
Figure 3.2.8. Binding of ^{125}I-NLDP to B16 cells at 0-4°C vrs cell density. Total $\bigcirc$; non-specific $\square$; specific $\triangledown$ bound after 0.5 hours; and total $\blacktriangledown$; non-specific $\bullet$; and specific $\blacksquare$ bound after 2 hours. Points represent the means of 4 sample wells.
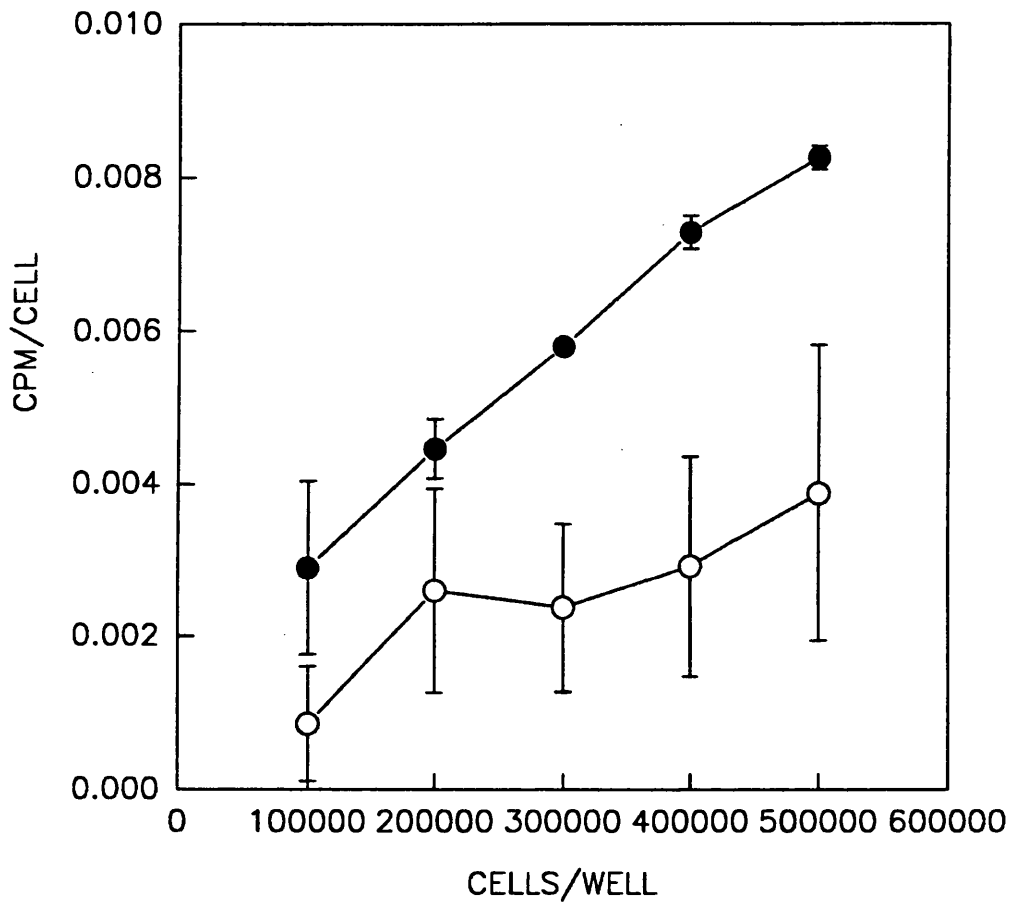
Figure 3.2.9. Binding of ^{125}I-NLDP to B16 cells at 0-4°C after 0.5 O ; and

2 ● hours vrs cell density. Bars indicate SD values of 4 sample wells.
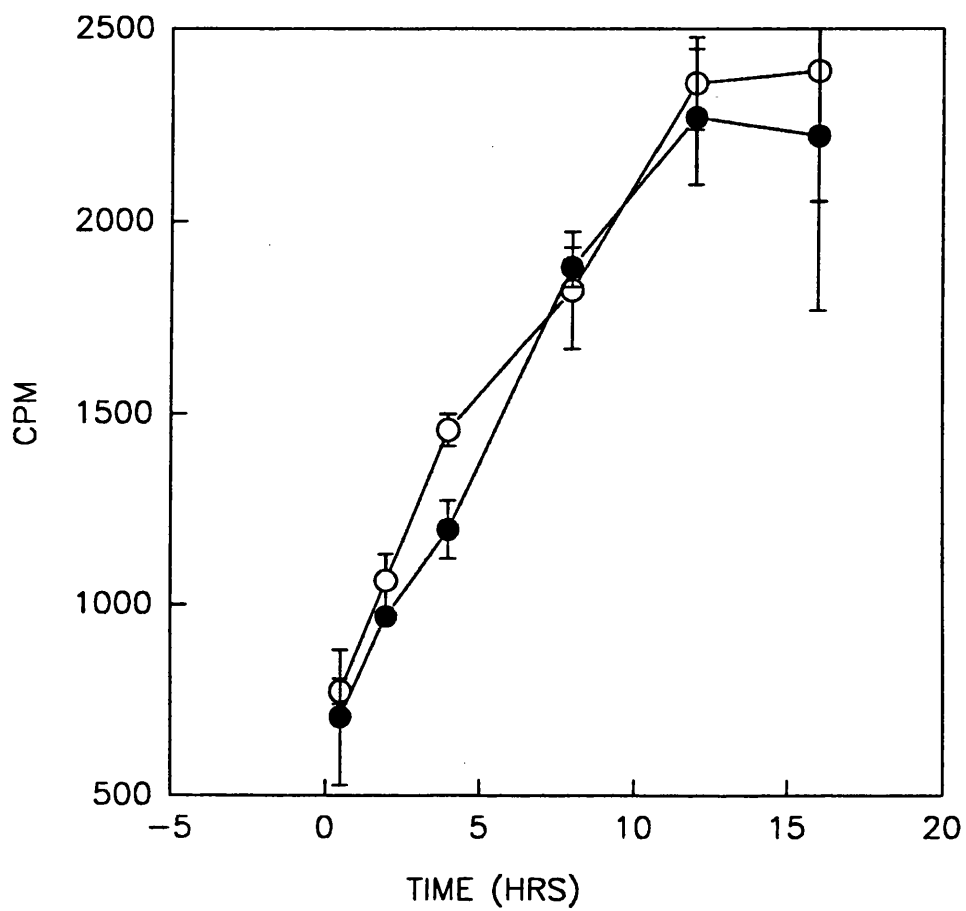
Figure 3.2.10. Binding of ^{125}I-NLDP to B16 cells at 0-4°C in media with O ; and without ● 0.3 mM 1,10-phenanthroline vrs time. Bars indicate SD values of 4 sample wells.
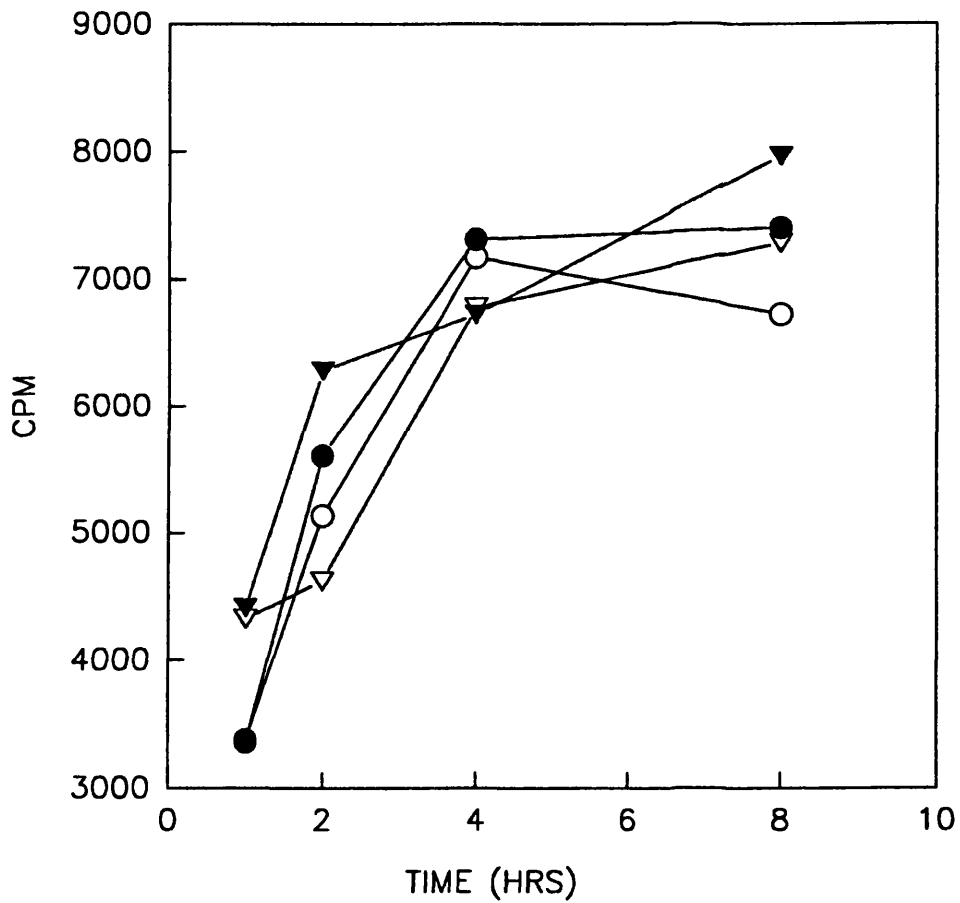
Figure 3.2.11. Binding of ^{125}I-NLDP to B16 cells at 0-4ºC in media with 10^{-5} M O ;

10^{-6} M ● ; 10^{-7} M ▽ ; and no ▼ collagenase inhibitor vrs time. Points represent the means of 4 sample wells.
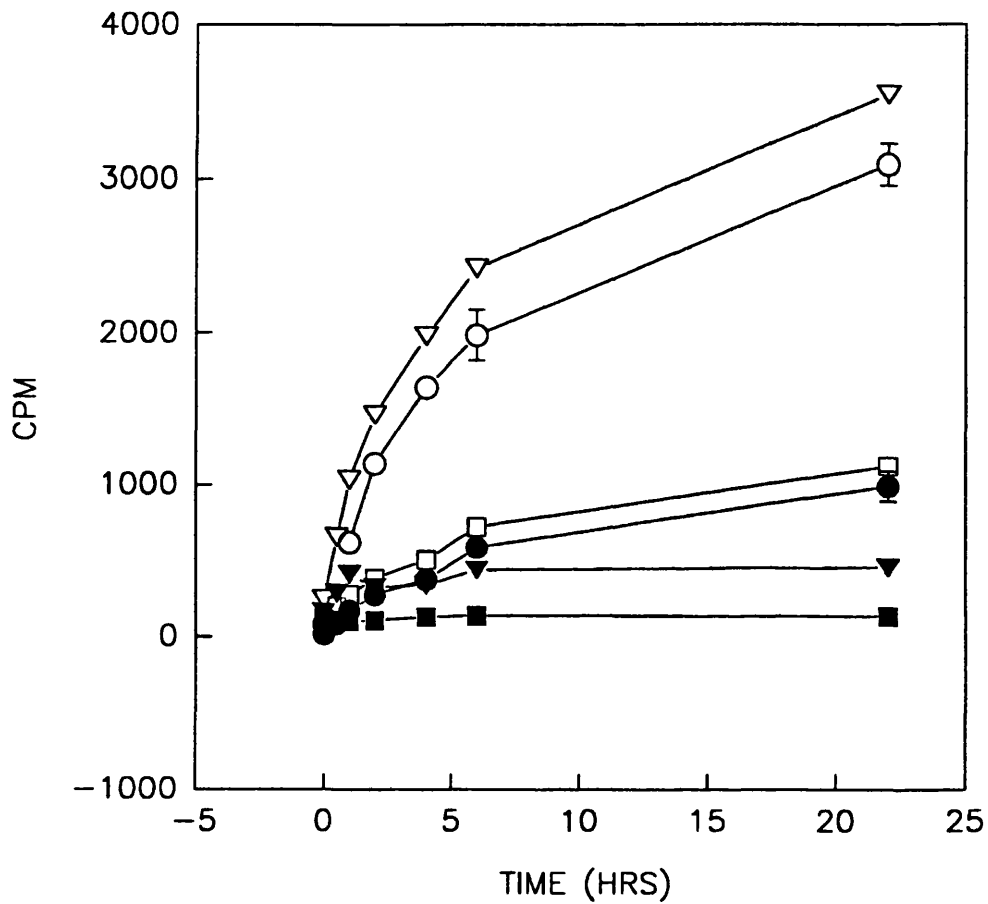
Figure 3.2.12. Binding of ^{125}I-NLDP to B16 cells at 0-4°C with 1.08×10^{-10} M tracer;

total $\triangledown$; non-specific $\blacktriangledown$; specific $\bigcirc$ bound; and 2.7×10^{-11} M tracer; total

$\square$; non-specific $\blacksquare$; and specific $\bullet$ bound vrs time. Bars represent SD values

of 4 sample wells.
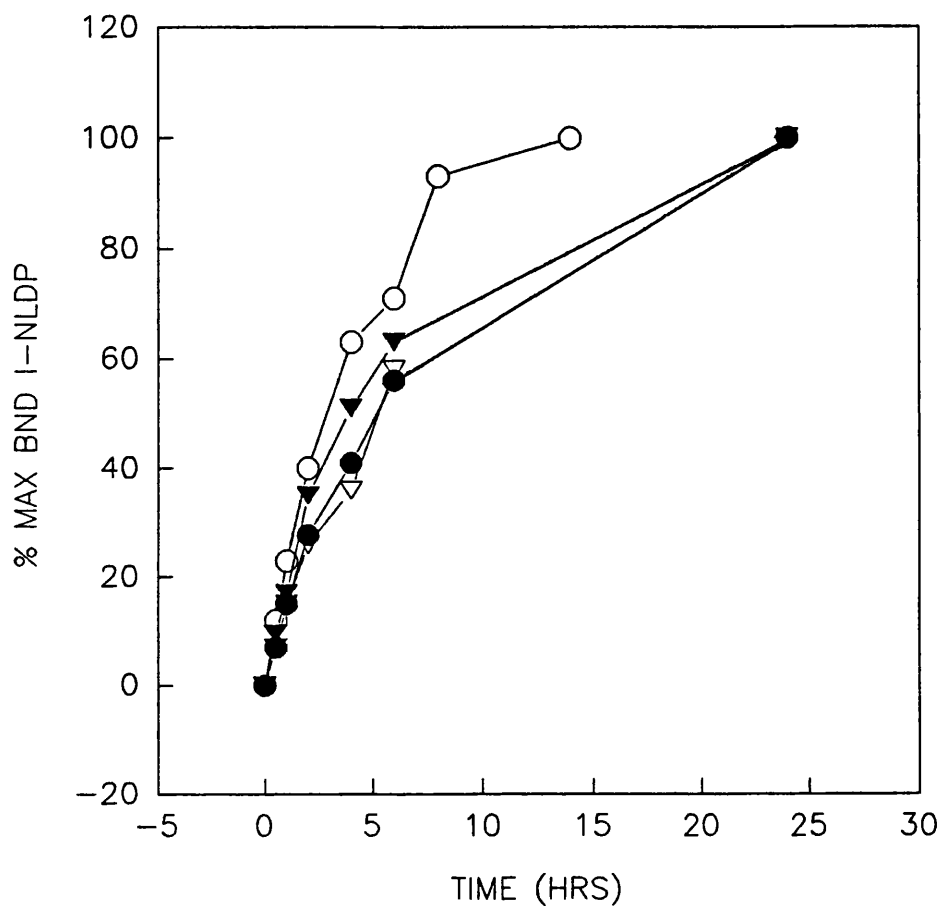
Figure 3.2.13. Percent maximum bound ^{125}I-NLDP to B16 cells at 0-4°C with tracer concentrations of 1.08x10^{-10} M ▼ ; 8.38x10^{-11} M ● ; 5.9x10^{-11} M O ; and 2.7x10^{-11} M ▽ vrs time. Assays using tracer concentrations of 1.08x10^{-10} M and 2.7x10^{-11} M were performed simultaneously (A), while the other assays (B) were performed 3 weeks apart. Points represent the means of 4 sample wells.
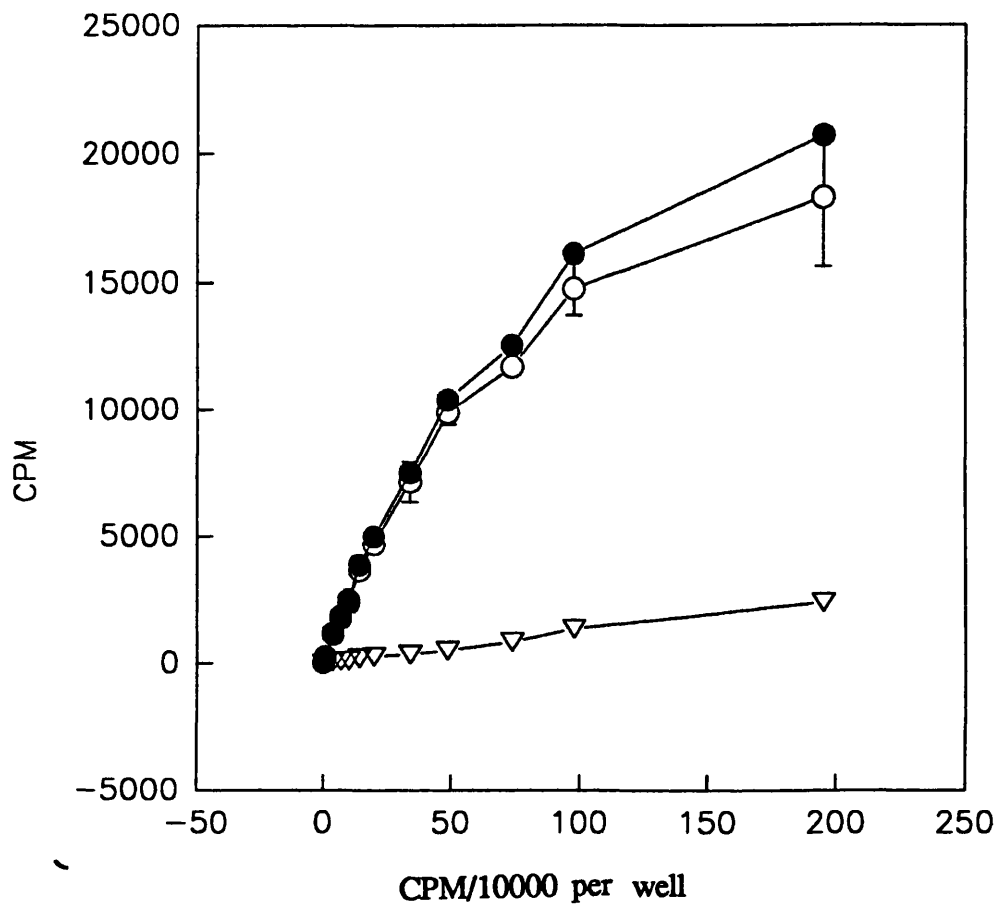
Figure 3.2.14. Saturation binding isotherm of CPM ^{125}I-NLDP bound vrs CPM/10000

added to each well, using B16 cells at 0-4°C for 8 hours. Total ● ; non-specific ▽

; and specific ○ ; binding of ^{125}I-NLDP vrs ^{125}I-NLDP added/well. Bars

indicate SD values of 4 sample wells.
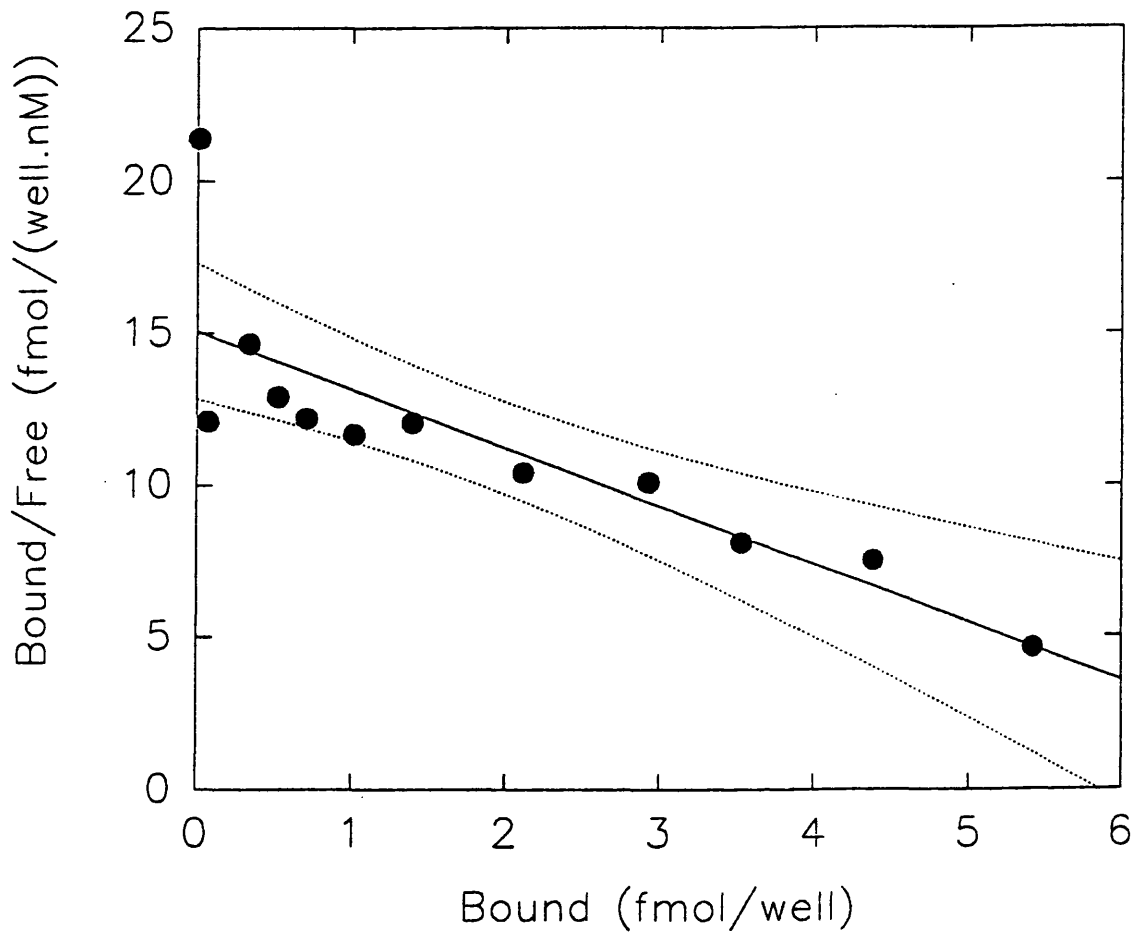
Figure 3.2.15. Scatchard Plot analysis of transformed data from Figure 3.2.14. saturation binding isotherm. Bound ^{125}I-NLDP/free ^{125}I-NLDP vrs bound ^{125}I-NLDP molar/cell. The Ka was estimated at $1.7(\pm0.11)\times10^9$ M^{-1}, the Kd was $5.85(\pm0.38)\times10^{-10}$ M, and n was $10,100(\pm400)$ receptors/cell. Dotted lines show the 95% confidence limits of regression.
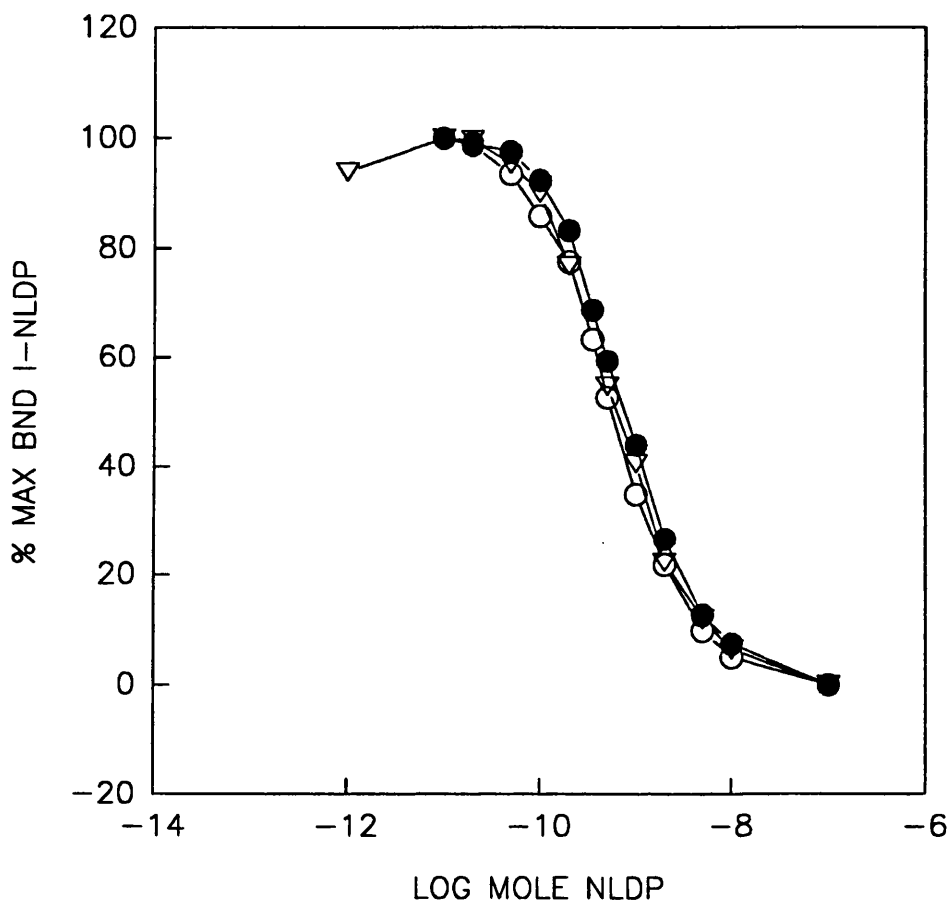
Figure 3.2.16. Competition binding assays of three preparations of NLDP against 1.25x10^{-10} M ^{125}I-NLDP. Percent maximum bound ^{125}I-NLDP vrs unlabelled NLDP. Sigma O ; Bath group ● ; 6 month old Bath group ∇ . Respective Kds are 2.13(±0.057)x10^{-9} M, 2.82(±0.107)x10^{-9} M, and 2.36(±0.113)x10^{-9} M. Points represent the means of 4 sample wells.
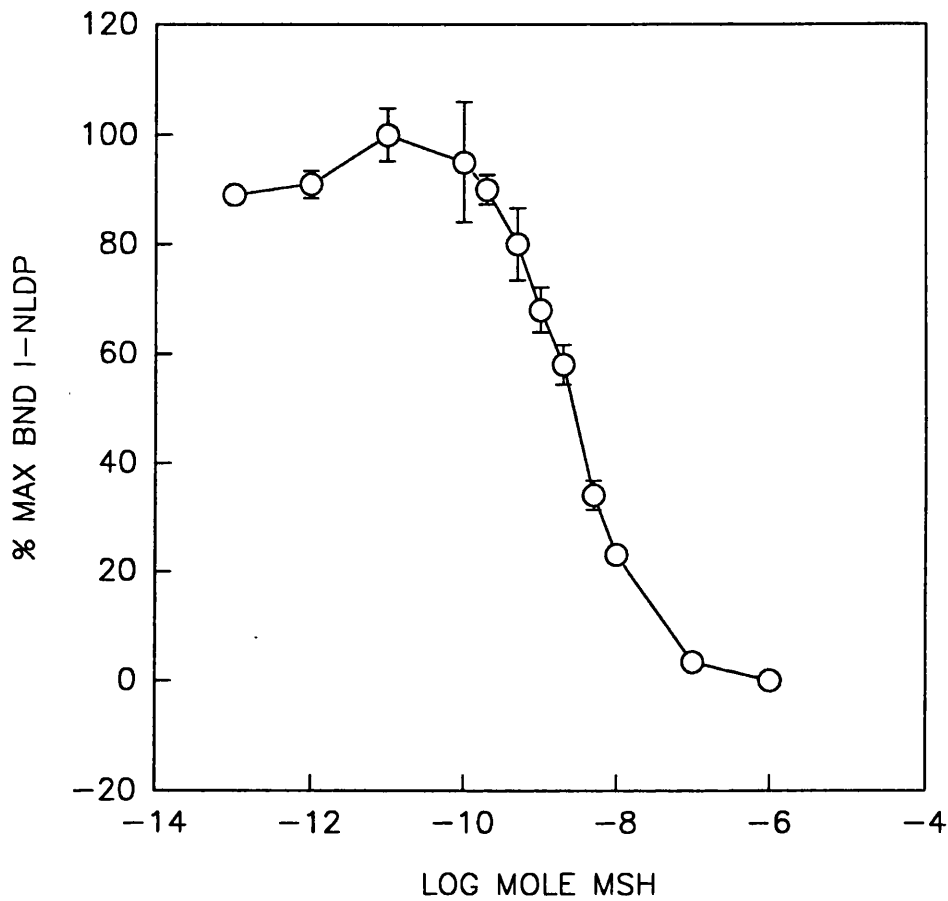
Figure 3.2.17. Competition binding assay of α–MSH against 1.42×10^{-10} M ^{125}I-NLDP. Percent maximum ^{125}I-NLDP bound vrs unlabelled α–MSH. Estimated Kd for α-MSH is $9.82(\pm 0.671) \times 10^{-9}$ M. Bars indicate SD values of 4 sample wells.
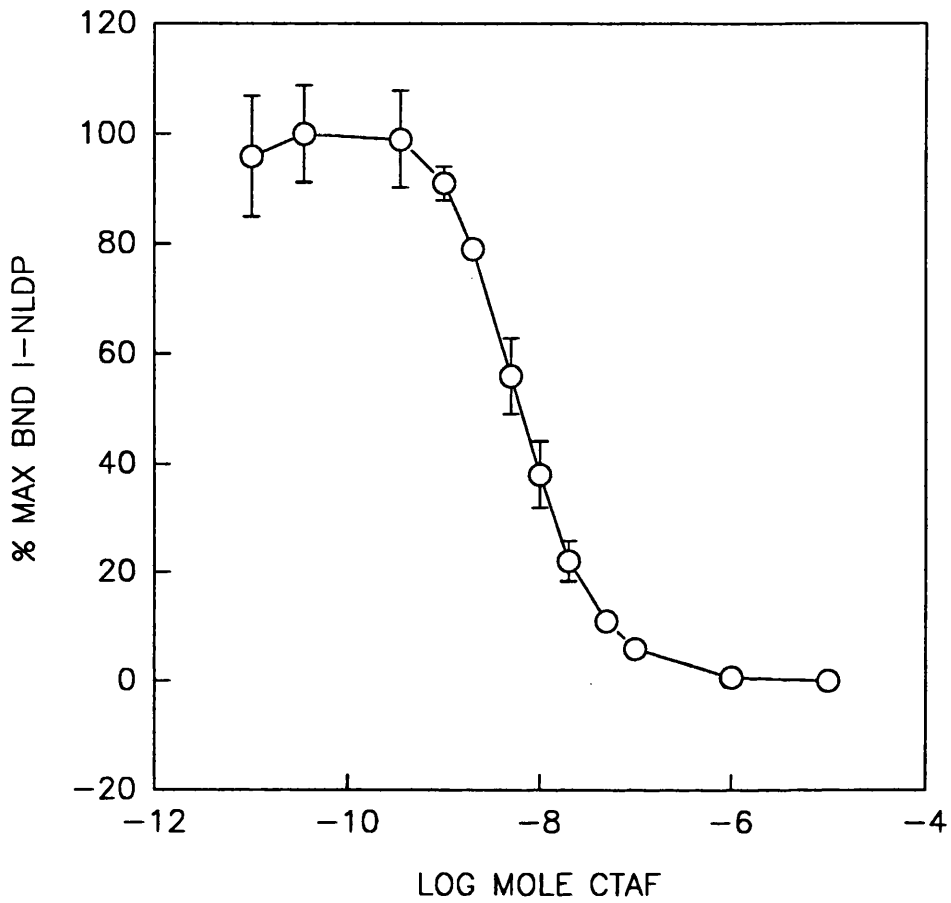
3.2.18. Competition binding assay of CTAF-NLDP against 1.28×10^{-10}M ^{125}I-NLDP. Percent maximum bound ^{125}I-NLDP vrs unlabelled CTAF-NLDP. Estimated Kd for CTAF-NLDP is $2.19(\pm 0.084) \times 10^{-8}$ M. Bars indicate SD values of 4 sample wells.
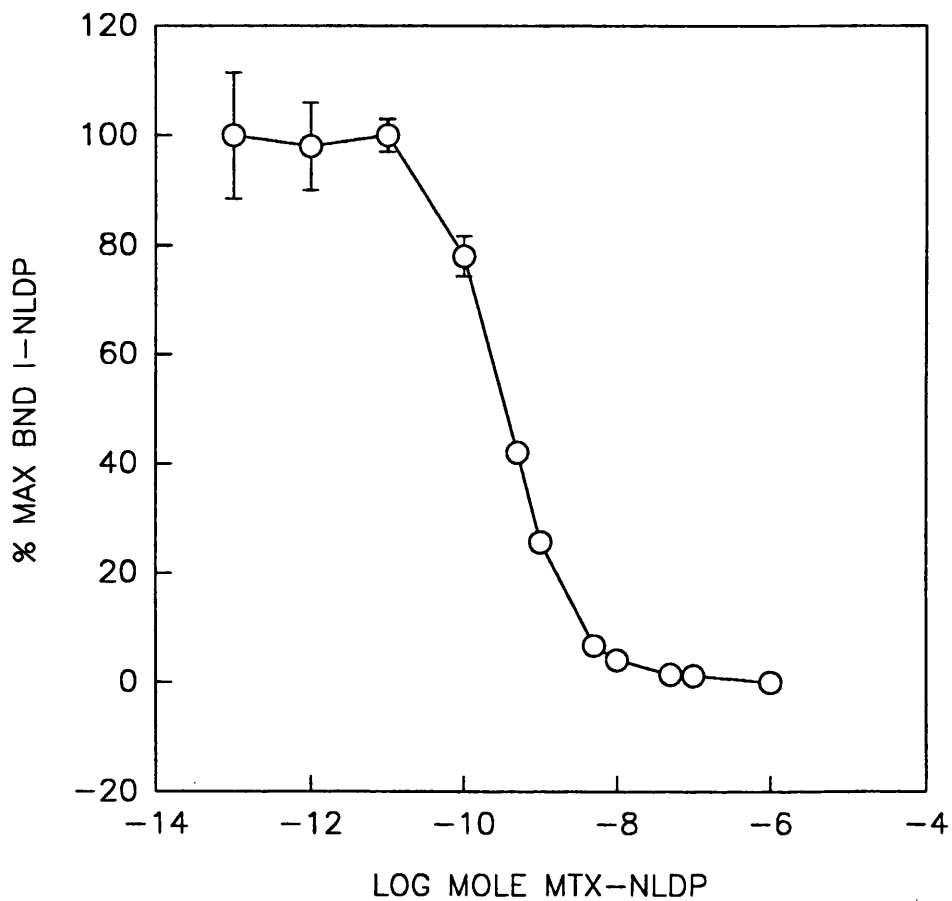
3.2.19. Competition binding assay of MTX-NLDP against 1.26×10^{-10} M ^{125}I-NLDP. Percent maximum bound ^{125}I-NLDP vrs unlabelled MTX-NLDP. Estimated Kd for MTX-NLDP is $1.71(\pm 0.095) \times 10^{-9}$ M. Bars indicate SD values of 4 sample wells.

% MAX BND I–NLDP

120

100

80

60

40

20

0

−20

−14   −12   −10   −8   −6

LOG MOLE BI–NLDP
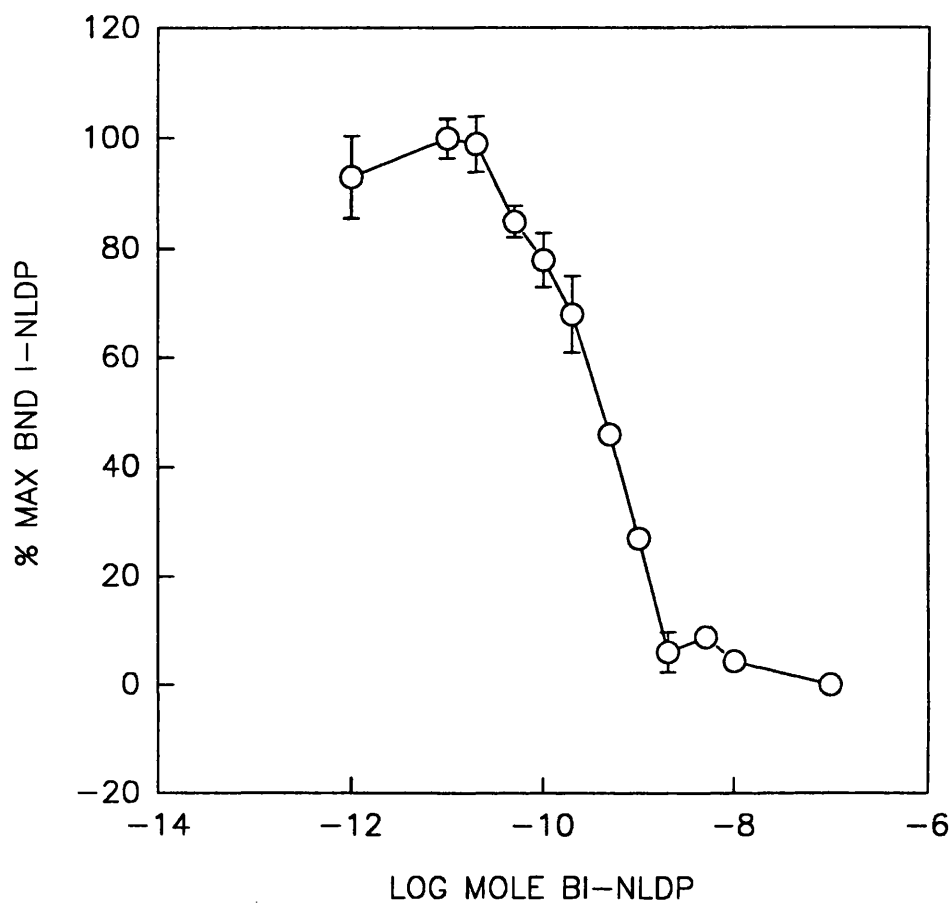
Figure 3.2.20. Competition binding assay of Bi-NLDP against 1.2×10^{-10} M ^{125}I-NLDP. Percent maximum ^{125}I-NLDP bound vrs unlabelled Bi-NLDP. Estimated Kd for Bi-NLDP is $1.12(\pm 0.108) \times 10^{-9}$ M. Bars indicate SD values of 4 sample wells.
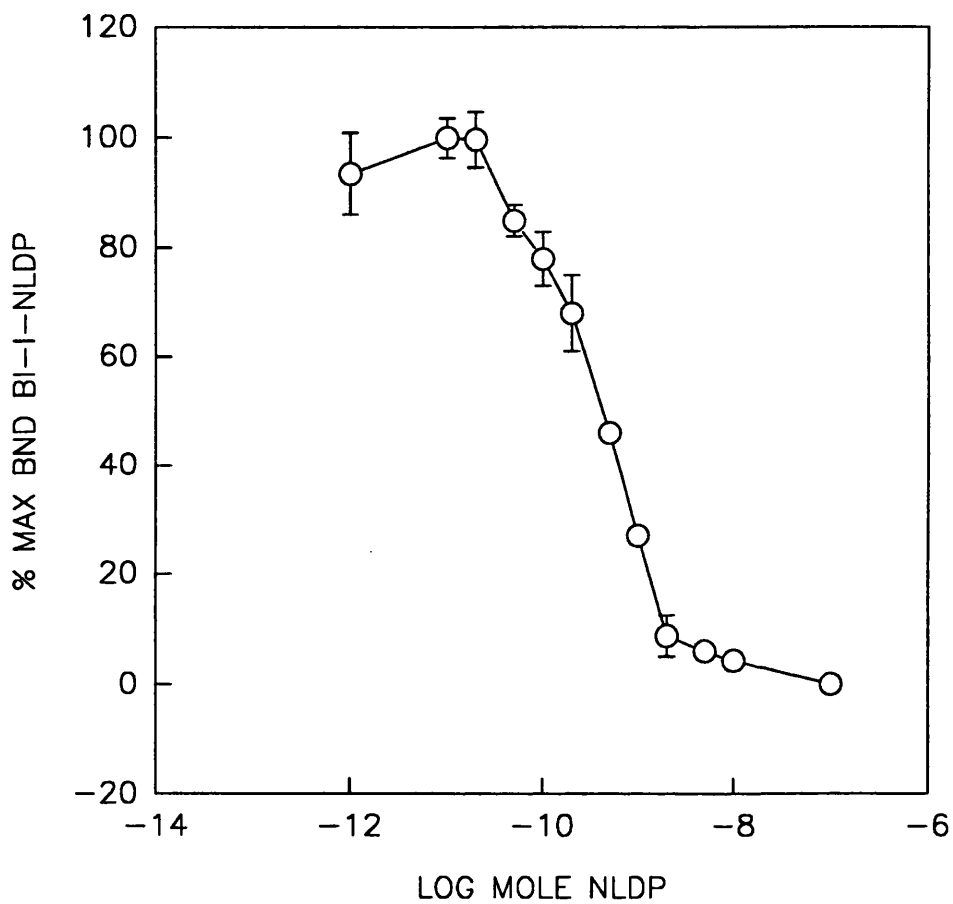
Figure 3.2.21. Competition binding assay of 1.34×10^{-10} M Bi-^{125}I-NLDP against NLDP. Percent maximum bound Bi-^{125}I-NLDP vrs unlabelled NLDP. Estimated Kd for Bi-^{125}I-NLDP is $7.31(\pm 0.707) \times 10^{-10}$ M. Bars indicate SD values of 4 sample wells.
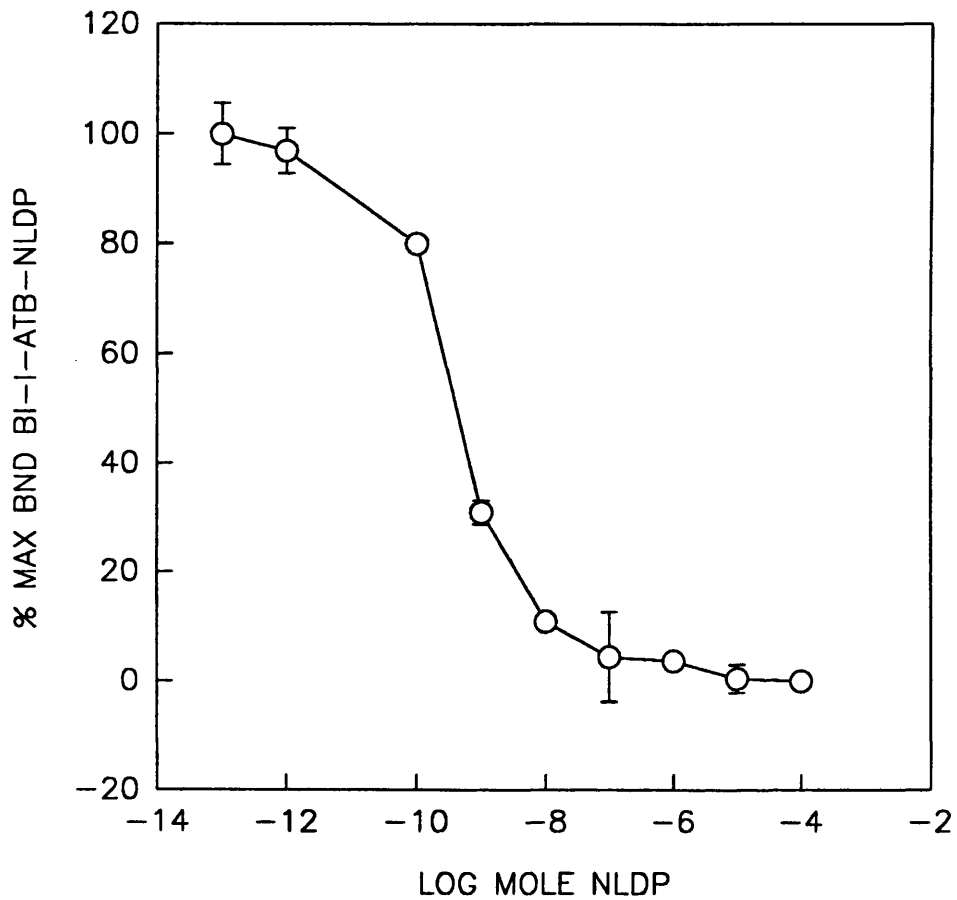
Figure 3.2.22. Competition binding assay of 1.43x10⁻¹⁰ M Bi-¹²⁵I-ATB-NLDP against NLDP. Percent maximum bound Bi-¹²⁵I-ATB-NLDP vrs unlabelled NLDP. Estimated Kd for Bi-¹²⁵I-ATB-NLDP is 6.17(±1.29)x10⁻¹⁰ M. Bars indicate SD values of 4 sample wells.
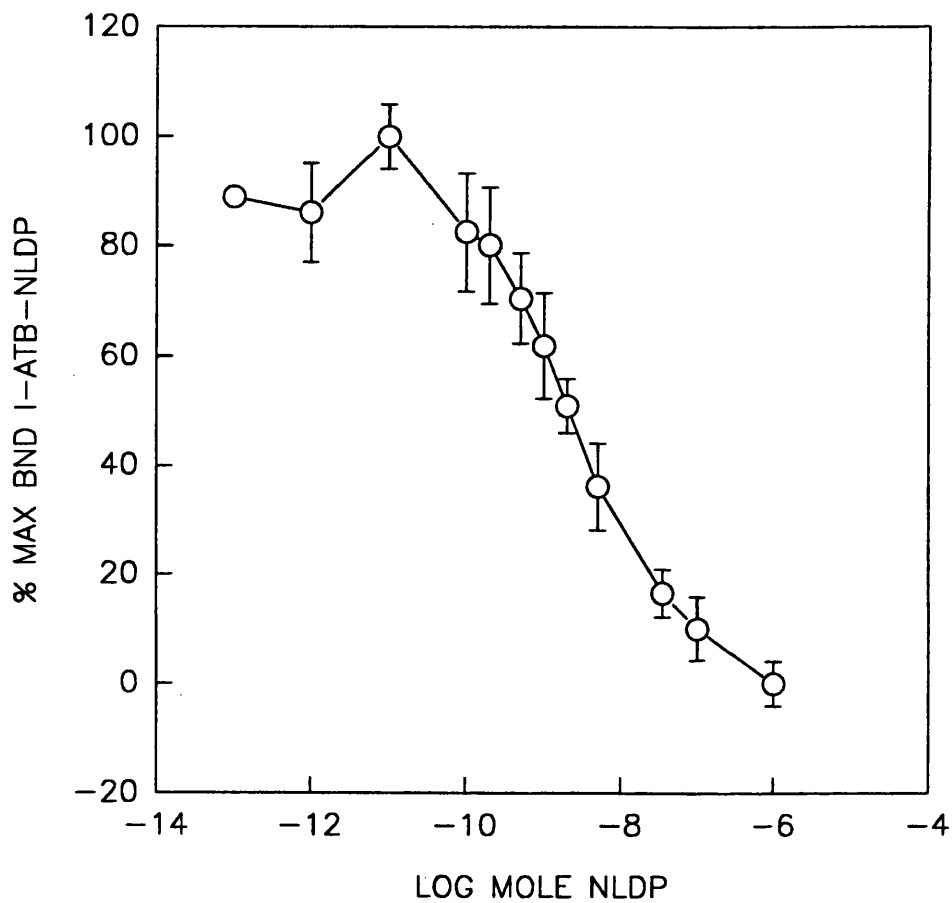
Figure 3.2.23. Competition binding assay of 1.37×10^{-10} M ^{125}I-ATB-NLDP against NLDP. Percent maximum bound ^{125}I-ATB-NLDP vrs unlabelled NLDP. Estimated Kd for ^{125}I-ATB-NLDP is $1.52(\pm 0.298) \times 10^{-10}$ M. Bars indicate SD values of 4 sample wells.
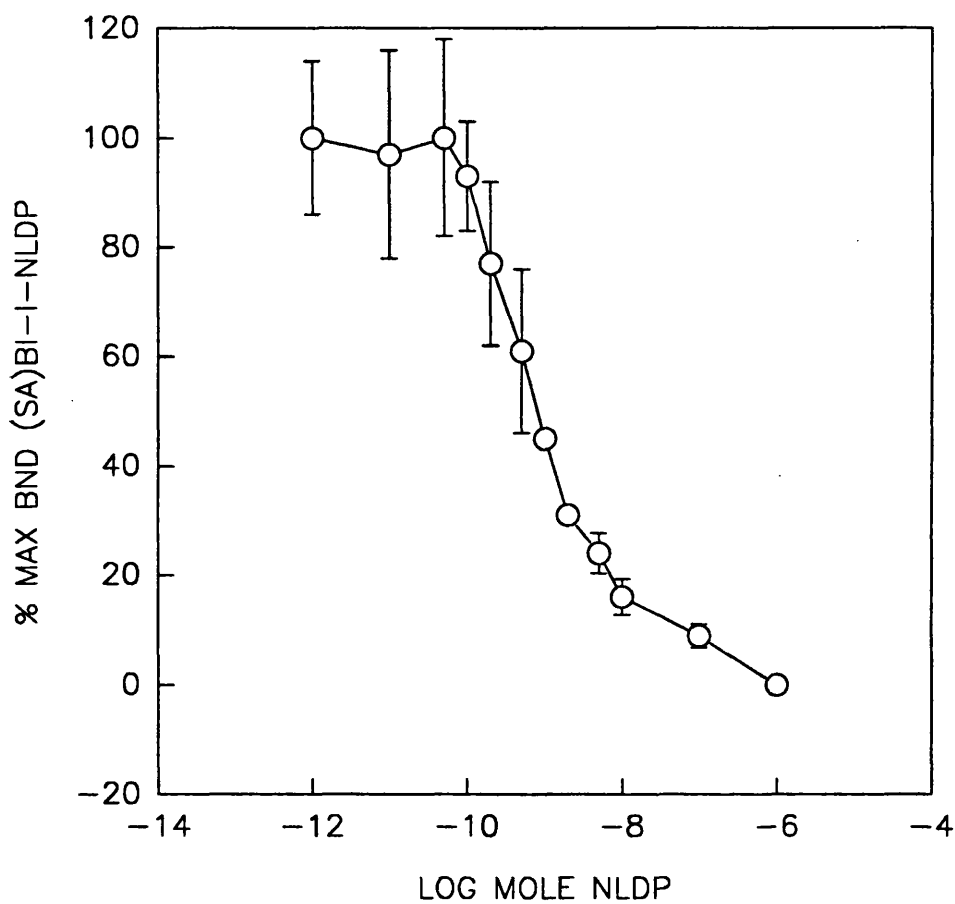
Figure 3.2.24. Competition binding assay of 1.50x10⁻¹⁰ M (Sa)-Bi-125I-NLDP against
NLDP. Percent maximum bound (Sa)-Bi-125I-NLDP vrs unlabelled NLDP. Estimated
Kd for (Sa)-Bi-125I-NLDP is 4.46(.10.660)x10⁻¹⁰ M. Bars indicate SD values of 4
sample wells.
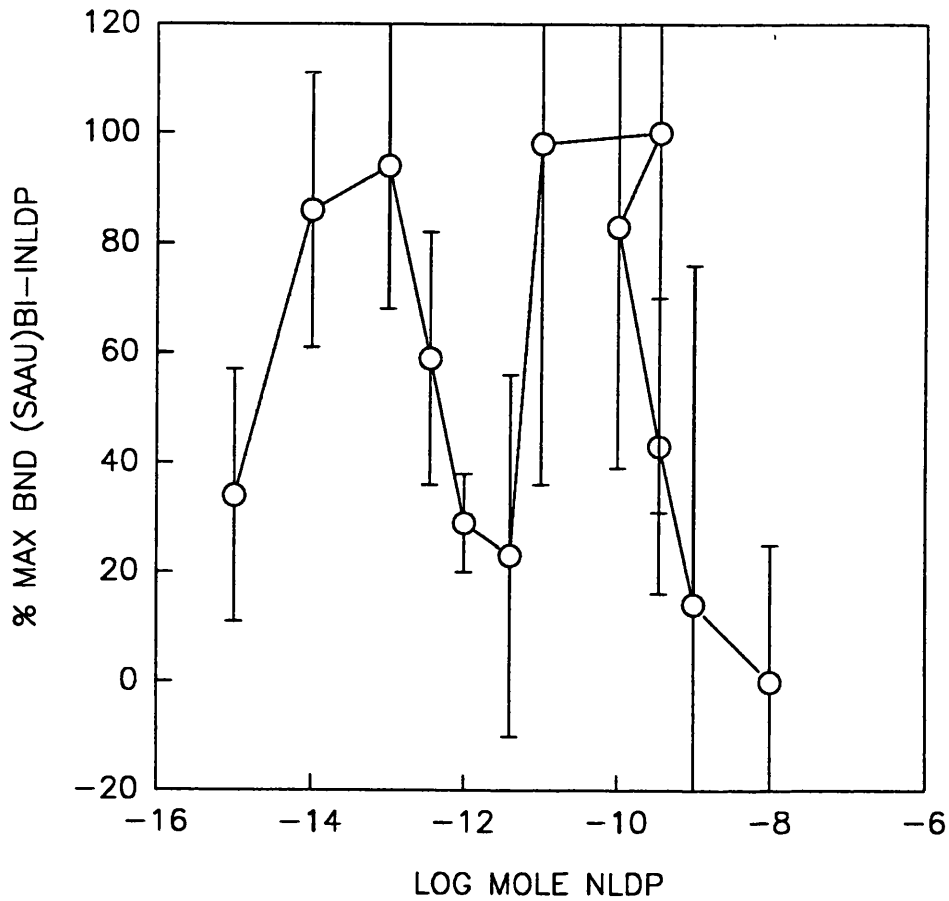
Figure 3.2.25. Competition binding assay of 1.34×10^{-10} M (Sa-Au)-Bi-^{125}I-NLDP against NLDP. Percent maximum bound (Sa-Au)-Bi-^{125}I-NLDP vrs unlabelled NLDP. There is no estimated Kd for (Sa-Au)-Bi-^{125}I-NLDP. Bars indicate SD values of 4 sample wells.

Table 3.2.2. Dissociation constants (Kd) and their standard deviations (SD) for all competition binding assays. Assays 1* are plotted in Figures 3.2.16.-3.2.25. All data are listed in Appendix 2.

α–MSH ANALOGUE	Kd (M)	SD (M)
NLDP 1*	2.13×10^{-9}	5.74×10^{-11}
2	2.82×10^{-9}	1.07×10^{-10}
3	2.36×10^{-9}	1.13×10^{-10}
4	1.19×10^{-9}	1.35×10^{-10}
5	2.12×10^{-9}	8.44×10^{-10}
6	1.63×10^{-9}	3.34×10^{-10}
7	2.61×10^{-9}	4.67×10^{-10}
8	2.52×10^{-9}	1.06×10^{-10}
9	2.71×10^{-9}	2.20×10^{-10}
10	2.16×10^{-9}	1.76×10^{-10}
α–MSH 1*	9.82×10^{-9}	6.72×10^{-10}
2	3.30×10^{-9}	4.04×10^{-10}
3	1.02×10^{-8}	8.17×10^{-10}
4	2.70×10^{-9}	4.15×10^{-10}
CTAF-NLDP 1*	2.19×10^{-8}	8.39×10^{-10}
2	5.83×10^{-8}	1.32×10^{-8}
3	5.92×10^{-8}	2.29×10^{-8}
MTX-NLDP 1*	1.32×10^{-9}	4.85×10^{-11}

2	1.71×10^{-9}	9.53×10^{-11}
3	1.59×10^{-9}	2.84×10^{-10}
BI-NLDP		
1*	1.12×10^{-9}	1.08×10^{-10}
2	4.13×10^{-10}	4.88×10^{-10}
3	5.25×10^{-10}	1.81×10^{-10}
4	3.42×10^{-10}	6.12×10^{-10}
5	3.70×10^{-10}	1.50×10^{-10}
BI-^{125}I-NLDP		
1*	7.31×10^{-10}	7.07×10^{-11}
2	5.19×10^{-10}	5.15×10^{-11}
3	4.26×10^{-10}	6.04×10^{-11}
BI-^{125}I-ATB-NLDP		
1*	6.17×10^{-10}	1.29×10^{-10}
2	4.35×10^{-9}	1.38×10^{-9}
^{125}I-ATB-NLDP		
1*	1.52×10^{-10}	2.99×10^{-11}
2	4.77×10^{-10}	5.24×10^{-11}
3	4.97×10^{-10}	3.07×10^{-10}
(SA)-BI-^{125}I-NLDP		
1*	4.46×10^{-10}	6.61×10^{-11}
2	5.97×10^{-10}	6.28×10^{-11}
3	1.75×10^{-10}	8.10×10^{-11}
(SA-AU)-BI-^{125}I-NLDP 1*	no detectable specific binding	
2	no detectable specific binding	

Table 3.2.3. The mean of the Kds, the standard deviations of the mean, the number of replicate assays, and the relative affinity to α-MSH, are listed for each analogue. The Kd of ^{125}I-NLDP* was determined with binding isotherms (Table 3.2.1.).

α-MSH ANALOGUE	MEAN Kd (M)	SD of MEAN Kd (M)	RELATIVE AFFINITY to α-MSH	NUMBER of REPLICATE ASSAYS
NLDP	2.25×10^{-9}	5.05×10^{-10}	2.92	10
α-MSH	6.46×10^{-9}	4.00×10^{-9}	1.0	4
CTAF-NLDP	4.64×10^{-8}	2.12×10^{-8}	0.139	3
MTX-NLDP	1.54×10^{-9}	2.01×10^{-10}	4.19	3
BI-NLDP	3.53×10^{-10}	1.51×10^{-10}	18.3	5
^{125}I-NLDP*	4.70×10^{-10}	7.60×10^{-11}	13.6	5
BI-^{125}I-NLDP	5.59×10^{-10}	1.57×10^{-10}	11.6	3
BI-^{125}I-ATB-NLDP	5.50×10^{-10}	9.41×10^{-11}	11.7	2
^{125}I-ATB-NLDP	3.76×10^{-10}	1.94×10^{-10}	17.2	3

(SA)-BI-^{125}I-NLDP	4.06×10^{-10}	2.14×10^{-10}	15.9	3
(SA-AU)-BI-^{125}I-NLDP	no detectable specific binding			2

3.3. TYROSINASE ASSAYS PERFORMED ON B16 CELLS TREATED WITH α-MSH ANALOGUES

3.3.1. INTRODUCTION

Melanoma and melanocytes produce a copper-containing enzyme, tyrosinase. It is essential in the biosynthesis of melanin pigment. MSH induced melanogenesis occurs with an increase in tyrosinase activity (100). Pomerantz (144) developed an assay which measured the extent of biological stimulation of pigment cells by hydroxylation of [3',5'-^{3}H]-L-tyrosine to ^{3}H$_2$O (144). During this study a modified version of this assay (52) was used to evaluate the biological potency of α–MSH analogues.

3.3.2. TYROSINASE ASSAY DEVELOPMENT

3.3.2.1. EFFECTS OF B16 CELL DENSITY AND INCUBATION TIMES ON TYROSINASE ACTIVITY

The number of B16 mouse melanoma cells/well and incubation times were varied to determine the best conditions for tyrosinase stimulation by α–MSH derivatives. Figure 3.3.1. shows the dose-response curves obtained using 24 wells seeded with 10^5 or 5×10^5 cells/well, and incubated for 1 day in a NLDP dilution series. Wells were also seeded with 5×10^4, 7.5×10^4, and 3.5×10^5 cells using a one day incubation time but these conditions did not result in comprehensive dose-response curves (data not shown). The tyrosinase assay was a better measurement of B16 cell stimulation at higher cell densities. These assays also displayed less variation (SD) between sample wells. 5×10^5 cells/well were more responsive to the agonist (Ec50 value of 3.5×10^{-12} M) with less standard deviation than wells seeded with 10^5 cells/well (Ec50 value of 3.5×10^{-11} M). But, the lower cell density (10^5 cells/well) was deemed more suitable since the change in specific response (maximum agonist stimulated ^3H_2O production) was three times greater (3×10^5 cpm versus 10^5 cpms) than those wells seeded at a higher cell density (5×10^5 cells/well).

In follow-up experiments, B16 cells were seeded with 10^5, 2.5×10^4, and 5×10^4 cells/well. The cells were incubated in a NLDP dilution series for 20, 27, and 43 hours. The best results were obtained at 27 hours with 10^5 cells/well. This was determined by the relatively large change in agonist-specific specific response obtained at 27 hours when compared to data collected at 20 and 43 hours (Figure 3.3.2., data for 20 and 43 hours not shown).

The assay was then conducted on cells seeded at a lower cell density for longer incubations. Cells seeded at 10^5 cells/well were incubated for 27 hours, while cells seeded at 3×10^4 cells/well were incubated for 2 and 3 days (Figure 3.3.3.). The largest response was obtained with a two day incubation of 3×10^4 cells/well, although the specific change was minimal. The standard deviations of ^3H_2O production of all three protocols were similar (data not shown). The largest differences in the NLDP-specific

response was obtained at 48 hours. Further tyrosinase assays were performed using a two day incubation of the agonist on 3×10^4 cells/well.

3.3.2.2. PROCEDURE FOR THE EXTRACTION OF UNREACTED [3',5'-^{3}H]-L-TYROSINE FROM THE ASSAY MEDIUM

The technique used during the charcoal extraction of unreacted [3',5'-^{3}H]-L-tyrosine from the cell supernatant was examined in an effort to reduce the intrasample variation. Supernatant was taken from wells following a 2 day tyrosinase assay of 3×10^4 cells/well, containing 1 ml of 10^{-9} M NLDP. It was then added to eppendorf tubes containing 0.4 mls of ice cold 10% charcoal in PBS. The tubes were agitated on a vortex mixer and subjected to one of the following treatments :

1) manually shaken for 15 minutes at room temperature.

2) manually shaken for 15 minutes at room temperature and mechanically shaken for 15 minutes at 4°C.

3) mechanically shaken for 30 minutes at 4°C.

4) and mechanically shaken for 1 hour at 4°C.

The smallest intrasample variation was observed at 4°C using protocol 3 (see Table 3.3.1. for standard deviations). In subsequent tyrosinase assays the conditioned supernatant and charcoal were mechanically shaken for 30 minutes at 4°C.

Table 3.3.1. The tyrosinase activity and its standard deviations as measured by supernatant ^3H_2O following the four charcoal separation techniques (Section 3.3.2.2.).

TREATMENT	DPM SUPERNATANT AFTER CHARCOAL	SD
1	86200	21700
2	71500	15000
3	81500	4970
4	78300	13900

3.3.3. TYROSINASE ACTIVITY OF B16 CELLS TREATED WITH α-MSH ANALOGUES

Estimates of half maximal tyrosinase stimulation (Ec50) of the melanoma cells by the peptides were obtained using INSTAT linear regression analysis (Section 2.6.4.) with Equation 2.6.4. :

Ec50 = antilog [dpm min + (1/2 x dpm specific - C)/M].

Alpha-MSH and its derivatives were tested over a two year period, using 34 different passages of B16 mouse melanoma cells. Figures 3.3.4.-3.3.8. show examples of a dose/response curve for each α-MSII analogue tested. Data for all assays are listed in Appendix 2. Table 3.3.2. lists the estimate of the curve slope (M), its standard error, the y-axis intercept (C), its standard error, and the derived Ec50 for each assay. Table 3.3.3. lists the mean Ec50 for each analogue, its standard deviation, its relative potency to α-MSH, its efficacy (Kd/Ec50), and the number of replicate assays. The standard deviations of the mean for the analogues were low considering they were performed with 34 different passages over a 2 year period.

Most dose/response curves displayed plateaus at non-specific and maximum tyrosinase activity. The plateaus were usually separated by a 2-3 log concentration span of the experimental peptide. There was often a drop in activity at ligand concentrations higher than those eliciting the maximal hormonal response. Occasionally, the straight line portion of the curve would be followed by a rise and fall in tyrosinase stimulation after non-specific activity (^3H_2O produced in the absence of added agonist) had been established (Figure 3.3.4.). These effects were not observed consistently throughout replicate assays.

The exchange of methionine for norleucine at position 4, and of D-phenylalanine for its L isomer at position 7 (NLDP) caused an 8 fold rise (<0.01 significance) in the biological stimulation of B16 cells by the agonist (Table 3.3.3.). Binding of the CTAF molecule to NLDP caused a 94 fold drop (<0.01) in tyrosinase activity. The addition of a methotrexate molecule to the N-terminus of NLDP had relatively little effect (0.668 significance) on the B16 cellular response. Conversely, biotinylation of NLDP caused a 3.4 fold drop (<0.01 significance) in biological stimulation of the cells by the ligand.

The hazards of gamma-radiation did not allow iodinated α–MSH derivatives to be lyophilised and weighed. Tracer concentration were determined by cpm after HPLC purification (Section 2.5.5.). Each tyrosinase assay required approximately 1.69×10^8 cpms of purified tracer. The yield of radio-ligand after iodination (usually 2×10^8) was not sufficient for routine tyrosinase assays in triplicate. After purification the concentration of iodinated ligand in the HPLC buffer was too dilute for concentrations above 10^{-9} M. During HPLC purification, the tracer was eluted with 49.5-50% methanol in 1% TFA HPLC buffer. The TFA and methanol in the HPLC buffer would cause cell death at tracer concentrations necessary for tyrosinase assays (10^{-13}-10^{-7} M). Hence, the α–MSH radio-tracers were not tested for biological activity with tyrosinase assays. Photoaffinity compounds were not tested for tyrosinase stimulation

due to their photo-reactive nature. The light sensitivity of the ATB compound would have caused technical difficulties during freeze-drying and experimental manipulations of the photoaffinity probes.
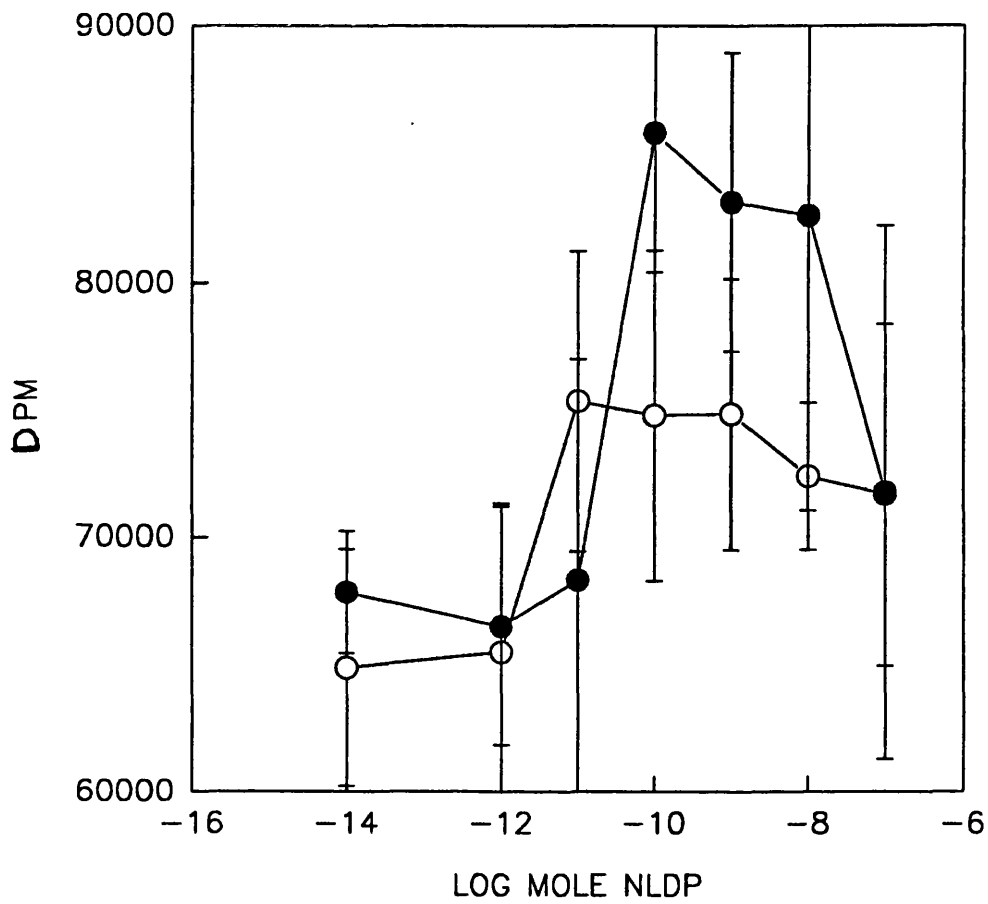
Figure 3.3.1. Tyrosinase activity assay of 10^5 ● ; and 5×10^5 ○ B16 cells/well in a NLDP dilution series for 24 hours. ^3H_2O production vrs NLDP. Bars indicate SD values of 4 sample wells.
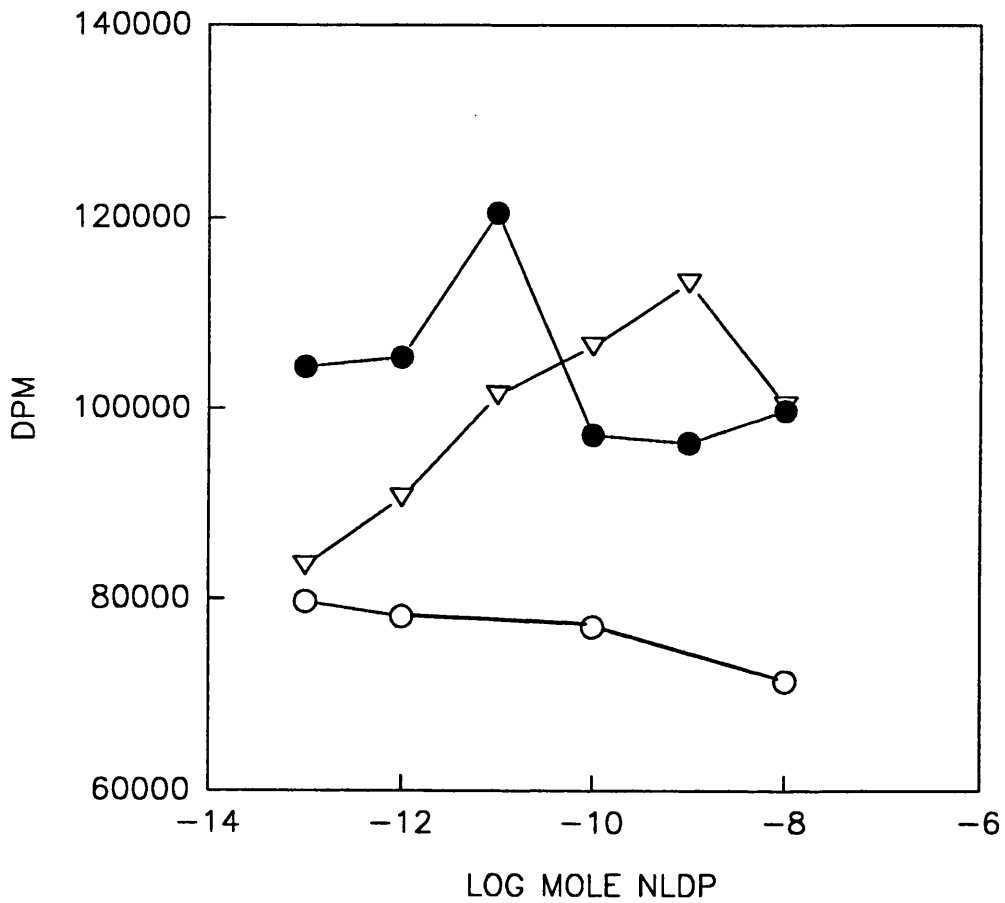
Figure 3.3.2. Tyrosinase activity assay of 10^5 ▽ ; 2.5×10^5 ● ; and 5×10^5 ○

B16 cells/well for 27 hours. ^3H_2O production vrs NLDP. Points represent the means of 4 sample wells.

250000

200000

DPM

150000

100000

50000

−18   −16   −14   −12   −10   −8   −6

LOG MOLE NLDP
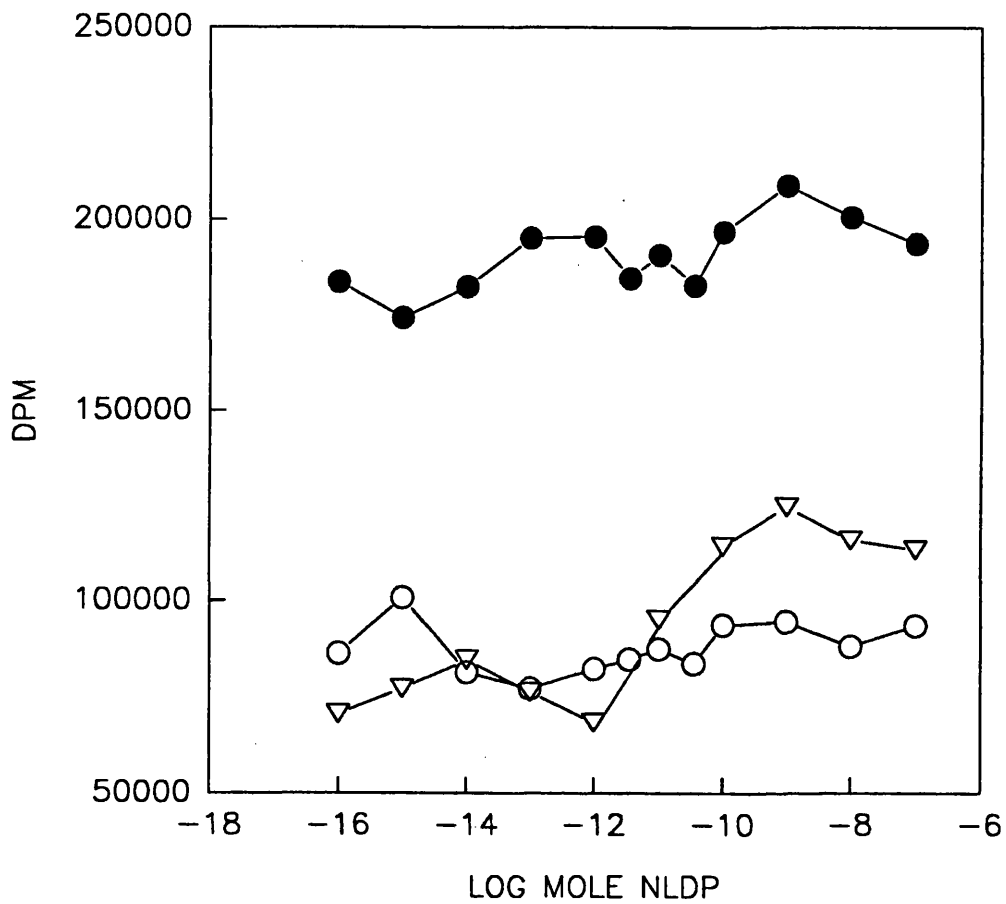
Figure 3.3.3. Tyrosinase activity assay of 10^5 B16 cells/well for 27 hours ◯ ; 3×10^4 B16 cells/well for 48 hours ▽ ; and 3×10^4 B16 cells/well for 72 hours ● ; in NLDP. ^3H_2O production vrs NLDP. Points represent the means of 4 sample wells.
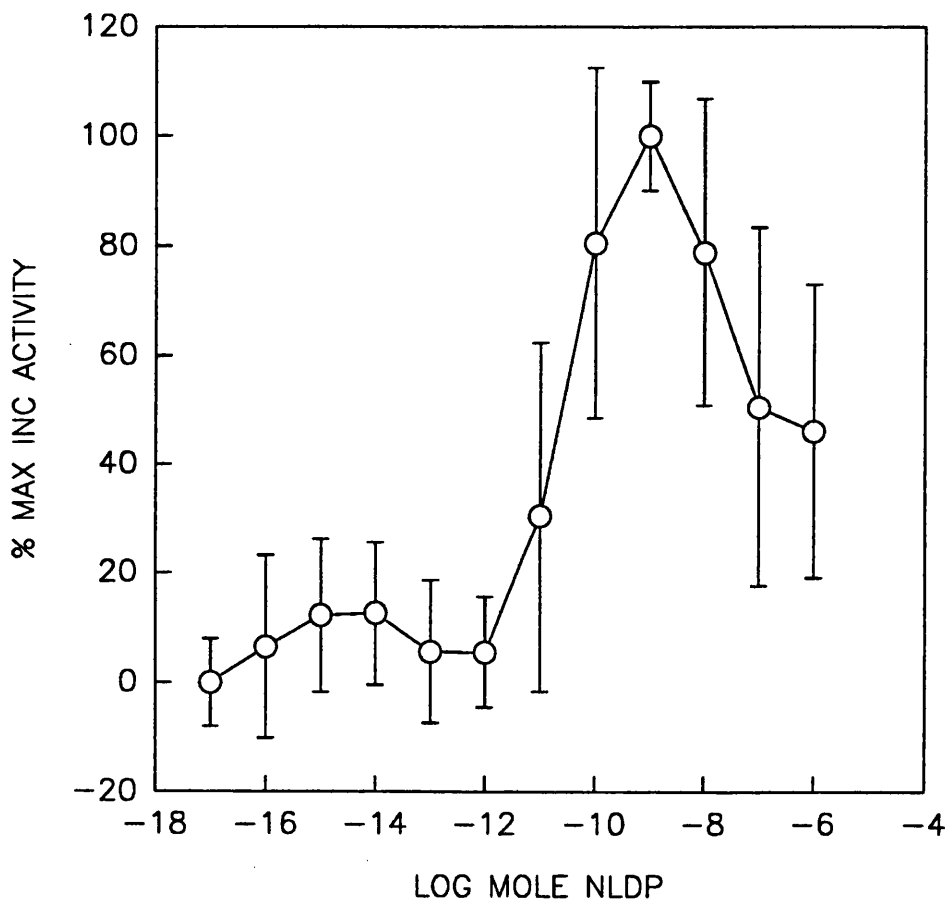
Figure 3.3.4. Tyrosinase activity of cells incubated in NLDP. Percent maximum increase in ^3H_2O production vrs NLDP. Estimated Ec50 for NLDP is 2.64×10^{-11} M. Bars indicate SD values of 4 sample wells.
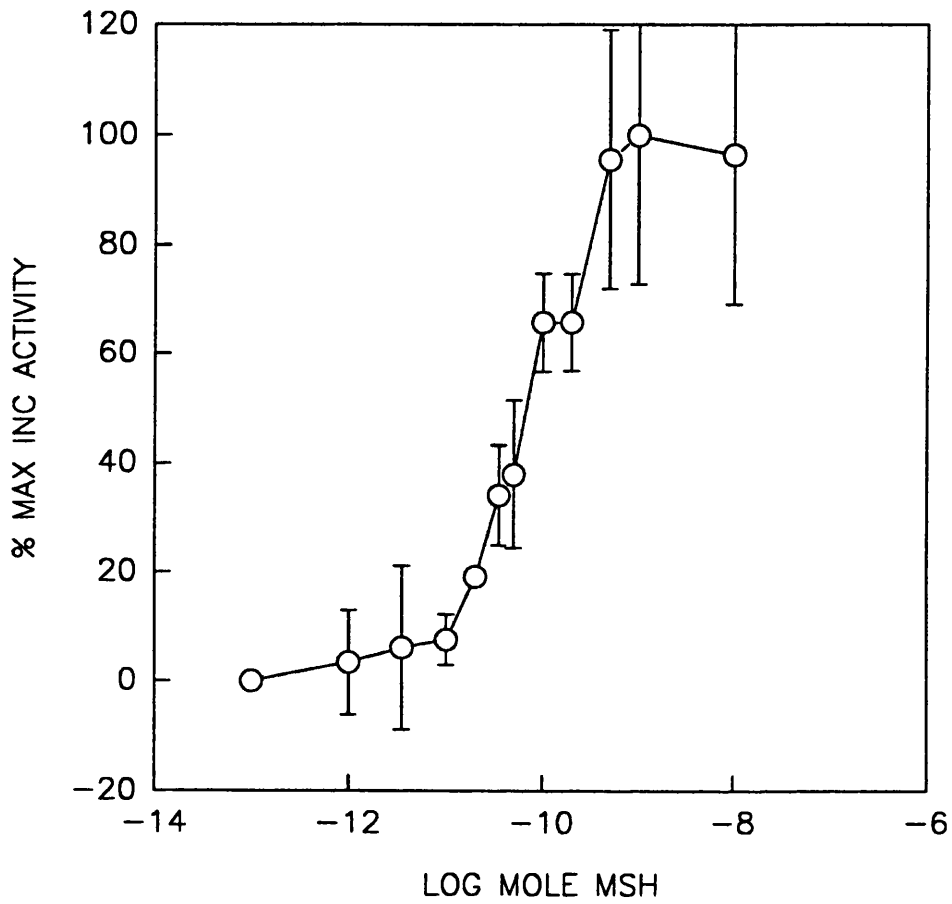
Figure 3.3.5. Tyrosinase activity of cells incubated in α–MSH. Percent maximum increase in ^3H_2O production vrs α- MSH. Estimated Ec50 for α-MSH is 4.25x10^{-10} M. Bars indicate SD values of 4 sample wells.
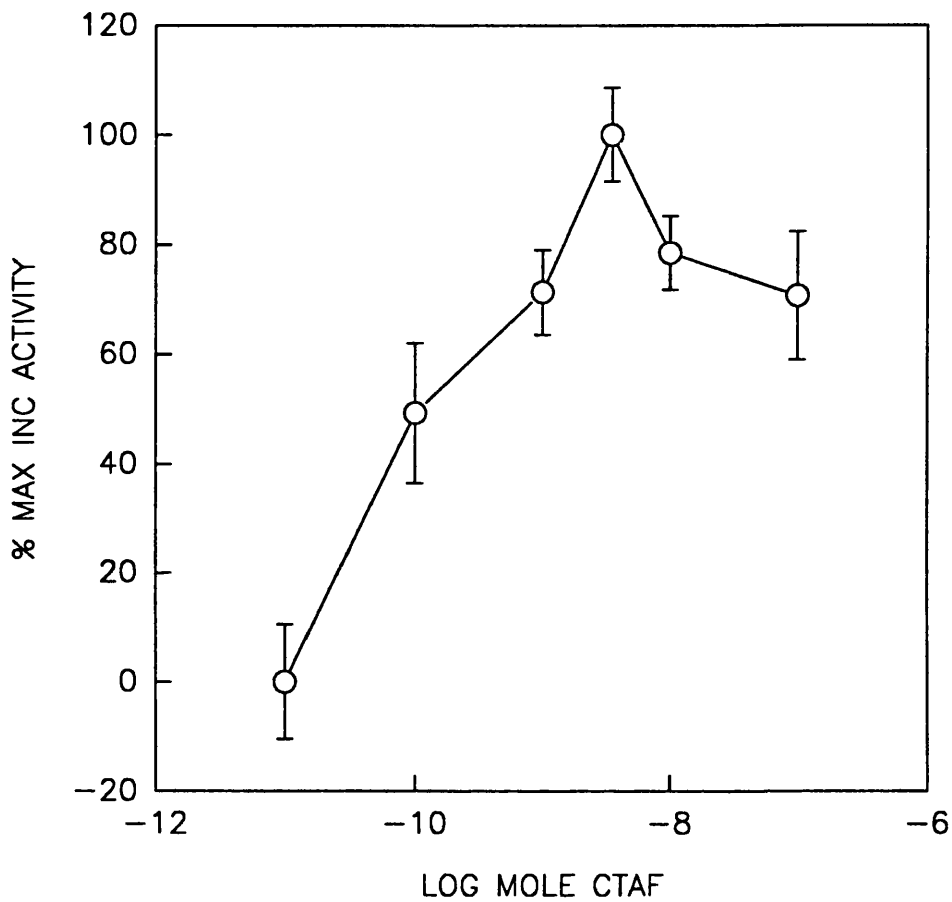
Figure 3.3.6. Tyrosinase activity of cells incubated in CTAF-NLDP. Percent maximum

increase in ^3H_2O production vrs CTAF-NLDP. Estimated Ec50 for CTAF-NLDP is

1.76x10^{-10}. Bars indicate SD values of 4 sample wells.
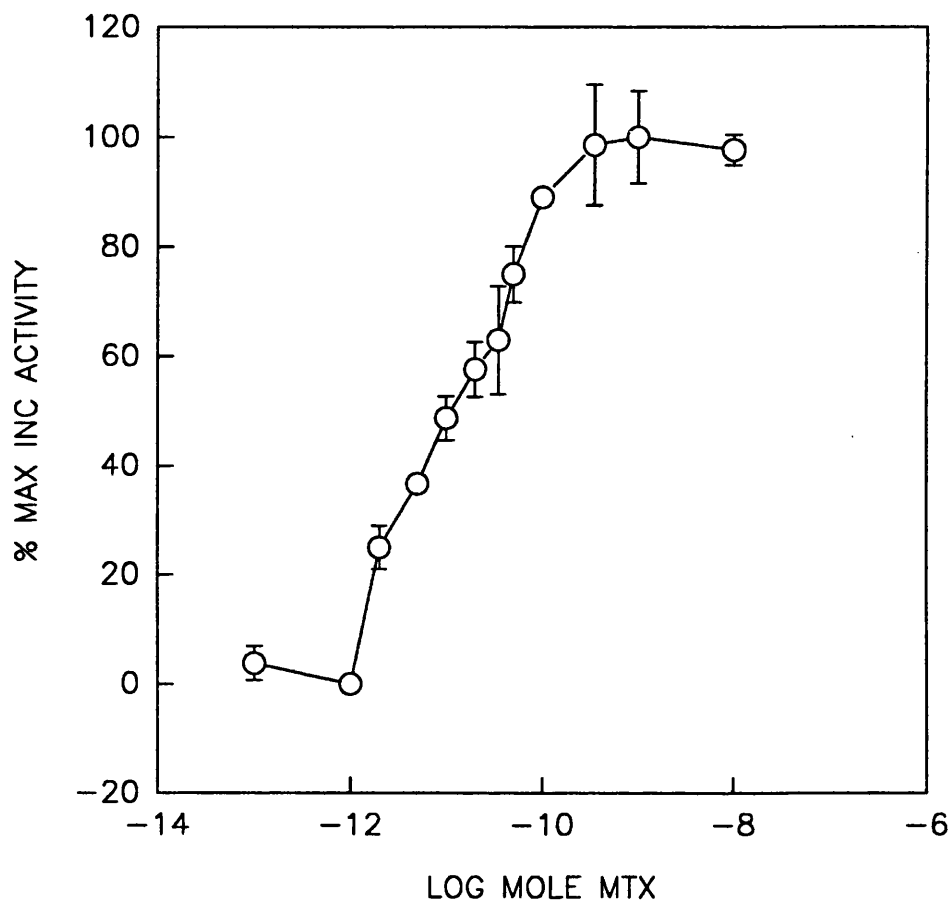
Figure 3.3.7. Tyrosinase activity of cells incubated in MTX-NLDP. Percent maximum

increase in ^3H_2O production vrs MTX-NLDP. Estimated Ec50 for MTX-NLDP is

1.73×10^{-11} M. Bars indicate SD values of 4 sample wells.
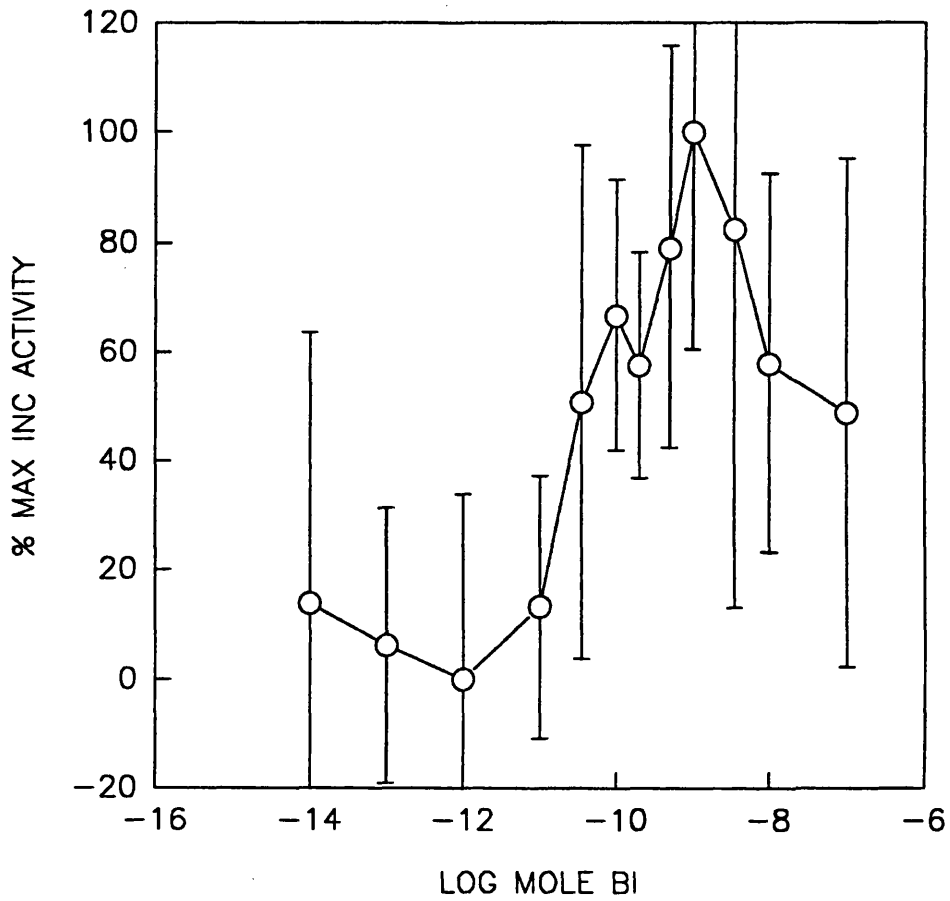
Figure 3.3.8. Tyrosinase activity of cells incubated in Bi-NLDP. Percent maximum increase in ^3H_2O production vrs Bi NLDP. Estimated Ec50 for Bi-NLDP is 9.29×10^{-11} M. Bars indicate SD values of 4 sample wells.

Table 3.3.2. The C(SE)s, M(SE)s, and resulting Ec50s, for all tyrosinase assays. Assay 1* of each analogue are plotted in Figures 3.3.4.- 3.3.8.. All data are recorded in Appendix 2.

α–MSH ANALOGUE		C($\pm$SE) DPM	M($\pm$SE) MOLE^{-1}	Ec50 MOLE
NLDP	1*	91600($\pm$6570)	1.00($\pm$2.66)x10^{10}	2.64x10^{-11}
	2	119000($\pm$4130)	1.29($\pm$1.42)x10^{10}	7.78x10^{-11}
	3	149000($\pm$2780)	4.30($\pm$0.95)x10^{11}	6.61x10^{-11}
	4	196000($\pm$5300)	6.66($\pm$15.8)x10^{9}	8.75x10^{-12}
	5	90600($\pm$7160)	2.46($\pm$2.35)x10^{13}	1.51x10^{-11}
	6	91600($\pm$6570)	2.14($\pm$22.6)x10^{9}	1.92x10^{-11}
	7	65900($\pm$4650)	1.83($\pm$1.60)x10^{12}	1.55x10^{-11}
	8	83900($\pm$6110)	2.94($\pm$2.10)x10^{11}	6.66x10^{-12}
	9	54200($\pm$5500)	1.86($\pm$1.89)x10^{12}	3.06x10^{-11}
	10	104000($\pm$4250)	1.31($\pm$1.38)x10^{12}	9.84x10^{-12}
α–MSH	1*	50100($\pm$94100)	2.55($\pm$1.44)x10^{11}	4.25x10^{-10}
	2	131000($\pm$8060)	2.98($\pm$2.66)x10^{10}	8.66x10^{-11}
	3	115000($\pm$96300)	5.43($\pm$21.0)x10^{9}	9.08x10^{-11}
	4	70500($\pm$4320)	7.60($\pm$21.8)x10^{9}	2.87x10^{-10}
CTAF-NLDP	1*	123000($\pm$13000)	1.15(($\pm$3.17)x10^{11}	1.76x10^{-10}
	2	207000($\pm$2570)	2.47($\pm$8.85)x10^{9}	2.96x10^{-9}
	3	131000($\pm$6330)	1.60($\pm$1.99)x10^{10} '	2.98x10^{-9}
	4	140000($\pm$6150)	1.33($\pm$2.11)x10^{10}	4.30x10^{-9}

MTX-NLDP 1*	65800(±5190)	$2.50(±1.78)\times10^{12}$	1.72×10^{-11}	
2	186000(±6030)	$2.69(±18.0)\times10^{9}$	2.25×10^{-11}	
3	190000(±5170)	$7.11(±15.4)\times10^{9}$	2.36×10^{-11}	
BI-NLDP 1*	184000(±5240)	$1.97(±18.0)\times10^{10}$	9.29×10^{-11}	
2	138000(±5660)	$1.79(±1.78)\times10^{10}$	9.70×10^{-11}	

Table 3.3.3. The mean of the Ec50s, the standard deviation of the mean, the relative activity to α–MSH, the efficacy determined by $Kd/Ec50$, and the number of replicate assays for each α–MSH analogue tested.

α–MSH ANALOGUE	MEAN Ec50 (±SD) MOLE	RELATIVE ACTIVITY to α–MSH	EFFICACY	NUMBER of REPLICATES
NLDP	$2.76(±2.47)$ $\times10^{-11}$	8.06	80.6	10
α–MSH	$2.22(±1.64)$ $\times10^{-10}$	1.0	29	4
CTAF-NLDP	$2.60(±1.74)$ $\times10^{-9}$	0.09	17.9	4
MTX-NLDP	$2.11(±0.34)$ $\times10^{-11}$	10.5	73	3
BI-NLDP	$9.50(±0.29)$ $\times10^{-11}$	2.35	3.7	2

3.4 *IN VITRO* GROWTH REGULATION OF B16 CELLS BY α-MSH AND NLDP

3.4.1. INTRODUCTION

Regulation of melanocyte and melanoma growth by α–MSH is a controversial subject. Some reports observe the inhibition of melanoma growth after exposure to α-MSH, whereas others have reported a stimulation of growth or negligible effects (Section 1.6.2-1.6.3.). Growth curves of B16 mouse melanoma cells *in vitro*, in the presence and absence of α–MSH or NLDP, are described in this section. Melanotropin induced growth inhibition was measured by the percent number of treated cells/well compared to untreated wells using Equation 2.7. (Section 2.7.).

3.4.2. EFFECTS OF PULSE OR CHRONIC DOSES OF NLDP ON B16 CELL GROWTH

1 nM NLDP was administered both chronically and for 30 minutes/day (see Section 2.7.). Figure 3.4.1. shows the effect of NLDP exposure upon B16 cell growth. Chronic exposure inhibited cell growth 30% after 3 days and 38% after 4 days. The 30 minute/day NLDP pulse had no effect on cell growth. Further trials of the chronic exposure of B16 cells to NLDP supported these findings (Table 3.4.1.).

3.4.3. EFFECTS OF α-MSH OR NLDP ON B16 CELL GROWTH

Figure 3.4.2. illustrates the effect of 10^{-9} M α–MSH and its NLDP analogue on B16 cell growth. Growth inhibition increased steadily over 4 days when wells were seeded with a density of 5×10^5 cells. Although inhibition was still increasing, it decelerated after 3 days. The decline in cell numbers for all wells on day 5 could be due to an experimental artefact. Alpha–MSH was less potent than NLDP in inhibiting cell growth. This became apparent after a 2 day exposure of the cells to the hormone. Wells with 10^{-9} M α–MSH contained cell numbers between hormone-free, and NLDP supplemented wells. An index of cell growth inhibition is listed in Table 3.4.1.

In all experiments, there was a marked alteration in cellular morphology 3-4 days after exposure to either α–MSH or NLDP. Cells became highly pigmented and granular, and the cell bodies became flattened and dendritic (on visual inspection). Cells incubated in α–MSH were less pigmented than those exposed to equal amounts of NLDP. It is concluded that under these conditions both α–MSH and NLDP increased melanogenesis while decreasing cell proliferation of B16 melanoma.

3.4.4. EFFECTS OF CELL DENSITY AND NLDP TREATMENT TIMES
ON B16 CELL GROWTH

When wells were seeded at low densities (10^4, Figure 3.4.3.) the cells displayed typical logarithmic growth in the presence or absence of 10^{-9} M NLDP over 4 days. The inhibitory effect of NLDP became more pronounced after the fourth day as cell density increased (5.6×10^5 cells/well, Table 3.4.1.). When cells were seeded at a high density (5×10^5 cells/well, Figure 3.4.9.), NLDP cell growth inhibition occurred earlier (2 days)

at a cell density of 9×10^5 cells/well (Figure 3.4.7., Table 3.4.1.). Wells seeded with, or under, 10^5 cells/well took 5 days to reach maximal inhibition. Those wells seeded with over 10^5 cells took 4 days (Figures 3.4.1., and 3.4.4-3.4.9.). NLPD induced growth inhibition gradually increased over time regardless of cell density, until a stationary phase of growth was reached. NLDP induced growth inhibition was influenced by cell density and length of chronic exposure.

3.4.5. EFFECTS OF NLDP DOSE CONCENTRATION ON B16 CELL GROWTH

Growth inhibition by chronic doses of NLDP was concentration-dependent. 10^{-7} M NLDP induced 34% cell growth inhibition after a five day exposure (Figure 3.4.10., Table 3.4.1.). A similar result was observed at concentrations below 10^{-9} M but the effect was diminished. B16 cell growth inhibition by NLDP increased most markedly from 10^{-11} to 10^{-9} M.
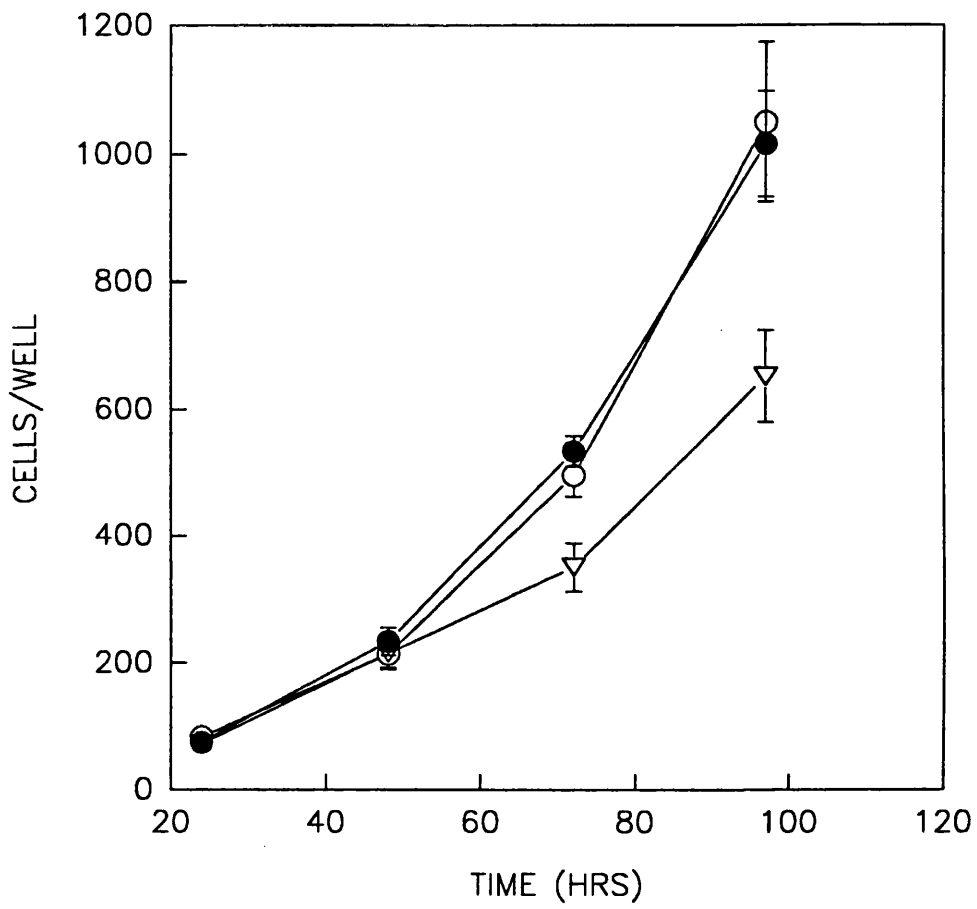
Figure 3.4.1. The effect of 1 nM NLDP doses of chronic ▽ ; pulse ○ ; and
untreated cells ● ; on B16 cell growth vrs time. Bars indicate SD values of 4
sample wells
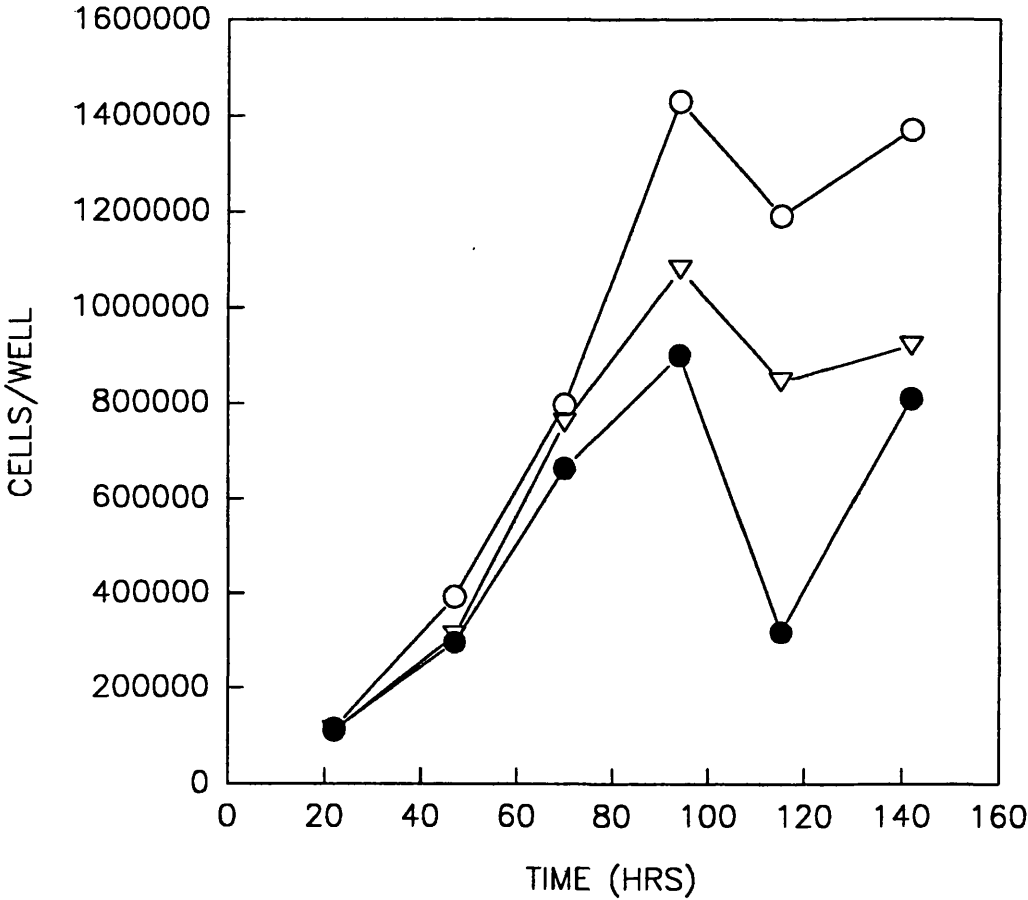
Figure 3.4.2. The effect of chronic doses of 1 nM NLDP ● ; α-MSH ▽ ; and
no treatment ○ on B16 cell growth vrs time. Points represent the means of 4
sample wells.
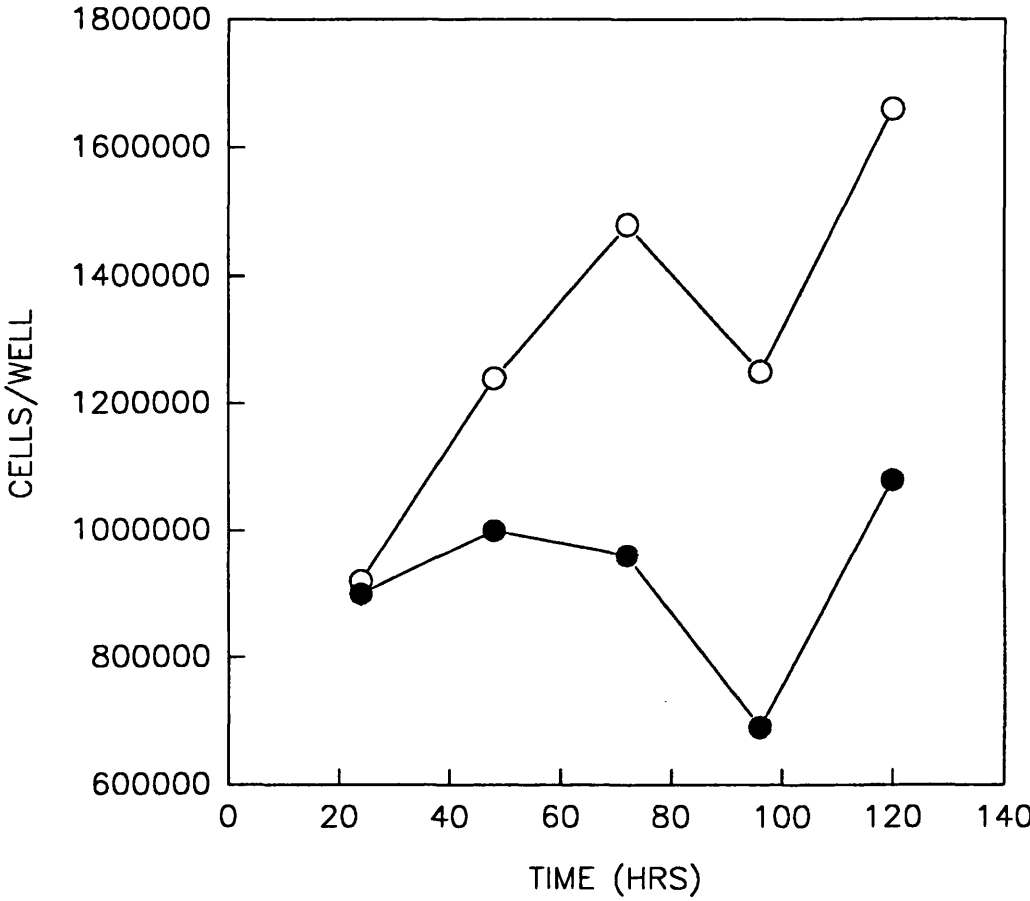
Figure 3.4.3. The effect of a chronic dose of 1 nM NLDP ● ; and no treatment

O on 10^4 B16 cells/well vrs time. Points represent the means of 4 sample wells.
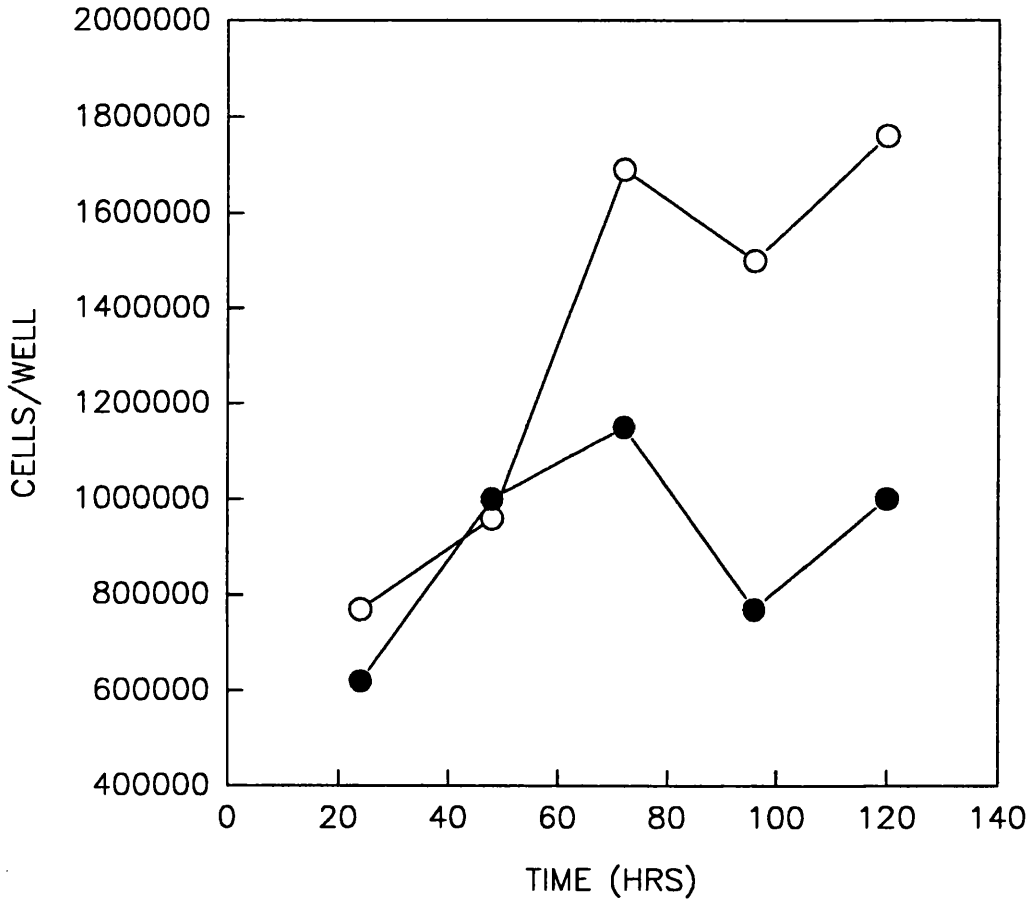
Figure 3.4.4. The effect of a chronic dose of 1 nM NLDP ● ; and no treatment

O on 2.5x10⁴ B16 cells/well vrs time. Points represent the means of 4 sample wells.
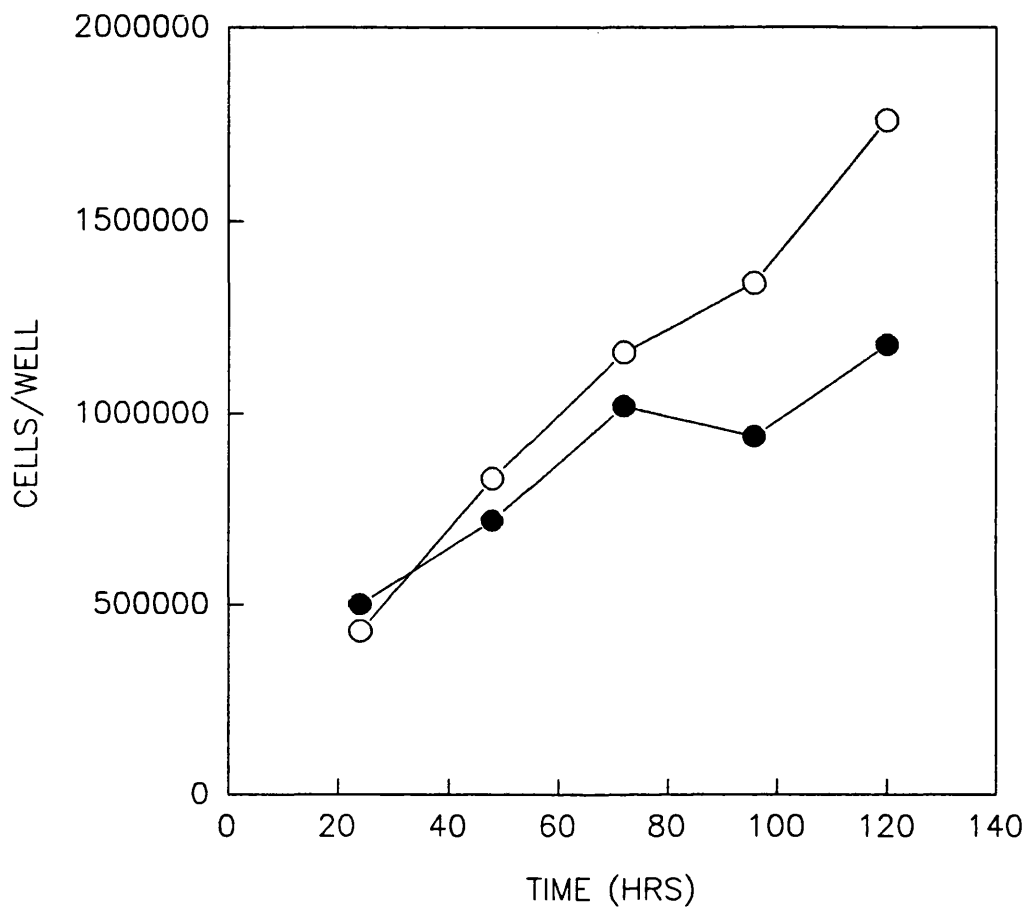
Figure 3.4.5. The effect of a chronic dose of 1 nM NLDP ● ; and no treatment

O   on 5x10⁴ B16 cells/well vrs time. Points represent the means of 4 sample wells.
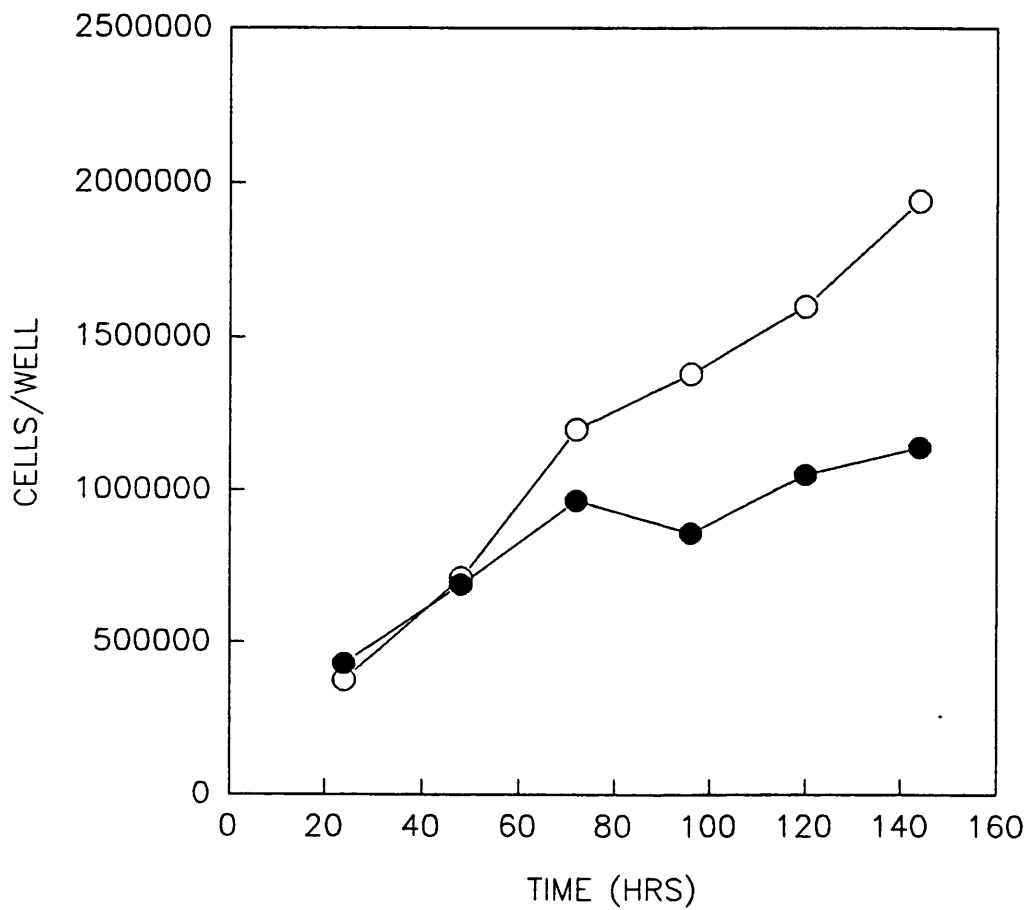
Figure 3.4.6. The effect of a chronic dose of 1 nM NLDP ● ; and no treatment

○ on 7.5x10⁴ B16 cells/well vrs time. Points represent the means of 4 sample wells.
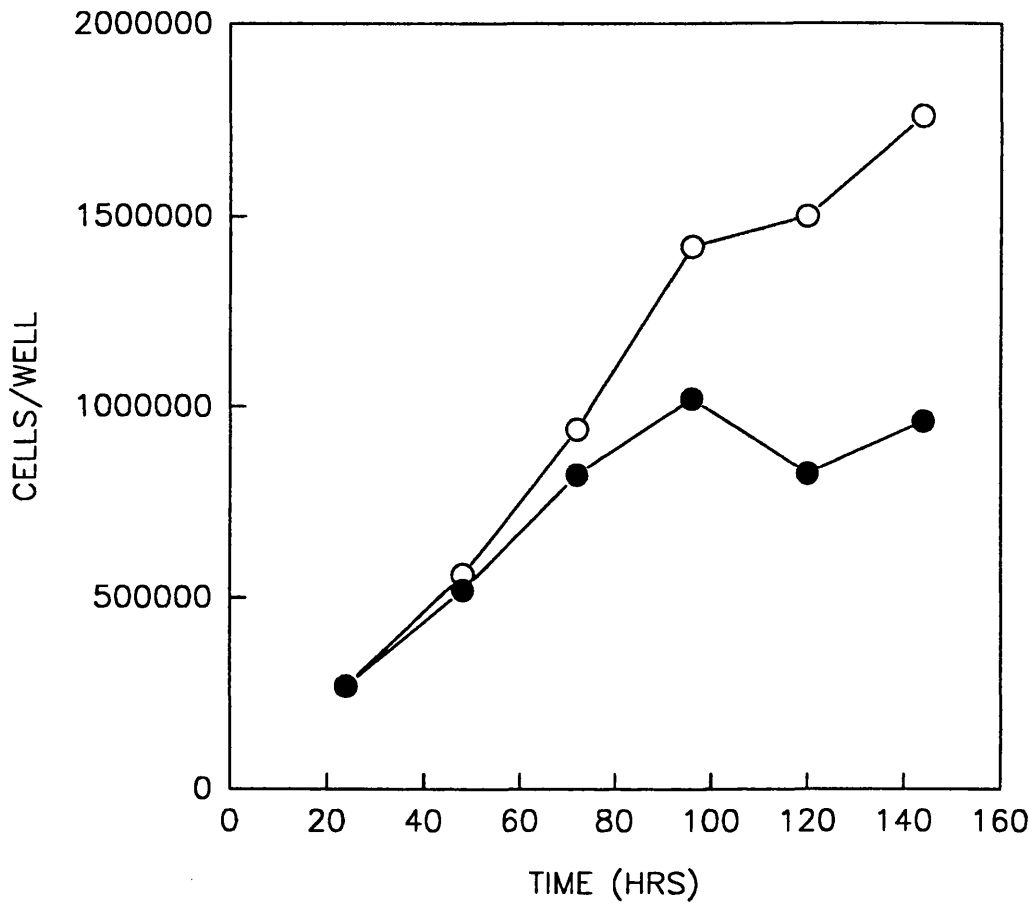
Figure 3.4.7. The effect of a chronic dose of 1 nM NLDP ● ; and no treatment

○ on 10^5 B16 cells/well vrs time. Points represent the means of 4 sample wells.
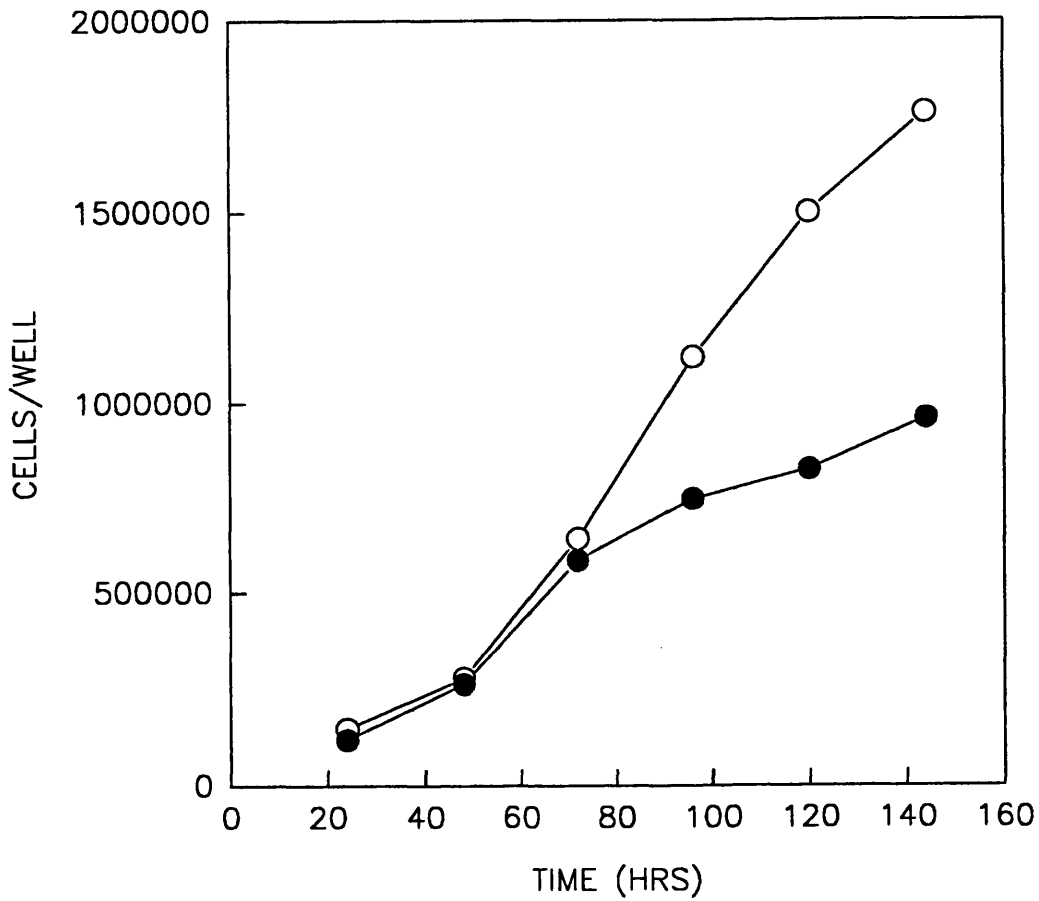
Figure 3.4.8. The effect of a chronic dose of 1 nM NLDP ● ; and no treatment

O on 2.5x10^5 B16 cells/well vrs time. Points represent the means of 4 sample wells.
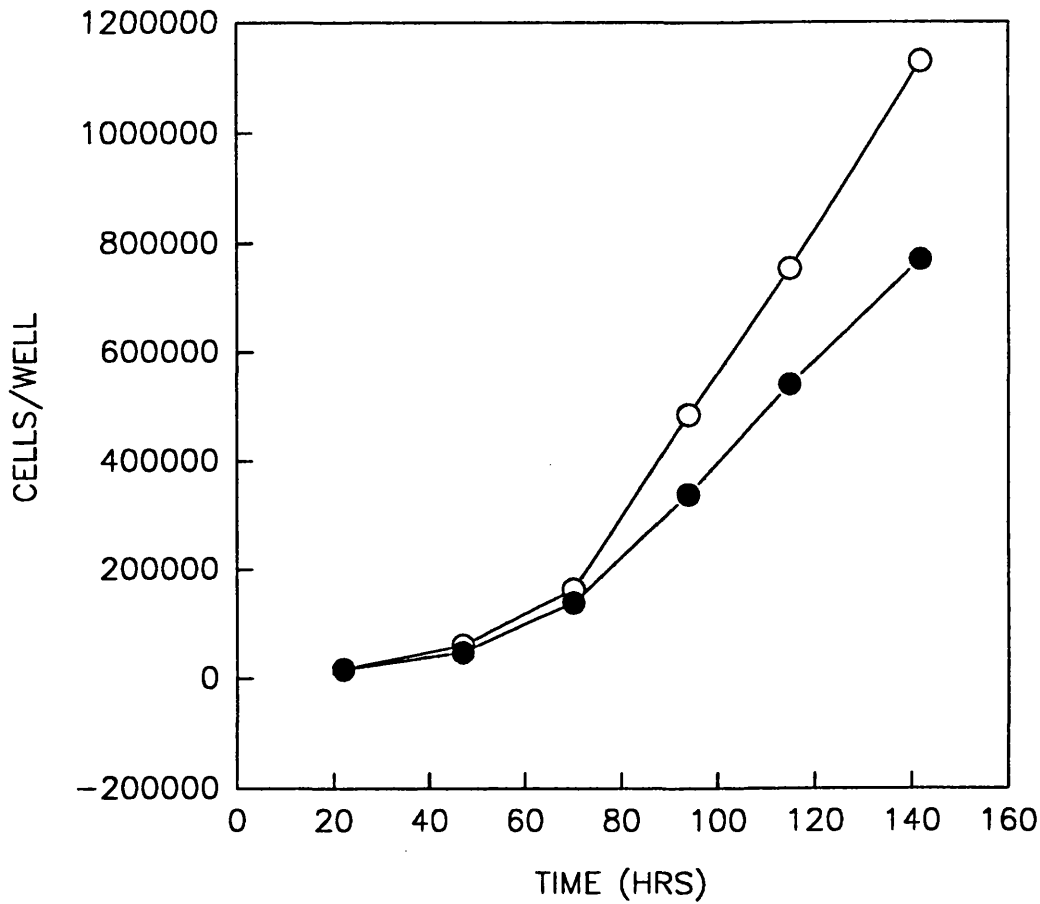
Figure 3.4.9. The effect of a chronic dose of 1 nM NLDP ● ; and no treatment

O   on 5x10⁵ B16 cells/well vrs time. Points represent the means of 4 sample wells.
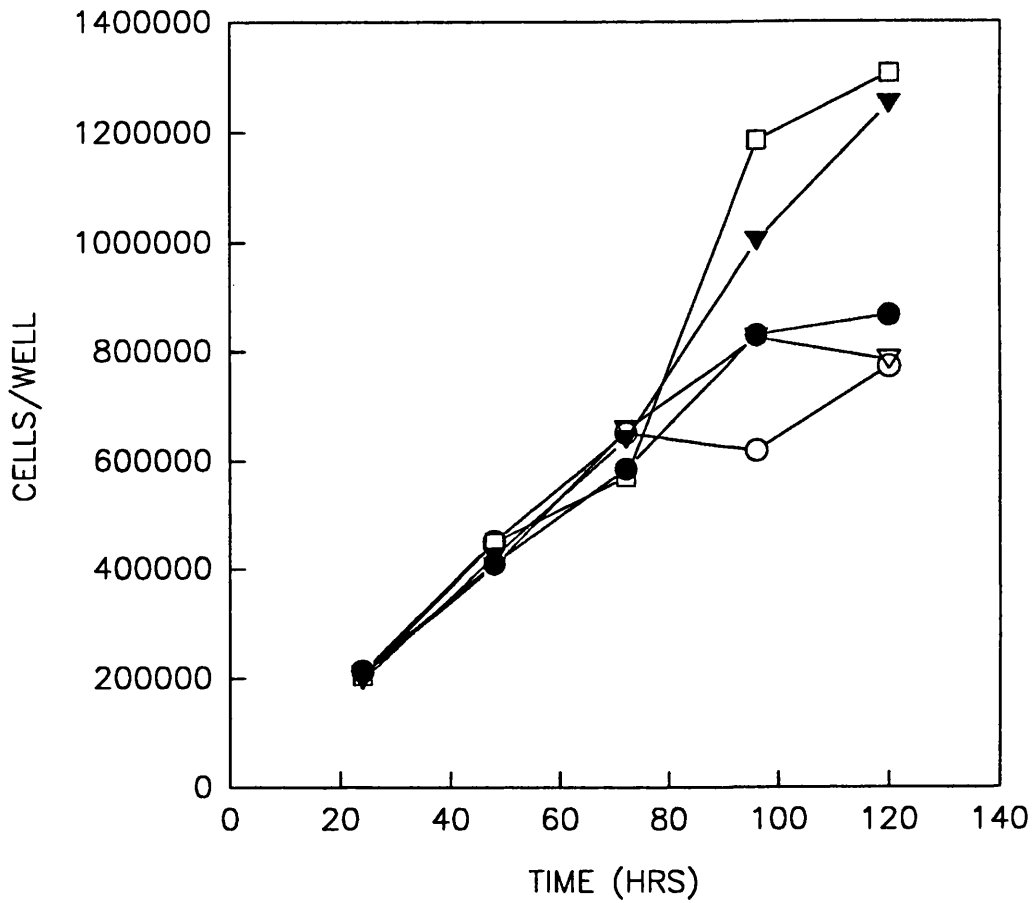
Figure 3.4.10. The effect of a chronic dose of 10^{-7} M $\bigcirc$; 10^{-8} M $\triangledown$;10^{-9} M

$\bullet$; 10^{-11} M $\blacktriangledown$; and no treatment $\square$ on 7×10^4 B16 cells/well vrs time. Points

represent the means of 4 sample wells.

Table 3.4.1. Percent melanotropin induced growth inhibition relative to untreated cells over time. All data are listed in Appendix 2.

FIGURE	DAYS 1	2	3	4	5	6
3.4.1. CHR PULSE	13.74 10.39	0 -9.30	29.4 -7.86	37.8 0.03		
3.4.2. α-MSH NLDP	3.48 2.60	20.9 24.5	4.64 16.7	24.5 37.1	29.1 33.2	
3.4.3.	2.35	20.0	14.8	30.2	28.3	28.0
3.4.4	18.9	7.14	8.89	33.4	45.0	45.4
3.4.5.	0	7.14	12.5	24.6	34.4	41.2
3.4.6.	-14.4	2.82	19.5	37.7	43.9	
3.4.7.	-16.3	13.2	12.1	29.8	32.9	
3.4.8.	19.5	-4.17	31.9	48.8	43.2	
3.4.9.	2.17	19.3	35.1	44.8	34.9	
3.4.10 M NLDP 10^{-11} 10^{-9} 10^{-8} 10^{-7}	-11.15 1.50 0 0	4.46 6.25 10.7 4.02	0 12.3 9.04 16.4	22.5 16.7 31.3 33.3	3.85 33.9 40.0 40.8	

4. DISCUSSION

4.1. POTENTIAL FOR MSH AS A CARRIER DURING SITE-SELECTIVE DRUG DELIVERY

The purpose of drug targeting is to reduce toxic side effects and increase the therapeutic index of the drug. Pharmaceutical and biological considerations demand that the ideal drug carrier should : 1) be biodegradable; 2) be non-immunogenic 3) be non-toxic; 4) be selectively delivered; 5) have a high carrier capacity; 6) be able to control the release of the drug; 7) have low production costs; 8) have reproducible properties; and 9) have a good shelf-life (5). In an effort to meet these criteria, drugs have been linked to a variety of carriers such as antibodies, glycoproteins, lectins, DNA, liposomes, and hormones. Hormones may be preferred since they are: 1) relatively easy to obtain in chemically pure form: 2) are not bound by Fc receptors on macrophages; and 3) do not cause allergic responses since hormones are structurally similar or identical in different species (188). Several toxins are extremely lethal at very low doses. These compounds are suited for targeted-delivery since their high potency enables effective dose concentrations to be low. A site-specific hormone conjugated to a potent toxin would need minimal amounts administered to the patient for cytotoxicity of the targeted cells. If the hormone bound selectively to its receptor with very little non-specific binding, and its receptor was only available at the target site, a high therapeutic index could be achieved. A hormone that exerts its effect merely by binding to a cell surface receptor is unlikely to be a good site-specific drug carrier. After binding, the receptor must mediate entry of the conjugate into the cell's interior in order for the toxin to exert its cytotoxic effect. The internalisation of a

hormone-receptor complex could be associated with intracellular activity and possible desensitisation of receptor binding.

One hormone being investigated as a drug carrier is alpha-melanocyte-stimulating hormone (α–MSH). Its receptors are found most frequently on melanocytes and melanoma cells. MSH related compounds could eventually serve as pharmaceuticals for clinical application in : 1) the treatment of pigment disorders; 2) treatment of certain forms of dementia; 3) the enhancement of nerve-regeneration and protection from nerve damage; 4) the control of fever and inflammation; and 5) diagnosis and therapy of melanoma (52). Although α–MSH receptors (MSH-Rs) are expressed in both melanoma and non-cancer pigment cells, killing of these non-cancer cells with drug-MSH conjugates is considered tolerable since only non-fatal de-pigmentation should occur. This study addresses the application of MSH in site-selective drug or probe delivery to, and within, melanoma cells.

The MSH analogue [Nle^4,D-Phe^7]-α–MSH (NLDP) is well suited as a targeting molecule for delivering therapeutic or imaging agents selectively to the α–MSH-R. It: 1) is biodegradable; 2) is non-immunogenic; 3) has no toxic side-effects when administered to mice as 2 mg/kg daily over four weeks; 4) can be used in transdermal drug delivery as NLDP diffuses reproducibly across mouse skin (45); 5) has a high specific affinity for the α–MSH-R resulting in prolonged cellular activation; 6) has a chemical structure which allows labels, toxins, and other compounds to be attached without compromising either its binding or stimulatory properties; 7) can be manufactured in mg quantities on a peptide synthesiser ; 8) has been well-characterised by several investigators; and 9) is stable for several years when suitably stored below 0°C.

Use of MSH as a vector in site-specific delivery requires more knowledge of its binding characteristics and its biological fate following binding. In an attempt to describe the

MSH/receptor interaction, the possible internalisation of the ligand-MSH-R complex or its separate elements, and its (their) metabolic fate, the group at Bath have synthesised and tested a number of melanotropic conjugates which have a selective affinity for MSH receptors. Several of these stimulate biological activity in a dose-dependent manner in B16 melanoma cells. They were used to: monitor, target toxins to, and extract the α–MSH receptor found in monolayers of B16 murine melanoma.

4.2. BINDING OF ^{125}I-NLDP TO α-MSH RECEPTORS OF B16 CELLS

Binding assays and tyrosinase assays were developed to measure the potential of various α–MSH derivatives as tools in the study and treatment of melanoma. Determination of endogenous α–MSH in the B16 melanoma growth media was undetectable (radio-immunoassay for α–MSH, Section 3.1.). Thus, all results were attributed to experimentally added α–MSH.

^{125}I-NLDP binding assays were performed on B16 monolayers in RPMI 1640 media containing 0.2% BSA. The time required for a relative equilibration of the tracer with the MSH-R at 0-4°C was longer than that observed by other investigators. Maximum binding was achieved on B16 murine melanoma monolayers by Siegrist *et al* (157) at 6, 3, and 0.5 hours at 4, 15, and 37°C, respectively. Our assays took 8, 6, and 1 hours to reach maximum binding at the same temperatures. The longer equilibrium times could be due to the secretion of protein endopeptidases by the melanoma cells during the assay (42). These peptidases could prolong the binding times of tracers to the MSH-R by continually degrading the ligand during the binding incubation. At 0-4°C there was a 2 hour difference

between our relative equilibrium binding times to those of Siegrist *et al* (157). Protein endopeptidase secretion were not expected to be responsible for ligand degradation at these temperatures as cells were not metabolically active. Preliminary binding experiments with the protease inhibitor 1,10-phenanthroline and a collagenase inhibitor had little effect on the binding of ^{125}I-NLDP to B16 melanoma. Either enzymatic degradation was not involved during receptor-binding incubations, or the collagenase inhibitor and 1,10-phenanthroline were unable to inhibit enzymatic degradation of the tracer. The variation in binding times could be due to the use of different B16 subclones, and/or a difference in experimental procedure not described in journal articles.

The minimal amount of acid-resistant ligand (7%), and the low non-specific binding (12%) of ^{125}I-NLDP (Section 3.2.4.5.) to α–MSH-Rs of B16 melanoma at 0-4ºC, allowed for the calculation of affinity constants of other α–MSH derivatives when competed with ^{125}I-NLDP (Section 3.2.4.8.). The assumption is made that if ^{125}I-NLDP is limited to external receptors of the plasma membrane, so are other α–MSH analogues.

4.3. CHARACTERISATION OF THE α-MSH RECEPTOR OF B16 CELLS

Scatchard plot analysis of saturation binding isotherms suggested a single α–MSH-R population with a mean of 18,022 (±13,022) receptors per B16 cell. These results are in agreement with receptor numbers observed by other investigators. B16 are quoted to have 9,570 (156), 2,805 (176), and 683-10,000 receptors/cell depending on the B16 sub-clone and growth media (167). In B16 tumours there were an estimated 14,700 receptors/cell

(159). Solca *et al* (166) estimated 20,000 α–MSH-Rs per B16-F1 cell using a photoaffinity Naps-NLDP tracer.

Studies with photoaffinity labels describe the α–MSH-R of B16 cells as a single population of 41-46 kDa, often composed of two proteins possibly representing two receptor moieties with one binding site (1, 152, 158, 167). Recently molecular cDNA techniques showed the MSH receptor of Cloudman murine melanoma, WM 266-4 human melanoma, and cervical cancer cells to be 34.795-35 kDa, 297, 317, and 361 amino acids long. It has a glycosylated N-terminal containing 7 membrane-spanning sequences, that bind GTPs proteins when activated (38, 62, 126).

4.4. STRUCTURE/FUNCTION ASPECTS OF α-MSH PROBES AND TOXIN FOR THE α-MSH-RECEPTOR OF B16 CELLS

4.4.1. α–MSH AND NLDP

The estimate for the dissociation constant (Kd) of NLDP was obtained by competition assays with ^{125}I-NLDP. It was 2.92 fold lower than the value observed for α–MSH. The biological potency of NLDP (Ec50) was measured with tyrosinase assays. It was 8 fold greater than the estimate observed for α–MSH. NLDP had a Kd of 2.22×10^{-9} M and an Ec50 value of 2.76×10^{-11} M for receptors of B16 murine melanoma. The corresponding α–MSH parameters were estimated to be 6.46×10^{-9} M and 2.22×10^{-10} M, respectively. These results are in accordance with Kd and Ec50 values for NLDP and α–MSH published by other researchers. Other studies reported NLDP to have a 6 fold greater

affinity for the α–MSH-R than α–MSH. Melanotropin receptors on B16 melanoma cells displayed a Kd of 3.2×10^{-10} M for NLDP compared to the Kd of 1.9×10^{-9} M for α–MSH (156). Siegrist (161) has observed a variation of α-MSH Kd values of $1.31-2.6 \times 10^{-9}$ M for different B16 sub-clones. Tyrosinase assays of α–MSH and NLDP on Cloudman mouse melanoma gave Ec50 estimates of $2.0-5.4 \times 10^{-9}$ M and 2.8×10^{-11} M, receptively (127, 150, 202).

In α–MSH the replacement of Met by Nle at position 4 and D-Phe for its L enantiomer at position 7 produced a stereo structural analogue [Nle^4,D-Phe^7]-α–MSH (NLDP) which: 1) maintained its binding and biological activities after iodination with chloramine T; 2) resisted enzymatic degradation by serum enzymes; 3) had a high affinity for the MSH receptor; and 4) displayed potent and prolonged biological stimulation as measured by raised tyrosinase levels (120, 150, 158).

4.4.2. ^{125}I-NLDP PROBE

Radio-labelled NLDP, ^{125}I-Tyr^2-NLDP (^{125}I-NLDP) displayed a high specific affinity for various human and mouse melanoma. The tracers affinity was similar to its unlabelled form when iodinated according to the equimolar chloramine T procedure. Conversely, iodination of α–MSH with chloramine T produced a tracer with 50% the activity of unlabelled α–MSH (53). This is thought to be due to the oxidation of the Met^4 residue during iodination. The α–MSH sequence 4-9 -Met^4-Glu^5-His^6-Phe^7-Arg^8-Trp^9- stimulates bioactivation and is particularly vulnerable to changes in the structure of the Met residue. The oxidation of the Met residue of α–MSH represents a mechanism for its inactivation *in vivo* (157). Replacement of Met^4 by norleucine increased the ability of the peptide to

induce cellular activation by 62.5% (157). The C-terminal 10-13 -Gly^{10}-Lys^{11}-Pro^{12}-Val^{13}-NH^2 of α–MSH potentiates the cellular response. The D-Phe residue at position 7 could protect the peptide from chemical degradation (51).

Iodination of NLDP increased the affinity of the peptide for its receptor 4.65 fold. Conversely, the binding affinity of Bi-NLDP (Section 4.4.4.) was not affected by iodination. Other researchers have found iodination of the Tyr^2 of melanotropins to have little effect on the peptide's affinity for the MSH-R. The binding affinity of unlabelled α–MSH was 1.9×10^{-9} M and 1.3×10^{-9} M after iodination to the [3'-Iodo-Tyr^2]-α–MSH analogue (49). The increase in the NLDP affinity following iodination could be due to an increase of the peptides hydrophobicity or experimental variability. All iodinated α–MSH and photoaffinity analogues were not examined for cellular stimulation with tyrosinase assays as explained in Section 3.3.2.2.

When designing tools for studies and possible therapy of melanoma, it was necessary to use a carrier that would: 1) have a high affinity for the α–MSH-R with low non-specific binding; 2) stimulate a biological response, hence possible internalisation of the ligand-α–MSH-R complex or its subunits; and 3) retain the above characteristics after iodination. Consequently, the NLDP carrier peptide was used instead of α–MSH when designing melanotropin-probes and toxins.

Conjugates of α–MSH generally maintained a high degree of biological activity when the hormone was attached to additional groups via its N-terminal. The C-terminal was less tolerant than the N-terminal. Eberle claims (52) it must consist of a basic side-chain at position 11 and a conformational stabilising element at position 12. Our studies of an alanine scan of α-MSH (postgraduate work in progress) has shown the replacement of Lys^{11} with alanine has no effect on binding or bioactivity of the peptide. The presence of a

residue at position 13 was not essential for biological activity (50). Chaturvedi *et al* (36) found the N-terminal Ser^1-Tyr^2-Ser^3- sequence of NLDP was not essential for the retention of biological activity. Hence, all melanotropin-probes or toxins used in this study were attached to the N-terminus of NLDP.

4.4.3. CTAF-NLDP PROBE

Addition of the large CTAF molecule to NLDP at its N-terminus lowered the binding affinity of the agonist 20 fold, raising   the Kd value to 4.64x10^{-8} M. This was reflected in a 94 fold drop in relative tyrosinase activity (Ec50 2.6x10^{-9} M). These results were expected since an increase in the size of an α–MSH analogue or a blockage of the peptide at its N-terminus with bulky groups, reduces its activity 2-10 fold in the first instance and 400 fold in the second (52). The CTAF molecule may sterically interfere with the binding sequence of NLDP to the α–MSH-R,   its subsequent internalisation, and internal signalling (tyrosinase expression). Alternatively, the CTAF-NLDP probe prepared in our laboratory may be too large for an easy access into the melanoma cytosol via the α–MSH-R.

4.4.4. BI-NLDP PROBES

Biotinylation of NLDP at its N-terminus increased its affinity for the α–MSH-R 6.31 fold in our binding assays. The Kd value for Bi-NLDP was 3.53x10^{-10} M. The reverse was observed in tyrosinase assays showing a 3.4 fold drop in the cellular response of B16 cells

to Bi-NLDP with an Ec50 estimation of 9.5×10^{-11} M. Eberle (52) found the biological activity of an α–MSH analogue would drop 2-10 fold if the lipophilicity of the peptide was increased. The hydrophobic properties of the biotin label could increase the affinity of an attached melanotropin for its receptor by bringing it in closer proximity to the α–MSH-R located in the lipoprotein bilayer of the plasma membrane. By the same mechanism, the label may then interfere with receptor-mediated internalisation of the receptor-ligand complex into the hydrophilic cytosol.

Neither iodination, the addition of the 4-(1-Azi-2,2,2-trifluoroethyl)benzoate (ATB) photoaffinity label or streptavidin interfered with the binding of Bi-NLDP to the α–MSH-R. Conversely, the incorporation of the gold (10 nm)-streptavidin complex in Bi-^{125}I-NLDP removed the ability of the probe to compete with NLDP for the α–MSH-R. This result could be interpreted as the probe losing its ability to bind to the α–MSH-R, or a high level of non-specific binding masking a specific effect. The reduced binding properties of the agonist might be caused by steric hindrance of the gold-streptavidin compound physically interfering with the binding domains of NLDP. Distancing the Sa-Au marker from NLDP with a linker might restore binding to the new (Sa-Au)-Bi-linker-^{125}I-NLDP probe. It would be interesting to insert a peptide linker between NLDP and the gold-streptavidin complex (Sa-Au) to test this hypothesis.

4.4.5. ATB-NLDP PHOTOAFFINITY PROBES

There was no change in the binding affinities when tracers ^{125}I-NLDP and Bi-^{125}I-NLDP were coupled with ATB to form ^{125}I-ATB-NLDP and Bi-^{125}I-ATB-NLDP, respectively. Incorporation of the ATB label into the NLDP molecule at the Lys[11] residue did not effect the binding properties of the agonist. These results are in agreement with our observation

that position 11 of α–MSH peptide can be exchanged for a neutral amide with no side chains, without a change in binding affinity or bioactivity of the ligand. Therefor, attachment of the ATB label to the Lys^{11} residue of NLDP did not interfere with the interaction of NLDP for the a-MSH-R and its subsequent cellular activity.

4.4.6. MTX-NLDP TOXIN

Addition of methotrexate (MTX) at the N-terminus of NLDP did not alter the peptide's affinity for the α–MSH-R, or interfere with its stimulation of the cell. The Kd and Ec50 of the MTX-NLDP conjugate were $1.54x10^{-9}$ M and $2.11x10^{-11}$ M. These values compare with the values observed for NLDP at $2.25x10^{-9}$ M and $2.76x10^{-11}$ M, respectively.

4.4.7. EFFICACY OF α–MSH PROBES AND TOXIN

In all cases, the tyrosinase Ec50 of B16 melanoma occurred at a lower concentration of the α–MSH analogues than was required for half maximum receptor binding. For all compounds tested in this study, the Ec50 estimates were consistently lower than their Kd values. The increase in sensitivity from binding to cellular activity was: 29 fold for α–MSH; 81 fold for NLDP; 18 fold for CTAF-NLDP; 3.7 fold for Bi-NLDP; and 73 fold for MTX-NLDP. As previously reported, the NLDP analogue was the most potent in eliciting a cellular response (120, 150). It was 12 fold more potent than α–MSH in B16 melanoma tyrosinase assays. This increase is thought to be caused by the prolonged binding of NLDP to the α–MSH-R with conformational properties related to the exchange of $L-Phe^{7}$ for D-

Phe[7] which stabilise the interaction. The loss of potency with the addition of the CTAF and Biotin labels to NLDP, could be caused by their hydrophobic properties or in the case of CTAF, its size.

This amplification of a cellular response as a consequence of agonist-receptor interactions is typical for a receptor that utilises stimulatory G proteins (guanine nucleotide-dependent regulatory proteins) as second messengers. G protein coupled receptors bind GDP (guanine diphosphate) by their α-subunits during their inactive state. Once activated, they exchange the GDP molecule for GTP (guanine triphosphate) and release of the GTP-α-subunit which regulates the activity of adenylate cyclase. Hydrolysis of the bound GTP to GDP by the α-subunit terminates the G protein signal (204). Amplification of an internal signal occurs as a single occupied MSH-R activates several Gs proteins which lead to a biological response. Additional specificity of a receptor effected event could be achieved with MSH-R-specific Gs proteins during MSH transmembrane signalling. G proteins also allow cells to respond rapidly to very low concentrations of extra-cellular stimuli (178). The low endogenous concentrations of MSH in the body (undetectabe-1 pM) suit this model. The functional coupling of a stimulatory G protein (Gs) to the MSH-Ris suggested by the code sequence of the cloned MSH-R, although this is not conclusive evidence. The high efficacy observed with the α-MSH analogues is probably due to a Gs regulatory mechanism employed by the α-MSH-R.

In our study, tyrosinase assays produced data with standard deviations of up to 40% (% maximum tyrosinase increase above basal levels) for replicate samples. Variations in experimental times, cell density, and techniques for the removal of unreacted [3',5'-^{3}H]-L-tyrosine could not eliminate this deviation. The Tyrosine Hydroxylase assay could be an improvement on the tyrosine assay employed in this study. The Tyrosine Hydroxylase assay uses L-[carboxy-^{14}C]tyrosine as the substrate, and releases $^{14}CO_2$ upon stimulation

of tyrosinase (200). Better measurements of MSH-related biological activity might be obtained with other *in vitro* biological assays such as the; *In situ* melanin (155), adenylate cyclase, and cAMP assays (63). Other researchers have found these assays to produce more accurate data than was observed in our tyrosinase assays (52).

4.5. RADIO-IMAGING OF MSH RECEPTORS OF MELANOMA CELLS USING MSH PROBES

Recently, the melanotropic tracer ^{125}I-NLDP was useful in quantifying MSH receptors of B16-F1 mouse melanoma tumours with auto-radiography (159). MSH tracers have also elucidated the distribution of MSH receptors in rodents (47, 175). Although the radio-signal was greater in melanoma tumours, its distribution was extensive. This is probably due to the pleiotropic nature of α–MSH.

Clinical targeting of human melanoma was achieved with a novel chelating α–MSH derivative (bisMSH-DTPA) which binds [111]indium firmly. Bard *et al* (9, 10) observed specific targeting of the compound to Cloudman melanoma *in vivo*. ^{111}In-bis-MSH-DTPA was successful in the diagnosis of 89% of melanoma lesions in 15 patients (201).

During our studies, Scatchard plot analysis of ^{125}I-NLDP binding isotherms gave a dissociation constant (Kd) of 4.76×10^{-10} M for α–MSH receptors on B16 mouse melanoma. Tatro *et al* (176) estimated the tracer to have a Kd an order of magnitude lower (5×10^{-11} M) for receptors of B16-F10 C23 melanoma. It is difficult to evaluate our results for ^{125}I-NLDP when so few Kd values of ^{125}I-NLDP have been published by other

researchers. Our tracer ^{125}I-NLDP appears to be suitable for localisation studies of the α–MSH-R on B16 melanoma cells *in vitro*.

4.6. POSSIBLE RECEPTOR-MEDIATED INTERNALISATION OF MSH PROBES BY MELANOMA CELLS

As previewed in Section 1.6.5., internalisation of plasma membrane MSH-R-ligand complexes is thought to occur after binding of an α-MSH agonist. Binding experiments of metabolically active melanoma with fluorescent, ferritin-labelled, or iodinated probes in combination with pulse-chase and acid wash treatments, have presented evidence for the internalisation of both human and mouse MSH-R-ligand complexes (43, 102, 158, 183, 184, 185). Further evidence for internalisation of the MSH-R-ligand was supported by the temperature and time-dependent association of ^{125}I-β-MSH with internal binding sites of Cloudman melanoma cells (132).

Orlow *et al* (132) observed specific internal binding sites for ^{125}I-β-MSH within the Cloudman melanoma cytosol after binding of the tracer at 12°C, followed by a 15 minute incubation at 37°C. Further studies showed these sites to be associated with a 50% sucrose gradient layer. These internal sites were of identical molecular weight (50-53 kDa), and shared common antigenic determinants with ^{125}I-β-MSH binding sites on the melanoma cell surface. Variant melanoma cells which differed from the wild-type with a lowered cellular response to β-MSH (changes in tyrosinase levels, dopa oxidase, and dopachrome conversion factor activities, melaninsation, proliferation, and morphology), had fewer internal binding sites, even though their ability to bind MSH on the outer cell

surface appeared normal. Thus, internal binding sites are thought to be involved during cellular responses to MSH.

In our studies, internalisation of the MSH-R-ligand was measured by the radiation associated with melanoma cells after an acid wash treatment. This treatment removes external cell-surface receptor-bound ligand (Section 1.6.5.). At 0-4°C, acid-resistant accumulation of ^{125}I-NLDP did not go above non-specific levels (Section 3.2.4.1.). The binding pattern of ^{125}I-NLDP to the B16 melanoma cell surface with possible internal binding sites (as determined by acid wash treatments) was similar to studies by researchers claiming internalisation of the MSH-R-ligand complex by melanoma cells. In all cases (including this study), the MSH probe was bound at 0-4°C, but was not observed intracellularly.

When the binding assay was performed at increased temperatures, the tracer accumulated in the cytosol. At 15°C, there was a steady increase in acid-resistant tracer over 25 hours, reaching a maximum of 42.1% of the total tracer bound (Section 3.2.3.). After 1 hour at 37°C, intracellular tracer reached a maximum plateau of 26-33.2% (Section 3.2.2.4.). Both cell-surface associated and acid resistant ^{125}I-NLDP reached maximum levels concurrently (1 hour at 37°C). There was a rapid rate of ^{125}I-NLDP dissociation from the cell surface once maximum binding was achieved, while intracellular levels remained stable (Section 3.2.2.4.). Similar results have been observed by other researchers also using the B16 murine melanoma system (Section 1.6.5.; 52, 133, 158).

The decline in surface binding of the α–MSH-R at 37°C may be influenced by a number of processes: 1) the temporary loss of receptor sites after ligand-stimulated receptor internalisation; 2) the loss of receptors due to lysosomal degradation; 3) recycling of the receptor back to the cell surface after dissociation of the ligand in an inactive state; 4)

down-regulation of the receptor (with the possible involvement of 1-3); and 5) release of the ligand either degraded or whole, back into the incubation medium. Siegrist *et al* (158) claimed that degradation of the MSH tracers by proteases in the incubation media caused the observed dissociation of the ligand from the melanoma cell plasma membrane (Section 4.2.). These questions could be addressed with the development of α–MSH probes in conjunction with microscopic technologies (light, fluorescent, confocal, and electron microscopy), and/or sub-cellular fractionation studies. In summary, the ^{125}I-NLDP tracer has a reproducibly high affinity for the α–MSH-R with low non-specific binding to B16 melanoma cells *in vitro*. After binding of an agonist, it appears to be transported with the α–MSH-R during intracellular cycling. These attributes make ^{125}I-NLDP a suitable probe for identifing the α–MSH receptor of B16 melanoma cells with potential use in future localisation and internalisation studies.

4.7. USE OF FLUORESCENT-MSH PROBES DURING STUDIES OF MSH RECEPTORS OF MELANOMA CELLS

The internalisation pathway of the MSH-R-ligand complex has yet to be explored with a sensitive fluorescent marker. Consequently, the fluorescent derivative N^α-((chlorotriazin-2-yl)amino)fluorescein-[Nle^4,D-Phe^7]-α–MSH was synthesised in our laboratory by attachment of the CTAF molecule to the N-terminal of NLDP (synthesised by Dr. George Olivier). The probe was tested for selective binding and cellular activation of the α–MSH-R of B16 melanoma cells. The CTAF-NLDP probe was determined to have specific binding and elicit a specific cellular response of the MSH-R of B16 cells. Thus, it is a candidate for monitoring the binding and subsequent intracellular route of receptor-bound agonists with light, electron, fluorescent, and confocal microscopy.

The localisation of fluorescein isothiocyanate-labelled-β–MSH (FITC-β–MSH) molecules in internal vesicles of melanoma has helped describe the possible internalisation pathway for α–MSH using a fluorescent marker (184, 185). Binding and biological activity of this compound were not characterised.

DiPasqual et al (43) synthesised a biologically active α–MSH-ferritin-FITC complex and which displayed specific labelling of receptors in the plasma membrane of Cloudman mouse melanoma, at both the fluorescent and electron microscopic levels. Its binding affinity was 7.7×10^{-10} M with a biological activity one third that of α–MSH during tyrosinase assays. Only 10-20% of the cells showed a patchy significant fluorescence when incubated with the α–MSH-ferritin-FITC probe. It is unknown if it was internalised as the cells were incubated with the probe at metabolically inactive temperatures (0-4°C). The patchy localisation of receptors on the melanoma cell surface could have been associated with developing clathrin-coated pits. The CTAF-NLDP probe examined in this study had a 50 fold lower affinity for the α-MSH-R than this MSH-ferritin-FITC probe.

Chaturvedi et al (37) prepared a fluorescein-labelled melanotropin [N^{α}-((chlorotriazinyl)amino)fluorescein-Ser^1,Nle^4,D-Phe^7]-α–MSH (CTAF-NLDP) using the NLDP agonist as the parent peptide. The fluorescein analogue was as potent as α–MSH in stimulating tyrosinase expression. Its binding affinity for the α–MSH receptor was not examined.

Wunderlin et al (202) constructed an α–melanotropin/tobacco mosaic virus disulphide (TMV-SS-α–MSH) conjugate with roughly 333 disulphide-liked α–MSH molecules per viron, as well as approximately 200 rhodamine molecules per viron. Its affinity for the α–MSH-R was 2-6 times higher than α–MSH, and had the same biological activity of NLDP

(7.52x10^{-10} M). As with the α–MSH-ferritin-FITC label, its binding was limited to 20-40% of the cells. They claimed 40% of the bound complex was internalised following a 30 minute incubation at 37°C. They were able to show a time-dependent accumulation of the TMV-α–MSH conjugate within the cell, but it could not be accredited to a localised area or organelle type. Our CTAF-NLDP probe was 3.37 fold less able to stimulate tyrosinase expression (Ec50 value of 2.6x10^{-9} M) than the TMV-SS-α–MSH conjugate. Its binding affinity for the α–MSH-R was a log cycle lower (4.64x10^{-8} M) than both the above mentioned melanotropin-fluorescent conjugates.

Considering the low α–MSH-R numbers observed on mouse (683-20,000) and human (400-2,000) melanoma cells, and the poor resolution given by fluorescent markers, the use of fluorescent probes may not be the optimal approach for mapping the intracellular route of the MSH-R and its agonists. Preliminary experiments with our CTAF-NLDP probe in localisation studies of the α-MSH pathway with flow cytometry were not encouraging. The signal was too weak and diffuse throughout the B16 melanoma cell for any specific binding to be recognised (postgraduate work in progress). Due to: a reduced binding affinity, reduced biological activity, and minimal visual localisation of the fluorescent signal; our CTAF-NLDP conjugate is not an improvement on existing fluorescent-melanotropin probes. Augmentation of the label could make future fluorescent-MSH probes more successful in monitoring the MSH-R cell cycle. This could be achieved by increasing the carrying capacity of the melanotropin via the strepavidin-biotin mechanism. There are 4 biotin binding sites for each streptavidin molecule (75). Combining a biotinylated-CTAF label with a (Sa)-Bi- NLDP peptide would increase the fluorescent label : peptide ratio from 1 : 1 (as for the CTAF-NLDP conjugate) to 4 : 1 with a maximum of 4 labels per receptor.

4.8. USE OF BIOTINYLATED-MSH PROBES DURING STUDIES OF MSH RECEPTORS OF MELANOMA CELLS

There are additional labels which allow the visualisation of the MSH-R besides MSH-radio ligands and MSH-fluorescent markers. Some of these are biotinylated compounds, and chemical (Section 4.1.) or photoaffinity labels. The biotin molecule is especially promising as a marker since the avidin-biotin system can be used to construct sensitive methods for the visual localisation of the MSH-R on/or within melanoma cells, at both the light and electron microscopic levels.

Chaturvedi *et al* (36) found that biotinylated NLDP equalled α–MSH in tyrosinase assays. The affinity of Chaturvedi's biotin-MSH probe was not calculated. A biotinylated derivative of $ACTH_{1-17}$ has been synthesised and biologically characterised (7). A dissociation constant of 1.67×10^{-9} M was determined with competition binding assays on mouse B16-F1 melanoma.. Our synthesis of Bi-NLDP followed the protocol of Chaturvedi *et al* (36). Both of the probes Bi-NLDP and Bi-^{125}I-NLDP developed by Dr. George Olivier displayed a 3 fold greater affinity for the α-MSH-R than the Bi-$ACTH_{1-17}$ derivative, with observed Kds of 3.5×10^{-10} M and 5.5×10^{-10} M, respectively. Ours is the first report of the application of a biotinylated-melanotropin probe to receptor studies on melanoma cells.

In an effort to both amplify and increase the resolution of the biotin signal at the ultrastructural level, the (Sa)-Bi-^{125}I-NLDP and (Sa-Au)-Bi-^{125}I-NLDP probes were constructed. The addition of streptavidin did not alter the affinity of the molecule, while the addition of the 10 nm gold marker completely inhibited specific binding of the (Sa)-Bi-

^{125}I-NLDP tracer. These results demonstrate that Bi-NLDP and its related derivatives (not containing gold markers), are useful tools during MSH-R microscopic studies of receptor targeting. This area of research has yet to define the sub-cellular localisation of the α-MSH-R, and subsequent cellular events.

4.9. USE OF PHOTOAFFINITY-MSH PROBES DURING STUDIES OF MSH RECEPTORS OF MELANOMA CELLS

The MSH receptor of melanoma cells must be isolated and purified before we can fully understand the ligand/MSH-receptor interaction and intracellular signalling pathways. Photoaffinity labels attached to α–MSH derivatives and fragments are useful in structure/function studies of the MSH-R of both human and murine melanoma. The most popular to date is the [Nle^4,(^{125}I)Tyr^2,D-Phe^7,Trp(Naps)^9]-α–MSH or Naps-^{125}I-NLDP tracer. Naps-^{125}I-NLDP specifically binds and activates the MSH-R. It is useful in the identification and purification of the MSH receptor protein(s) from melanoma (Section 4.3.) (152, 158, 166, 167). Unfortunately, affinity estimations of Naps-^{125}I-NLDP for the MSH-R were not examined.

The biotinylation of NLDP has proven useful in more ways than the visual monitoring of the α–MSH-R. Due to the strong affinity of biotin for avidin (Ka = 10^{15} M $^{-1}$) it allowed us to partially isolate and purify the MSH receptor from B16 murine melanoma cells in combination with a 4-(1-azi-2,2,2-trifluroethyl)benzoic acid (ATB) photoaffinity label. Dr. George Olivier synthesised the photoaffinity label [^{125}I-Tyr^2,Nle^4,D-Phe^7,ATB-Lys^{11}]-α–MSH by attaching ATB to the Lys^{11} residue of NLDP. Its Kd for α–MSH-R sites on the cell surface of B16 mouse melanoma was 3.75x10^{-10} M. The addition of the biotin

molecule to the ^{125}I-ATB-NLDP label, resulted in the irreversible binding of the receptor complexes to streptavidin beads. The α–MSH-R was extracted from the plasma membrane of B16 melanoma using N^{α}-Bi-SS-^{125}I-ATB-NLDP and streptavidin-coated magnetic beads (1). The incorporation of the cleavable disulphide bridge between the biotin and peptidyl ligand allowed for the elution of the MSH-R-ligand complexes from the beads with DTT (1). Although the Bi-SS-^{125}I-ATB-NLDP compound was not tested in assays for specific α–MSH-R binding, both it and the ^{125}I-ATB-NLDP probe partially purified a doublet band of 43 and 46 kDa (1). This result implies similar binding characteristics for the two labels of the α–MSH-R.

The strong affinities of both the Bi-^{125}I-ATB-NLDP and ^{125}I-ATB-NLDP photoaffinity labels make them useful tools for the labelling of the α–MSH-R during: 1) auto-radiography; 2) histological localisation at both the light and electron microscopic levels; and 3) extraction and characterisation with SDS-PAGE techniques. The ^{125}I-ATB-NLDP and the Bi-^{125}I-NLDP derivatives enabled comparisons with other ATB-NLDP analogues such as the Bi-SS-^{125}I-ATB-NLDP compound.

4.10. SITE-SELECTIVE DRUG DELIVERY TO MELANOMA CELLS VIA MSH ANALOGUES

4.10.1. INTRODUCTION

Targeting of cytotoxic agents with α–MSH analogues via the melanogenesis pathway is not a novel idea (133, 194). MSH derivatives have been studied as potential treatments for

melanoma in the following site-selective drug delivery therapies: 1) radio-therapy; 2) cytotoxic MSH related complexes; and 3) melanoma growth retardation.

Treatment with chlorpromazine is an example of creating selective enhancement of the cytotoxic effects of gamma-radiation for melanoma via the melanotropin pathway. Animals were pre-treated with chlorpromazine (which selectively binds to melanin) in order to selectively increase the radio-sensitivity of melanotic melanoma above non-melanoma cells (20). Pretreated animals showed a marked tumour regression, decreased transplant ability of melanoma, and decreased metastasis after irradiation (40). Mishima (124) proposed the use of [10]B-labelled chlorpromazine in combination with slow neutron activation of boron atoms. When compared to gamma-radiation, the [10]B isotope capture of slow neutrons can be an efficient method of killing cells causing less damage to the surrounding tissue (61). The thermal neutron-induced emission of high LET α–particles and lithium atoms have a limited travelling range equal to the diameter of individual melanoma cells (10-14 μm). [10]B-labelled chlorpromazine depressed the growth rate of malignant melanoma in hamsters and pigs (124). Mishima (125) then synthesised hybrid compounds of [10]B with analogues of the melanin precursor, DOPA. Radio-biological studies showed enhanced melanoma cell-killing effect when these compounds were used in combination with neutron-radiation. He treated 9 cases of primary and metastic melanoma lesions with the DOPA hybrid [10]B$_1$-BPA molecule (125). Unfortunately, large doses of [10]B-BPA (10,000 atoms/cell) are needed for cell death.

Liu et al (115) prepared an α–MSH/T cell receptor antibody conjugate for activation and targeting of cytotoxic T lymphocytes to melanoma. Antibodies to the CD3 component of the T cell receptor were conjugated to the N-terminal of NLDP. When the NLDP portion was bound to the α–MSH-R of melanoma cells, and the CD3 antibody was bound to T lymphocytes, significant lysis of mouse (B16-F10) and human (6137 and M1313)

145

melanoma cells occurred (115). Excess α–MSH or CD3 antibody suppressed the cytolytic effect of the conjugate. This complex was not examined *in vivo*.

4.10.2. USE OF MSH-TOXIN CONJUGATES DURING MELANOMA THERAPY

Four types of toxins have been linked to MSH analogues in an effort to target and treat melanoma: 1) daunomycin; 2) N-nitrosocaramates; 3) melphalan; and 4) diphtheria toxin.

Daunomycin attached to β–MSH was 3 fold more toxic to cultured Cloudman S91 murine melanoma than free daunomycin. It was non-toxic to 3T3 fibroblast cells (102, 186). Cytotoxicity occurred via specific interaction with MSH receptors on the cell surface (197). There were no studies for its use *in vivo*. C-terminal fragments of α–MSH coupled to 2-chloroethlnitrosocarbamoyl yielded compounds with marked growth-inhibitory actions on melanoma tumours in mice (92). Selective cytotoxicity was not achieved with α–MSH fragments containing melphalan either *in vitro* or *in vivo*. Although, the α–MSH carrier peptide was able to reduce the toxic action of melphalan (an alkylating agent) to MSH-R negative cells without affecting its anti-tumour potency (171, 172). Thus, making the α–MSH-melphalan conjugate a potentially safer therapeutic agent for melanoma.

Murphy *et al* (127) constructed a chimeric diphtheria toxin-α–MSH gene with the toxin receptor-binding domain replaced by the α–MSH gene sequence. The protein (DAB$_{389}$-MSH) was selectively toxic for human melanoma containing the α–MSH-R. Binding of DAB$_{389}$-MSH to α–MSH-Rs in biopsy specimens of human and mouse metastases was confirmed by its ability to inhibit binding of ^{125}I-NLDP. Its binding affinity for the α–

MSH-R was 3 fold lower than α–MSH in human biopsies, and 5 fold lower than ^{125}I-NLDP in mouse sections (177).

4.10.3. SITE-SELECTIVE DRUG DELIVERY WITH THE MTX-NLDP TOXIN TO MELANOMA

In this study the anti-metabolite methotrexate (MTX; 76) was attached to the N-terminus of NLDP. Methotrexate is used against a variety of cancers since its toxicity is primarily against growing, self-renewing tissues (93). It exerts its cytological action through competitive inhibition with dihydrofolate reductase (DHFR) for DHF substrates. The conjugate's ability to bind and stimulate cellular activity of α–MSH-Rs found in B16 melanoma plasma membranes, was compared to other α–MSH derivatives.

The Kd and Ec50 values obtained for the MTX-NLDP conjugate (1.54×10^{-9} M and 2.11×10^{-11} M) were similar to those observed for NLDP (2.22×10^{-9} M and 2.76×10^{-11} M). Attachment of MTX to NLDP did not compromise the peptides affinity for the α–MSH-R or its cellular response. Non-specific binding of the conjugate to the cell surface of B16 cells was comparable to ^{125}I-NLDP (12% over 8 hours at 0-4°C). The ability of MTX-NLDP to raise tyrosinase expression suggests agonistic action of the α–MSH-R, and its likely receptor-mediated internalisation (as described for ^{125}I-NLDP at 37°C). The specific binding of MTX-NLDP to the α–MSH-R with a high affinity, low non-specific binding, and probable internalisation, are all characteristics of an effective drug compound site-selectively delivered to melanoma.

147

Unfortunately, an estimated 10^6 MTX molecules are required for cell death. The low receptor numbers of α–MSH on human melanoma cells (400-2,000) and the reduction of external α–MSH binding sites after a 1 hour exposure at 37ºC, are not conducive to the intracellular accumulation of 10^6 molecules of MTX. There are 3 possible solutions to this problem: 1) replace MTX with a more potent toxin; 2) increase the number of MTX molecules per peptide and/or MSH-R; 3) up-regulation of the α–MSH-R during treatment with MTX-NLDP.

Replacing the MTX molecule with a more cytotoxic compound such as ricin would lower the number of internalised toxin molecules necessary for cell death. This approach would only be acceptable if non-melanoma binding was minimal.

Modification of NLDP to carry more MTX molecules per peptide is another option. Increasing the MTX carrier load might be achieved with a (Bi-MTX)-(Sa)-Bi-NLDP compound. This would change the MTX : NLDP ratio from 1 : 1 up to 4 : 1. The (Bi-MTX)-(Sa)-Bi-NLDP conjugate would be better suited as a site-specific toxin for melanoma since fewer receptor sites would be needed for cytotoxicity. Another means of increasing the number of MTX molecules transported by a melanotropin into the melanoma cytosol might be the attachment of MTX to a TMV-α–MSH fusion gene product (Section 4.7.). In earlier studies, the TMV-α–MSH gene product carried up to 200 rhodamine molecules per viron and displayed intracellular accumulation (202). By replacing MTX for rhodamine molecules, up to 200 MTX molecules might be carried/receptor into melanoma cells via the TMV-α–MSH gene product. Thus, activation of only 5,000 α–MSH-Rs would cause cell death.

There are a number of procedures for the up-regulation of MSH-Rs of melanoma cells. MSH receptor up-regulation has been reported with the following treatments: 1) MSH-

related compounds; 2) retinoic acid; 3) interferons; and 4) ultraviolet light. A short exposure (hours) of 10^{-6} M L-DOPA increased binding of ^{125}I-α-MSH in six human melanoma cell lines. Cyclic AMP added to the growth media also increased α-MSH-R binding with two optima at 10^{-11} M and 10^{-8} M. Added tyrosine also significantly increased specific binding of α-MSH after an hour incubation (72). These results verify earlier studies showing a 3 fold increase in the numbers of MSH-Rs after a 48 hour exposure of Cloudman mouse melanoma cells to dopa phosphates (123). The effect increased with dose. Similar results were observed with Bomirski hamster melanoma cultured for 24-48 hours in the presence of 2×10^{-4} M L-tyrosine. After the L-tyrosine treatment melanoma displayed a 3-4 fold increase in their ability to bind ^{125}I-β-MSH (162). It was suggested that compounds which activate melanogenesis, up-regulate receptor expression via a positive feedback mechanism (72).

Siegrist and Eberle (161) have found that MSH-R regulation varies with the melanoma cell line used. They observed a time and dose-dependent up-regulation of MSH-Rs in two human lines. The increase of α-MSH binding was maximal after an incubation of 24 hours with 10^{-7} M α-MSH. Up-regulation appeared to be caused by the recruitment of spare receptors since it was independent of protein synthesis. Conversely, a 12 hour incubation in α-MSH caused MSH-R down-regulation of Cloudman and B16-F1 mouse, and HBL human melanoma cells. Alpha-MSH (10^{-9} M) caused the disappearance of 85-90% of the cell surface MSH-Rs from B16-F1 melanoma cells. This down-regulation may be a consequence of receptor internalisation. Our observed decrease in binding of ^{125}I-NLDP to B16 plasma membrane receptors after an hour incubation at 37°C is in agreement with similar results for B16-F1 cells (161).

Up-regulation of the β-MSH-R (3-4 fold) was evident in Cloudman mouse melanoma cells after a 3 hour incubation in 2×10^{-6} M retinoic acid (32). Interferon's (α-, β-, and γ-) in

combination with α-MSH also increased the expression of surface MSH-Rs of a primary JB/MS murine melanoma line. There was a 2.5 fold increase in bound ligand after a 4 day combined treatment of $2x10^{-7}$ M α–MSH and interferons (94, 95).

Exposure of Cloudman melanoma cells to UVB radiation increased the binding of ^{125}I-MSH 2-10 fold within 24 hours (23). UVB radiation raised IL-1 levels in the melanoma cell supernatant. Interleukin-1 added to the growth media of melanoma cells increased the dose-dependent binding of ^{125}I-β-MSH to its receptor. Birchall et al (18) claimed ultraviolet light indirectly up-regulated both cell surface and internal MSH-R activity in Cloudman melanoma and RHEK human carcinoma cells by stimulating the secretion of interleukin-1 by these cells. In this manner, ultraviolet light might trigger an autocrine up-regulatory system of MSH-Rs of melanoma cells.

Any, or all, of these pre-treatments may increase the selective delivery of α–MSH-drugs to melanoma cells by increasing the number of available α–MSH-Rs at the cell surface.

4.11. INDUCTION OF MELANOMA GROWTH INHIBITION
WITH MELANOTROPINS

Our studies showed the growth inhibition of B16 mouse melanoma cells by the melanotropins α–MSH and NLDP. The response was time, concentration, and cell density dependent. Pulse doses of 10^{-9} M NLDP of 30 minutes per day, had no effect on melanoma growth. Melanization, dendritic process development, and cell flattening of B16 cells occurred after a 4-6 day chronic exposure to both the melanotropins. NLDP indused

a morphological change and inhibited melanoma proliferation more effectively than α–MSH.

NLDP gradually retarded melanoma growth up to 49% after 4-6 days at 10^{-9} M. This inhibition of cell growth was concentration-dependent as well as time-dependent. A clear effect was observed at 10^{-9}-10^{-7} M, but was not observed at dilutions of 10^{-10} M or lower. Apparently, a higher concentration of peptide is needed to inhibit melanoma growth than is needed for tyrosinase stimulation (Ec50 = 3×10^{-11} M). B16 cells had a similar response to α–MSH, but inhibition was less pronounced than observed with NLDP. This was expected as α–MSH is less potent than NLDP in eliciting melanoma cellular responses such as tyrosinase activity and melanin biosynthesis.

Our findings are in agreement with other studies concerning the effects of MSH on mouse melanoma (Section 1.6.2.). Pawelek *et al* (136, 141) observed similar results with Cloudman S91 murine melanoma cells. He found MSH extended the doubling time of the S91 melanoma cells from 38 to 64 hours, and caused a 25% decrease in cellular DNA. After 14 days, there was a 30% growth arrest in the Cloudman S91 PS4 sub-clone. The growth medium was changed every 3 days. Pawelek suggested MSH inhibited cell proliferation only in the G1 or early S phase of the cell cycle. Cells blocked in metaphase with colchicine had twice as much DNA than controls when melanoma cells were incubated in MSH. Wick (195) also observed growth inhibition of Cloudman melanoma cells (34%) after 3 days of 5×10^{-8} M MSH, with a cell density of 10^5 cells/well. He observed maximum inhibition after 4 days.

Both Wick and Pawelek (138, 195) found theophylline enhanced the effects of MSH. Theophylline inhibits the hydrolysis of cAMP by cyclic nucleotide phosphodiesterase, thus raising intracellular cAMP levels. Cyclic-AMP levels are raised when the MSH-R is

activated. Raised intracellular levels of cAMP have been shown to inhibit cell growth in other cell systems. These results suggest the involvement of cAMP during melanoma growth inhibition. Other MSH activated intracellular messengers which are thought to inhibit melanoma proliferation are cytosolic myoinositol phosphates and protein kinase C (28, 73, 164).

During melanogenesis, tyrosine is catalysed by tyrosinase to form dopa. Dopa also reacts with tyrosinase to form dopaquinone. A series of well characterised biosynthetic steps give rise to pigmented quinone derivatives, leading to the formation of melanochrome and melanin (Section 1.5.3.; 136). Both tyrosine and N-acetyltyrosine have been shown to be toxic to melanotic Cloudman S91 cells. The dopa analogue levodopa methyl ester, had anti-tumour activity against B16 melanoma *in vivo* (191). Dopamine was also a potent inhibitor of B16 melanoma *in vitro* and *in vivo* (193). Melanoma growth retardation by α–MSH could be caused by the accumulation of toxic melanogenic products and metabolic by-products in the surrounding cellular environments (122, 192). It is suggested that the above compounds owe their cytotoxic effect to the generation of super oxide free radicals within the cell (194). One component of the pathway, 5,6-dihydroxindole conversion factor, is thought to protect the cells from cytotoxic melanin precursors in the absence of MSH. Thus, MSH stimulated cells would undergo auto-toxicity during MSH stimulated melanogenesis. This explanation is contradictory to our results. We observed growth inhibition of B16 melanoma with frequent media changes and optimal culture conditions. Although, intracellular accumulation of cytotoxic by-products from melanogenesis were not accounted for.

Growth stimulation whs also beenreported as a cellular response to melanotropins (Section 1.6.3.). MSH has been shown to encourage metastases in melanoma. It stimulated the metastatic capacity of melanoma (118) and; increased melanoma cloning

and proliferative potentials in agar bilayers (122). It is suggested that this effect is due to MSH-induced autocrine growth factors or intracellular messengers (27, 118, 122, 205).

The cellular response of melanoma cells to MSH has been observed to be dependent on cell density, substrate, cell line, and metastatic potential. Niles and Makarski (130) found that two B16 subclones responded differently to cAMP or MSH depending on their metastatic potential. Growth of B16-F1 cells with a low metastatic potential were inhibited by MSH and cAMP while cells with a high metastatic potential (B16-F10), were not significantly effected. A correlation between the loss of hormonal regulation with increased metastatic potential might explain why some cell lines have a high colony-forming ability in the presence of MSH.

As cell density increased, Cloudman melanoma cells lost their ability to demonstrate an MSH-induced increase in tyrosinase activity (59, 121). Neither theophilline (10^{-6} M) or dibutyryl cyclic AMP (10^{-4} M), stimulated tyrosinase activity in melanoma cells cultured at densities exceeding 6×10^4 cells/cm^2. This loss in hormone responsiveness occurred before confluency was reached and was not reversed by exposure of cells to increasing concentrations of MSH (59). We observed a different effect with B16 mouse melanoma cells. We found growth inhibition (a cellular response to melanotropins) increased at B16 cell densities exceeding 1.25×10^5 cells/cm^2. Maximum inhibition occurred more quickly when the cells were seeded at higher densities. Malek *et al* (121) also reported the inhibition of melanoma cells by melanotropins, but only when they were plated at very high densities. He proposed this reduction of cell growth with an increase in cell density was caused by cell contact growth inhibition, and or, the depletion of media nutrients. Our results do not agree with the latter explanation as the cell growth media was frequently changed. Melanoma cell density may effect MSH induced tyrosinase expression and growth inhibition in different ways. It appears that hormonal control over pigment cell

153

melanogenesis and cell growth is complicated and controversial at our level of understanding.

4.12. CONCLUSION

We report the suitability of a panel of melanotropin probes as tools to localise, diagnose, monitor, and characterise and extract the α-MSH-R and its cell cycle. We also present a novel MTX-NLDP toxin conjugate which is potentially useful during melanoma therapy. Both the probes and toxin operate via an α–MSH carrier which selectively delivers compounds (probe or drug) to α–MSH-Rs found on B16 murine melanoma cells *in vitro*. Our studies also report the inhibition of B16 melanoma cell growth by melanotropins. The MSH induced growth retardation of melanoma also appears to operate via the MSH cellular pathway. This is an additional advantage for the use of melanotropins during treatment against melanoma.

Results obtained with the melanotropin probes and MTX-toxin conjugate may be summarised as follows :

1) ^{125}I-NLDP specifically binds and activates α–MSH-Rs of B16 melanoma cells *in vitro*. It is potentially useful for the localisation, diagnosis, characterisation, and monitoring agonist-α–MSH-R complexes during binding and internalisation when used in combination with cell fractionation and auto-radiographic studies.

2) CTAF-NLDP specifically binds and activates α–MSH-Rs of B16 melanoma cells *in vitro*. It has limited potential for visualising the binding, internalisation, and cellular processing of α–MSH-R agonists due to its low affinity for the α-MSH-R.

3) Bi-NLDP specifically binds and activates α–MSH-Rs of B16 melanoma cells *in vitro*. It

is a potentially useful probe for the visualisation of the binding and metabolic fate

of α–MSH-R agonists at both the light and electron microscopic levels.

4) Bi-^{125}I-NLDP specifically binds to α–MSH-Rs of B16 melanoma cells *in vitro*. It is

suitable for α–MSH-R localisation studies at the cellular (auto-radiography) and

subcellular (cell fractionation studies, light and electron microscopic studies)

levels.

5) (Sa)-Bi-^{125}I-NLDP specifically binds to α–MSH-Rs of B16 melanoma cells *in vitro*. It

allows for the possible augmentation of the probe signal when combined with

biotinylated labels.

6) (Sa–Au)-Bi-^{125}I-NLDP does not bind selectively to the α–MSH-R of B16 melanoma *in*

vitro. Thus, it is not suitable for future studies of the α–MSH-R.

7) ^{125}I-ATB-NLDP photoaffinity label specifically binds to the α–MSH-R of B16

melanoma *in vitro*. It is potentially useful for irreversibly binding and monitoring

the α–MSH-R during receptor localisation and bioactivation studies.

8) Bi-^{125}I-ATB-NLDP photoaffinity label specifically binds the α–MSH-R of B16

melanoma *in vitro*. It led to the development of the Bi-SS-^{125}I-ATB-NLDP

complex which covalently binds, localises, and allows for the partial purification

and characterisation of the α–MSH-R when used in combination with streptavidin

magnetic beads and SDS-PAGE techniques.

9) MTX-NLDP specifically binds and activates α-MSH-Rs of B16 melanoma cells *in*

vitro. It is potentially useful during site-selective delivery of the MTX toxin to

melanoma cells.

Melanotropins are potentially useful for treating melanoma. The NLDP analogue of α-

MSH both inhibits melanoma proliferation and selectively delivers a drug and probes to

the α–MSH-R of B16 melanoma cells *in vitro*. Unfortunately, the wide distribution of

radio-iodinated and tritiated α–MSH and NLDP in rodents implies the need for melanotropins to be more selective for melanoma *in vivo* (175). There needs to be a reduction in binding of melanotropins by non-melanoma tissues before MSH can be regarded seriously as a targeting agent to melanoma *in vivo*. This may not be possible considering the vast distribution of POMC related receptors within the body (Section 1.2.). Although melanotropins show promise for selective drug delivery to melanoma in culture conditions, experiments *in vivo* are often disappointing (58). Regardless, there have been many advancements in this area, and MSH-drug conjugates have been successful in selectively targeting and killing (or reducing growth) of melanoma lesions in humans (Section 4.10.). Parameters for the future role of melanotropins in the study and treatment of melanoma can only be defined by more MSH studies in animal and human models.

REFERENCES

1. Ahmed A.R.H., Olivier G.W.J., Adams G., Erskine M.E., Kinsman R.G., Branch S.K., Moss S.H., Notarianni L.J., Pouton C.W. Isolation and partial purification of a melanocyte-stimulating hormone receptor from B16 murine melanoma cells. *Biochem. J.* 286:377-382, 1992.

2. Al-Obeidi F., Hruby V.J., Hadley M.E., Sawyer T.K., Castrucci A.M. Design, synthesis, and biological activities of a potent and selective α–melanotropin antagonist. *Int J Peptide Protein Res* 35:228-234, 1990.

3. Al Zein M., Luntz-Bucher B., Koch B. Modulation by Leu-enkephalin of peptide release from perfused neurointermediate pituitary. II. Inhibition of calcium-mediated secretion of α–MSH and β–endorphin. *Neuroendocrinology* 42:248-254, 1986.

4. Arai H., Moroji T., Kosaka K., Iizuka R. Extrahypophyseal distribution of α–melanocyte-stimulating hormone (α–MSH)-like immunoreactivity in post-mortem brains from normal subjects and Alzheimer-type dementia patients. *Brain Res* 377:305-310, 1986.

5. Artursson P. The fate of micro particulate drug carriers after intravenous administration. In Illum I., Davis S.S. (eds) Polymers in controlled drug delivery pp. 15-24, 1987.

6. Atherton E., Sheppard R.C. Solid phase synthesis : a practical approach. IRL Press, Oxford, 1989.

7. Bagutti C., Eberle A.N. Synthesis and biological properties of a biotinylated derivative of $ACTH_{1-17}$ for MSH receptor studies. *J Receptor Res* 13(1-4):229-244, 1993.

8. Bajzer Z., Pavelic K., Vuc-Pavlovic S. Growth self-incitement in murine melanoma B16: a phenomenological model. *Science* 225:930-932, 1984.

9. Bard D.R., Knight C.G., Page-Thomas D.P. A chelating derivative of alpha-melanocyte-stimulating hormone as a potential imaging agent for malignant melanoma. *British J Cancer* 62:919-922, 1990.

10. Bard D.R., Knight C.G., Page-Thomas D.P. Targeting of a chelating derivative of a short-chain analogue of alpha-melanocyte-stimulating hormone to Cloudman S91 melanomas. *Biochem Soc Trans* 18:882-883, 1990.

11. Barnea A., Cho G., Pilotte N.S., Porter J. C. Regional differences in the molecular weight profiles of corticotropin and α–melanotropin in the hypothalamus. *Endocrinology* 108:150-156, 1981.

12. Bateman A., Dell A., Whitehouse B.J., Vinson G.P. Non-ACTH components of adult human pituitary extracts which stimulate adrenal steroidogenesis. *Neuropeptides* 7:381-390, 1986.

13. Bertagna X., Lenne F., Comar D., Massias J.F., Wajcman H., Baudin V., Luton J.P., Girard F. Human β–melanocyte-stimulating hormone revisited. *Proc Natl Acad Sci USA* 83:9719-9723, 1986.

14. Beynon R.J., Bond J.S. Proteolytic enzymes a practical approach. Oxford University Press, Oxford.

15. Birnbaumer L. Which G protein subunits are the active mediators in transduction? *Trends Pharmacol Sci* 8:109-211, 1987.

16. Bitensky M.W., Demopoulos H.B. Activation of melanoma adenyl cyclase by MSH. *J Invest Dermatol* 54:83, 1970.

17. Bitensky M.W., Demopoulos H.B., Russell V. MSH-responsive adenyl cyclase in the Cloudman S91 melanoma. In Riley V (ed) Pigmentation, its genesis and biologic control, pp. 247-255, Appleton-Century-Crofts, New York, 1973.

18. Birchall N., Orlow S.J., Kupper T., Pawelek J. Interactions between ultraviolet-light and interleukin-1 on MSH binding in both mouse melanoma and human squamous carcinoma-cells. *Biochem Biophys Res Comm* 175(3):839-845, 1991.

19. Bjorklund A., Nobin A. Fluorescence histochemical and microspectrofluorimetric mapping of dopamine and noradrenaline cell groups in the rat diencephalon. *Brain Res* 51:193-205, 1973.

20. Blois M.S. On chlorpromazine binding *in vivo*. *J Invest Dermatol* 45:475-481, 1965.

21. Bogdahn U., Apfel R., Hahn M., Gerlach M., Behl C., Hoppe J., Martin R. Autocrine tumour-cell growth-inhibiting activities from human-malignant melanoma. *Cancer Res* 49:5358-5363, 1989.

22. Bolander F.F. Molecular Endocrinology. pp. 64-76, Academic Press, London, 1989.

23. Bolognia J., Murray M., Pawelek J.M. UVB-induced melanogenesis may be mediated through the MSH-receptor system. *Soc Invest Derm* 92(5):651-656, 1989.

24. Bolognia J.L., Myerson N., Pawelek J.M. Ultraviolet light-induced pigmentation of Cloudman S91 melanoma cells requires the cyclic AMP system. *J Invest Derm* 96(4):632, 1991.

25. Bordoni R., Fine R., Murray D., Richmond A. Characterisation of the role of melanoma growth stimulatory activity (MGSA) in the growth of normal melanocytes, nevocytes, and malignant melanocytes. *J Cell Biochem* 44:207-219, 1990.

26. Bowley T.J., Rance T.A., Baker B.I. Measurement of immunoreactive α–melanocyte-stimulating hormone in the blood of rainbow trout, kept under different conditions. *J Endocrinology* 97:267-275, 1983.

27. Bregman M.D., Malek Z.A.A., Meyskens F.L. Anchorage-independent growth of murine melanoma in serum-less media is dependent on insulin or melanocyte-stimulating hormone. *Exp Cell Res* 157:419-428, 1985.

28. Brooks G., Wilson R.E., Dooley T.P., Goss M.W., Hart I.R. Protein kinase C down-regulation, and not transient activation, correlates with melanocyte growth. *Cancer Res* 51:3281-3288, 1991.

29. Buffey J., Thody A.J., Bleehen S.S., Mac Neil S. Alpha-melanocyte-stimulating hormone stimulates protein kinase C activity in murine B16 melanoma. *J Endocrinology* 133:333-340, 1991.

30. Bustamante J., Guerra L., Bredeston L., Mordoh J., Boveris, A. Melanin content and hydroperoxide metabolism in human melanoma cells. *Exp Cell Res* 196:172-176, 1991.

31. Chakraborty A.K., Mishima Y., Inazu M., Hatta S., Ichihashi M. Melanogenic regulatory factors in coated vesicles from melanoma cells. *J Invest Derm* 93:616-620, 1989.

32. Chakraborty A.K., Orlow S.J., Pawelek J.M. Stimulation of the receptor for melanocyte-stimulating hormone by retinoic acid. *FEBS Letters* 276(1-2):205-208, 1990.

33. Chakraborty A.K., Pawelek J.M. Internal binding sites for MSH in Cloudman S91 melanoma cells co-purify with coated vesicles and are regulated by UVB radiation. *J Invest Derm* 94(4):512, 1990.

34. Chakraborty, A.K. Orlow, S.J, Bolognia, J.L. Pawelek J.M. Structural/functional relationships between internal and external MSH receptors: modulation of expression in Cloudman melanoma cells by UVB radiation. *J Cell Physiol* 147:1-6, 1991.

35. Chang A.C.Y., Cochet M., Cohen S.N. Structural organisation of human genomic DNA encoding the pro-opiomelanocortin peptide. *Proc Natl Acad Sci USA* 77:4890-4894, 1980.

36. Chaturvedi A.N., Knittel J.J., Hruby V.J., de L. Castrucci A.M., Hadley M.E. Highly potent peptide hormone analogues: synthesis and biological actions of biotin-labelled melanotropins. *J Med Chem* 27:1406-1410, 1984.

37. Chaturvedi A.N., Hruby V.J., Castrucci A.M., Kreutzfeld K.L., Hadley, M.E. Research articles: synthesis and biological evaluation of the superagonist [N-Chlorotriazinylaminofluorescein-Ser¹,Nle⁴,D-Phe⁷]-alpha-MSH. *J Pharm Sci* 74(3):237-240, 1985.

38. Chhajlani V., Wikberg J.E.S. Molecular cloning and expression of the human melanocyte-stimulating hormone receptor cDNA. *FEBS Letters* 309(3):417-420, 1992.

39. Cobb J.P., McGrath A. *In vitro* effects of melanocyte-stimulating hormone, adrenocorticotropic hormone, 17 β–estradiol, or testosterone propionate on Cloudman S91 mouse melanoma cells. *J Natl Cancer Inst* 52:567-570, 1974.

40. Cooper M., Mishima Y. The radio-response of malignant melanomas pretreated with chlorpromazine. In Kawamura T. et al (eds) Biology of normal and abnormal melanocytes, pp 141-147, University of Tokyo Press, Tokyo, 1971.

41. Daynes R.A., Robertson B.A., Cho B.H., Burnham D.K., Newton R. α–Melanocyte-stimulating hormone exhibits target cell selectivity in its capacity to affect interleukin 1-inucible responses *in vivo* and *in vitro. J Immunology* 139:103-109, 1987.

42. Deschodt-Lanckman M., Vanneste Y., Loir B., Michel A., Libert A., Ghanem G., Lejeune F. Degradation of alpha-MSH by calla/endopeptidase 24.11 expressed by human melanoma cells in culture. *Int J Cancer* 46:1124-1130, 1990.

43. DiPasquale A., Varga J.M., Moellmann G., McGuire J. Synthesis of a hormonally active conjugate of alpha-MSH, ferritin, and fluorescein. *Analytical Biochem* 84:37-48, 1978.

44. Donatien P.D., Hunt G., TaYeb A., Lunec J., Thody A.J. The demonstration of functional MSH receptors on cultured human melanocytes. *J Endocrinology*. 132:124-128, 1992.

45. Dorr R.T., Dawson B.V., Al-Obeidi F., Hadley M.E., Levine N., Hruby V.J. Toxicological studies of a super potent α–melanotropin, [Nle⁴,D-Phe⁷]α–MSH. *Invest New Drugs* 6:251-258, 1988.

46. Drouin J., Goodman H.M. Most of the coding region of rat ACTH/ β–LPH precursor gene lacks intervening sequences. *Nature* 288:610-613, 1980.

47. Dupont A., Kastin A.J., Labrie F., Pelletier G., Puvianti, R., Schally A.V. Distribution of radioactivity in the organs of the rat and mouse after injection of [125I]alpha-melanocyte-stimulating hormone. *J Endocrinology* 64:237-241, 1975.

48. Durkacz B.W., Lunec J., Grindley H., Griffin S., Horner O., Simm A. Murine melanoma cell differentiation and melanogenesis induced by poly(ADP-ribose) polymerase inhibitors. *Exp Cell Res* 202:287-291, 1992.

49. Eberle A., Hubscher W. Alpha-melanotropin labelled at its tyrosine[2] residue: synthesis and biological activities of 3'-iodotyrosine[2], 3'-[125]iodotyrosine[2], 3',5'-diiodotyrosine[2]-, and (3',5'-[3]H$_2$)tyrosine[2]-α–melanotropin, and related peptides. *Helv Chem Acta* 62(7):2460-2483, 1979.

50. Eberle A.N., de Graan P.N.E., Hubscher W. Synthesis and biological properties of p-azidophenylalanine[13]-α–melanotropin, a potent photoaffinity label for MSH receptors. *Helv Chim Acta* 64:2645-2653, 1981.

51. Eberle A.N., de Graan P.N.E. General principles for photoaffinity labelling of peptide hormone receptors. *Methods Enzymol* 109:129-156, 1985.

52. Eberle A.N. The melanotropins: chemistry, physiology and mechanisms of action. Karger, Basel, 1988.

53. Eberle A.N., Verin V.J., Solca F., Siegrist W., Kuenlin C., Bagutti C., Stutz S., Girard J. Biologically active monoiodinated α–MSH derivatives for receptor binding studies using human melanoma cells. *J Receptor Res* 11(1-4):311-322, 1991.

54. Eisinger M., Marko O., Darzynkiewicz Z., Houghton A.N. Long-term cultures of normal human melanocytes in the presence of phorbol esters: characterisation of the differentiated phenotype. In: Bagnara J., and et al (eds) Pigment Cell, pp. 377-388, University of Tokyo Press, Tokyo, 1985.

55. Evans C.J., Lorenz R., Weber E., Barchas J.D. Variants of α–melanocyte-stimulating hormone in rat brain and pituitary: evidence that acetylated α–MSH exists only in the intermediate lobe of the pituitary. *Biochem Biophys Res Commun* 106:910-919, 1982.

56. Fitzpatrick T.B., Szabo G., Seiji M., Quevedo W.C. Biology of melanin pigmentary system. In Fitzpatrick T.B., Eisen A.Z., Wolff K., Freedberg I.M., Austen K.F. (eds) Dermatology in general medicine, pp. 131-163, McGraw-Hill, New York, 1979.

57. Fritsch P., Varga J.M. Melanocyte-stimulating hormone receptors on cultured guinea-pig melanocytes. *J Invest Dermatol* 67:538-540, 1976.

58. Friend D.R., Pangburn S. Site-specific drug delivery. *Medicinal Research Reviews* 7(1):53-106, 1987.

59. Fuller B.B., Lebowitz J. Decay of hormone responsiveness in mouse melanoma cells in culture as a function of cell density. *J Cellular Physiol* 103:279-287, 1980.

60. Fuller B.B., Lunsford J.B., Iman D.S. α–Melanocyte-stimulating hormone regulation of tyrosinase in Cloudman S91 mouse melanoma cell culture. *J Biol Chem* 262:4024-4033, 1987.

61. Gabel D., Holstein H., Larsson B., Gille L., Ericson, Sacker D., Som P., Fairchild R.G. Quantitative neutron capture radiography for studying the biodistribution of tumour-seeking boron-containing compounds. *Cancer Res* 47:5451-5454, 1987.

62. Gantz I., Konda Y., Tashiro T., Shimoto Y., Miwa H., Munzert G., Watson S.J., DelValle J., Yamada T. Molecular cloning of a novel melanocortin receptor. *J Biol Chem* 268:8246-8250, 1993.

63. Gerst J.E., Sole J., Mather J.P., Salomon Y. Regulation of adenylate cyclase by β–melanotropin in the M2R melanoma cell line. *Mol Cell Endocrinology* 46:137-147, 1986.

64. Gerst J.E., Sole J., Salomon Y. Dual regulation of β–melanotropin receptor function and adenylate cyclase by calcium and guanosine nucleotides in the M2R melanoma cell line. *Mol Pharmacology* 31:81-88, 1987.

65. Gerst J.E., Salomon Y. Inhibition by melittin and fluphenazine of melanotropin receptor function and adenylate cyclase in M2R melanoma cell membranes. *Endocrinology* 121:1766-1772, 1987.

66. Gerst J.E., Salomon Y. A synthetic analogue of the calmodulin-binding domain of myosin light chain kinase inhibits melanotropin receptor function and activation of adenylate cyclase. *J Biol Chem* 263(15):7073-7078, 1988.

67. Gerst J., Miriam B., Schimmer A., Salomon Y. Phorbol ester impairs melanotropin receptor function and stimulates growth of cultured M2R melanoma cells. *Euro J Pharm.* 172:29-39, 1989.

68. Gerst, J., Salomon Y. Calcium and guanosine nucleotide modulation of melanotropin receptor function and adenylate cyclase in the M2R melanoma cell line. *NATO ASI SER SER A* 133:117-126, 1990.

69. Geschwind I.I. Chemistry of the melanocyte-stimulating hormones. In Della Porta G., Muhlbock O. (eds) Structure and control of the melanocyte, pp. 28-44, Springer, Berlin, 1966.

70. Geschwind I.I., Horowitz J.M., Mikuckis G.M., Dewey R.D. Iontophoretic release of cyclic AMP and dispersion of melanosomes within a single melanophore. *J Cell Biol* 74:923-939, 1977.

71. Ghanem G.E., Comunale G., Libert A.J., Vercammen-Grandjean A., Lejeune F.J. Evidence for alpha-melanocyte-stimulating hormone (α–MSH) receptors on human malignant melanoma cells. *Int J Cancer* 41:248-255, 1988.

72. Ghanem G., Verstegen J., De Rijcke S., Hanson P., Van Onderbergen A., Libert A., Del Marmol V., Arnould R., Vercammen-Grandjean A., Lejeune F. Studies on factors influencing human plasma α–MSH. *Anticancer Res* 9:1691-1696, 1989.

73. Gordon P.R., Gilchrest B.A. Human melanogenesis is stimulated by diacylglycerol. *J Invest Derm* 93(5):700-702, 1989.

74. Gossuin A., Ghanem G., Temmerman A., Coel J., Henry P.E., Legros, F. ^{125}I-α–MSH binding in human melanoma cell lines. *Protides Biol Fluids* 29:555-558, 1982.

75. Green N.M. Avidin. In Anfinsen C.B., Edsall J.T., Richards F.M. (eds) Advances in protein chemistry, volume 29. pp. 85-130, Academic Press, London, 1975.

76. Griffin J.P., Krakoff I.H. Cancer chemotherapy: part VI. antimetabolites-methotrexate. *Hospital Formulary*:254-265, 1980.

77. Griffiths E.C., McDermott J.R. Biotransformation of neuropeptides. *Neuroendocrinology* 39:573-581, 1984.

78. Harris J.L., Lerner A.B. Amino-acid sequence of the α-melanocyte-stimulating hormone. *Nature* 179:1346-1347, 1957.

79. Halaban, R., Lerner A.B. The dual effect of melanocyte-stimulating hormone (MSH) on the growth of cultured mouse melanoma cells. *Exp Cell Res* 108:111-117, 1977.

80. Halaban R., Lerner A.B. Tyrosinase and inhibition of proliferation of melanoma cells and fibroblasts. *Exp Cell Res* 108:119-125, 1977.

81. Halaban R., Pomerantz S.H., Marshall S., Lambert D.T., Lerner A.B. Regulation of tyrosinase in human melanocytes grown in culture. *J Cell Biol* 97:480-488, 1983.

82. Hatta S., Mishima Y., Ichihashi M., Ito S. Melanin monomers within coated vesicles and premelanosomes in melanin synthesising cells. *J Invest Dermatol* 91:181-184, 1988.

83. Herlyn M., Mancianti M.L., Jambrosic J., Bolen J.B., Koprowski H. Regulatory factors that determine growth and phenotype of normal human melanocytes. *Exp Cell Res* 79:322-331, 1988.

84. Hill S.E., Buffey J., Thody A.J., Oliver I., Bleehen S.S., MacNeil S. Investigation of the regulation of pigmentation in alpha-melanocyte-stimulating hormone responsive and unresponsive cultured B16 melanoma cells. *Pigment Cell Res* 2:161-166, 1989.

85. Hirobe T., Takeuchi T. Induction of melanogenesis *in vitro* in the epidermal melanoblasts of new-born mouse skin by MSH. *In vitro Cell Dev Biol* 13:311-315, 1977.

86. Hirobe T. Melanocyte-stimulating hormone induces the differentiation of mouse epidermal melanocytes in serum-free culture. *J Cellular Physiol* 152(2):337-345, 1992.

87. Hopkins, C. Coated pits and their role in membrane receptor internalisation. In Cohen, Houslay (eds) Molecular mechanisms of transmembrane signalling pp. 337-357, Elsevier Science Publishers, 1985.

88. Horikoshi T., Onodera H., Miura S., Hanada N., Takahashi H. The possible role of protein kinase C in the regulation of melanocyte growth and pigmentation. *Clinical Res* 38(2):536, 1990.

89. Horowitz J.M., Mikuckis G.M., Longshore M.A. The response of single melanophores to extracellular and intracellular iontophoric injection of melanocyte-stimulating hormone. *Endocrinology* 106:770-777, 1980.

90. Howe A., Thody A.J. Histochemical differentiation of oxidative enzymes in the adenohypophysis of the pig, with particular reference to the pars intermedia. *J Endocrinology* 39:351-359, 1967.

91. Ito K., Takeuchi T. Melanocyte differentiation in black-eyed white mice. In Seiji M. (ed) Pigment Cell pp. 185-188, University of Tokyo Press, Tokyo, 1981.

92. Jeney A., Kopper L., Nagy P., Lapis K., Suli-Vargha H., Medzihradszky K. Anti-tumour action of N-(2-choroethyl)-N-nitrosocarbamoyl derivatives of biologically active polypeptide hormone fragments. *Cancer Chemother Pharmacol* 16:129-132, 1986.

93. Jolivet J., Cowan K.H., Curt G.A., Clendeninn N.J. and Chabner B. A. The pharmacology and clinical use of methotrexate. *New Eng J Med* 3:1094-1102, 1983.

94. Kameyama K., Montague P.M., Hearing V.J. Expression of melanocyte-stimulating hormone receptors correlates with mammalian pigmentation, and can be modulated by interferons. *J Cellular Physio* 137:35-44, 1988.

95. Kameyama K., Tanaka S., Ishida Y., Hearing V.J. Interferons modulate the expression of hormone receptors on the surface of murine melanoma cells. *J Clinical Invest* 83:213-221, 1989.

96. Kastin A.J., Schally A.V., Viosca S., Miller M.C. MSH activity in plasma and pituitaries of rats after various treatments. *Endocrinology* 84:20-27, 1969.

97. Kennelly P.J., Krebs E.G. Mini review: consensus sequences as substrate specificity determinants for protein kinases and protein phosphatases. *J Biol Chem* 266(24):15555-15558, 1991.

98. Kitano, Y. Stimulation by melanocyte-stimulating hormone and dibutyryl adenosine 3,5-cyclic monophosphate of DNA synthesis in human melanocytes. *Arch Derm Res* 257:47-52, 1976.

99. Kitano, Y. Effects of melanocyte-stimulating hormone and theophylline on human melanocytes *in vitro*. *Arch Derm Res* 255:163-168, 1976.

100. Lee T.H., Lee M.S., Lu M. Effects of α–MSH on melanogenesis and tyrosinase of B16 melanoma. *Endocrinology* 91:1180-1188, 1972.

101. Lee T.H., Lee M.S. MSH-specific desensitisation of MSH-sensitive adenylate cyclase of mouse melanoma. *Pigment Cell* 4:130-135, 1979.

102. Leffert H.L., Moran T., Boorstein R., Koch K.S. Melanotropin-daunomycin conjugate shows receptor-mediated cytotoxicity in cultured murine melanoma cells. *Nature* 267:56-61, 1977.

103. Legros F., Coel J., Doyen A., Hanson P., Van Tieghem N., Vercammen-Grandjean, A., Fruhling J., Lejeune F.J. Alpha-melanocyte-stimulating hormone binding and biological activity in a human melanoma cell line. *Cancer Res* 41:1539-1544, 1987

104. Lerner A.B., Shizume K., Bunding I. The mechanism of endocrine control of melanin pigmentation. *J Clin Endocrinol Metab* 14:1463-1490, 1954.

105. Lerner A.B., Lee T.H. Isolation of a homogeneous melanocyte-stimulating hormone from hog pituitary gland. *J Am Chem Soc* 77:1066-1067, 1955.

106. Lerner A.B., Takahashi Y. Hormonal control of melanin pigmentation. *Recent Prog Hormone Res* 12:303-320, 1956.

107. Lerner A.B., McGuire J.S. Effect of α– and β–melanocyte-stimulating hormones on the skin colour of man. *Nature* 189:176-179, 1961.

108. Lerner A.B. On the aetiology of vitiligo and grey hair. *Am J Med* 51:141-147, 1971.

109. Lerner A.B. Melanocyte-stimulating hormones (MSH); bioassay. In Berson S.A., Yalow R.S. (eds) Methods in investigative and diagnostic endocrinology, pp. 411-415, North-Holland, Amsterdam, 1973.

110. Levitzki A. Regulation of hormone-sensitive adenylate cyclase. *Trends Pharmacol Sci* 8:299-303, 1987.

111. Lichtstein D., Rodbard D. A second look at the second messenger hypothesis. *Life Sci* 40:2041-2051, 1987.

112. Limbird L.E. Cell surface receptors: a short course on theory and methods. Martinus Nijhoff Pub, Boston, 1986.

113. Ling N., Ying S., Minick S., Guillemin R. Synthesis and biological activity of four γ–melanotropin peptides derived from the crypic region of the adrenocorticotropin/ β–lipotropin precursor. *Life Sci* 25:1773-1780, 1979.

114. Lipton J.M. MSH in CNS control of fever and its influence on inflammation/immune responses. In Hadley M.E. (ed) The melanotropic peptides, Vol 2, CRC Press, Boca Raton, 1988.

115. Liu M.A., Nussbaum S.R., Eisen H.N. Hormone conjugated with antibody to CD3 mediates cytotoxic T cell lysis of human melanoma cells. *Science* 239:396-398, 1988.

116. Lucas A.M., Thody A.J., Shuster S. The role of calcium in MSH stimulated melanosome dispersion. *Peptide* 8:955-960, 1987.

117. Lucas A.M. Thody A.J., Shuster S. Role of protein kinase C in the pigment cell of the lizard (Anolis carolinensis). *J Endocrinology* 112:283-287, 1987.

118. Lunec J., Fisher C., Parker C., Sherbet G.V., Thody A.J. Possible autocrine control of growth and progression of melanoma by α–MSH. *Brit J Cancer* 58(2):227, 1988.

119. MacNeil S., Buffey J., Hill S.H., Dobson J., Bleehen S.S. Intracellular signalling in the control of melanogenesis. *Pigment Cell Res Sup* 2:154-161, 1992.

120. Malek, Z.A.A., Kreutzfeld K.L., Marwan M.M., Hadley M.E., Hruby V.J., Wilkes B.C. Prolonged stimulation of S91 melanoma tyrosinase by [Nle⁴,D-Phe⁷]-substituted alpha-melanotropins. *Cancer Res* 45:4735-4740, 1985.

121. Malek Z.A.A., Kreutzfeld K.L. Hadley M.E., Bregman M.D., Hruby V.J., Meyskens F.L. Long-term and residual melanotropin-stimulated tyrosinase activity in S91 melanoma cells is density dependent. *In vitro Cell Dev Biol* 22:75-81, 1986.

122. Malek, Z.A.A., Hadley, M.E., Bregman, M.D., Meyskens, F.L. and Hruby, V.J. Actions of melanotropins on mouse melanoma cell growth *in vitro*. *JNCI* 76:857-863, 1986.

123. McLane J., Osber M., Pawelek J.M. Phosphorylation isomers of L-dopa stimulate MSH binding-capacity and responsiveness to MSH in cultured melanoma-cells. *Biochem Biophys Res Comm* 145(2):719-725, 1987.

124. Mishima Y. Neutron capture treatment of malignant melanoma using ^{10}B-chlorpromazine compound. Pigment Cell pp. 215-221 Karger, Basel, 1973.

125. Mishima Y. A post melanosomal era: control of melanogenesis and melanoma growth. *Pigment Cell Res Suppl* 2:3-16, 1992.

126. Mountjoy K.G., Robbins L.S., Mortrud M.T., Cone R.D. The cloning of a family of genes that encode the melanocortin receptors. *Science* 257:1248-1251, 1992.

127. Murphy J.R., Bishai W., Borowski M., Miyanohara A., Boyd J., Nagle S. Genetic construction, expression, and melanoma-selective cytotoxicity of a diphtheria toxin-related α–melanocyte-stimulating hormone fusion protein. *Proc Natl Acad Sci USA* 83:8258-8262, 1986.

128. Nakanishi S., Inoue A., Kita T., Nakamura M., Chang A.C.Y., Cohen S.N., Numa S. Nucleotide sequence of cloned cDNA for bovine corticotropin-β–lipotropin precursor. *Nature* 278:423-427, 1979.

129. Nakanishi S., Teranishi Y., Noda M., Notake M., Watanabe Y., Kakidani H., Jingami H., Numa S. The protein-coding sequence of the bovine ACTH-β–LHP precursor gene is split near the signal peptide region. *Nature* 287:752-755, 1980.

130. Niles R.M., Makarski J.S. Hormonal activation of adenylate cyclase in mouse melanoma metastatic variants. *J Cell Physiol* 96:355-360, 1978.

131. Nishizuka Y. Studies and perspectives of protein kinase C. *Science* 233:305-312, 1986.

132. Orlow S.J., Hotchkiss S., Pawelek J.M. Internal binding sites for MSH: analyses in wild-type and variant Cloudman melanoma cells. *J Cellular Physiol* 142:129-136, 1990.

133. Panasci L.C., McQuillan A., Kaufman M. Biological activity, binding, and metabolic fate of Ac-[Nle^4,D-Phe^7]α–MSH$_{4-11}$NH$_2$ with the F1 variant of B16 melanoma cells. *J Cell Physiol* 132:97-103, 1987.

134. Pankovich J.M., Jimbow K. Tyrosine transport in a human-melanoma cell-line as a basis for selective transport of cytotoxic analogues. *Biochem J* 280:721-725, 1992.

135. Parker C.R., Porter J.C., Subcellular localisation of immunoreactive α–melanocyte-stimulating hormone in human brain. *Brain Res Bull* 4:535-538, 1979.

136. Pawelek J.M., Wong G., Sansone M., Morowitz J. Molecular biology of pigment cells: molecular controls in mammalian pigmentation. *Yale J Biol Med* 46:430-443, 1973.

137. Pawelek J.M., Sansone M., Koch N., Christie G., Halaban R., Hendee J., Lerner A.B., Varga J. Melanoma cells resistant to inhibition of growth by melanocyte-stimulating hormone. *Proc Natl Acad Sci USA* 72(3):951-955, 1975.

138. Pawelek J.M. Factors regulating growth and pigmentation of melanoma cells. *J Invest Derm* 66(4):201-209, 1976.

139. Pawelek J.M., Lerner A.B. 5-6-dihydroxyindole is a melanin precursor showing potent cytotoxicity. *Nature* 276:627-628, 1978.

140. Pawelek J.M., Korner A., Bergstrom A., Bolognia J. New regulators of melanin biosynthesis and the autodestruction of melanoma cells. *Nature* 286:617-619, 1980.

141. Pawelek, J., Bolognia, J., McLane, J., Murray, M., Osber, M. and Slominski, A. A possible role for melanin precursors in regulating both pigmentation and proliferation of melanocytes. *Prog Clin Biol Res* 256:143-154, 1990.

142. Pedersen R.C., Ling N., Brownie A.C. Immunoreactive γ-melanotropin in rat pituitary and plasma: a partial characterisation. *Endocrinology* 110:825-834, 1982.

143. Pichon F., Lagarde A.E. Autoregulation of MeWo metastatic melanoma cell growth: characterisation of intracellular (FGF, MGSA) and secreted (PDGF) growth factors. *J Cell Physiol* 140: 344-358, 1989.

144. Pomerantz S.H. The tyrosine hydroxylase activity of mammalian tyrosinase. *J Biol Chem* 241(1):161-168, 1966.

145. Prota G., Nicolaus R.A. On the biogenesis of phaeomelanins. *Adv Biol Skin* 8:323-328, Pergamon Press, Oxford, 1967.

146. Quevedo W.C. Fitzpatrick T.B., Szabo G., and Jimbow K. Biology of melanocytes. In Fitzpatrick T.B., Eisen A.Z., Wolff K., Freedberg I.M., Austen K.F. (eds) Dermatology in general medicine pp. 224-250, McGraw-Hill, New York, 1979.

147. Robertson B.A., Gahring L.C., Daynes R.A. Neuropeptide regulation of interleukin-1 activities. Capacity of α–melanocyte-stimulating hormone to inhibit interleukin-1-inducible responses *in vivo* and *in vitro* exhibits target cell selectivity. *Inflammation* 10:371-385, 1986.

148. Rodeck U., Melber K., Kath R., Menssen H., Varello M., Atkinson B., Herlyn M. Constitutive expression of multiple growth factor genes by melanoma cells but not normal melanocytes. *Society Invest Derm* 97(1):20-25, 1991.

149. Salomon, Y. Melanocortin receptors: targets for control by extracellular calcium. *Mol Cell Endrocrinol* 70:139-145, 1990.

150. Sawyer T.K., Sanfilippo P.J., Hruby V.J., Engel M.H., Heward C.B., Burnett J.B., Hadley M.E. 4-Norleucine,7-D-phenylalanine-α–melanocyte-stimulating hormone: a highly potent α–melanotropin with ultralong biological activity. *Proc Natl Acad Sci USA* 77:5754-5758, 1980.

151. Schliwa M. Aspects of cytoskeletal organisation in fish chromatophores. In Seiji M. (ed) Pigment Cell pp. 409-414 University of Tokyo Press, Tokyo, 1981.

152. Scimonelli T., Eberle A.N. Photoaffinity labelling of melanoma cell MSH receptors *FEBS Letters* 226:134-138, 1987.

153. Sheppard J.R., Kerr S.T., Brown D.R., Burger M.M. Lectin-resistant B16 melanoma cells exhibit an altered response to MSH and cholera toxin. *Exp Cell Res* 149:577-581, 1983.

154. Shizume K. 35 years of progress in the study of MSH. *Yale J Biol Med* 58(6):561-570, 1985.

155. Siegrist W., Eberle A.N. In situ melanin assay for MSH using mouse B16 melanoma cells in culture. *Analytical Biochem* 159:191-197, 1986.

156. Siegrist W., Oestreicher M., Stutz S., Girard J., Eberle A.N. Radioreceptor assay for α–MSH using mouse B16 melanoma cells. *J Receptor Res* 8(1-4):323-343, 1988.

157. Siegrist W., Stutz S., Girard J., Eberle A.N. Binding assay for the study of melanoma cell MSH receptors. In Bresciani F., King R.J.B., Lippman M.E., Raynaud J.P. (eds) Progress in Cancer Research and Therapy, Vol. 35: Hormones and Cancer 3, pp. 314-317, New York: Raven Press Ltd, 1988.

158. Siegrist W., Solca F., Stutz S., Giuffre L., Carrel S., Girard J., Eberle A.N. Characterisation of receptors for alpha-melanocyte-stimulating hormone on human melanoma cells. *Cancer Res* 49:6352-6358, 1989.

159. Siegrist W., Girard J., Eberle A.N. Quantification of MSH receptors on mouse melanoma tissue by receptor autoradiography. *J Receptor Res* 11(1-4):323-331, 1991.

160. Siegrist W., Bagutti C., Solca F., Girard J., Eberle A.N. MSH receptors on mouse and human melanoma cells: receptor identification, analysis and quantification. *Prog Histochem Cytochem* 26(1-4):110-118, 1992.

161. Siegrist W., Eberle A.N. Homologous regulation of the MSH receptor in melanoma cells. *J Receptor Res* 13(1-4):263-281, 1993.

162. Slominski A., Pawelek J. MSH binding in Bomirski amelanotic hamster melanoma cells is stimulated by L-tyrosine. *Biosci Reports* 7(12):949-954, 1987.

163. Slominski A., Moellmann G., Kuklinska E. MSH inhibits growth in a line of amelanotic hamster melanoma-cells and induces increases in cyclic-AMP levels and tyrosinase activity without inducing melanogenesis. *J Cell Science* 92:351-359, 1989.

164. Slominski A., Costantino R. Molecular mechanism of tyrosinase regulation by L-dopa in hamster melanoma cells. *Life Science* 48:2075-2079, 1991.

165. Slominski A., Costantino R., Wortsman J., Paus R., Ling N. Melanotropic activity of γ– MSH peptides in melanoma cells. *Life Science* 50:1103-1108, 1992.

166. Solca F., Siegrist W., Drozdz R., Girard J., Eberle A.N. The receptor for alpha-melanotropin of mouse and human melanoma cells: application of a potent α–melanotropin photoaffinity label. *J Biol Chem* 264(24):14277-14281, 1989.

167. Solca, F.F., Salomon, Y. and Eberle, A.N. Heterogeneity of the MSH receptor among B16 murine melanoma subclones. *J Receptor Res* 11(1-4):379-390, 1991.

168. Stoeckel M.E., Schmitt G., Porte A. Fine structure and cytochemistry of the mammalian pars intermedia. *Ciba Found Symp* 81:101-122, 1981.

169. Stoeckel M.E., Schimchowitsch S., Garaud J.C., Schmitt G., Vaudry H., Porte A. Immunocytochemical evidence of intragranular acetylation of α-MSH in the melanotrophic cells of the rabbit. *Cell Tissue Res* 230:511-515, 1983.

170. Sugumaran M., Dali H., Semensi V. The mechanism of tyrosinase-catalysed oxidative decarboxylation of α-(3,4-dihydroxyphenyl)-lactic acid. *Biochem J* 277:849-853, 1991.

171. Suli-Vargha H., Jeney A., Kopper L., Olah J., Lapis K., Botyanszki J., Csukas I., Gyorvari B., Medzihradszky K. Investigations on the antitumour effect and mutagenicity of alpha-MSH fragments containing melphalan. *Cancer Letters* 54:157-162, 1990.

172. Suli-Vargha H., Botyanszi J. Medzihradszkyschweiger H., Medzihradszky K. Synthesis of α-MSH fragments containing phenylalanine mustard for receptor studies. *Intern J Peptide Protein Res* 36(3):308-315, 1990.

173. Tanaka K., Nicholson W.E., Orth D.N. Diurnal rhythm and disappearance half-time of endogenous plasma immunoreactive β-MSH (LPH) and ACTH in man. *J Clin Endocrinol Metabolism* 46:883-890, 1978.

174. Tanaka I., Nakai Y., Jingami H., Fukata J., Nakao K., Oki S., Nakanishi S., Numa S., Imura H. Existence of gamma-melanotropin (γ-MSH)-like immunoreactivity in bovine and human pituitary glands. *Biochem Biophys Res Comm* 94:211-217, 1980.

175. Tatro J.B., Reichlin S. Specific receptors for alpha-melanocyte-stimulating hormone are widely distributed in tissues of rodents. *Endocrinology* 121(5):1900-1907, 1987.

176. Tatro J.B., Entwistle M., Lester B.R., Reichlin S. Melanotropin receptors of murine melanoma characterised in cultured cells and demonstrated in experimental tumours in Situ. *Cancer Res* 50:1237-1242, 1990.

177. Tatro J.B., Wen Z., Entwistle M.L., Atkins M.B., Smith T.J., Reichlin S., Murphy J.R. Interaction of an alpha-melanocyte-stimulating hormone-diphitheria toxin fusion protein with melanotropin receptors in human-melanoma metastases. *Cancer Res* 52:2545-2548, 1992.

178. Taylor C.W. Review article: the role of G proteins in transmembrane signalling. *Biochem J* 272:1-13, 1990.

179. Thody A.J., Wilson C.A. Melanocyte-stimulating hormone and the inhibition of sexual behaviour in the female rat. *Physiol Behaviour* 31:67-72, 1983.

180. Tilders F.J.H., Parker C.R., Barnea A., Porter J.C. The major immunoreactive α–melanocyte-stimulating hormone (α–MSH)-like substance found in human fetal pituitary tissue is not α–MSH but may be desacetyl α–MSH (adrenocorticotropin$_{1-13}$NH$_2$). *J Clin Endocrinol Metab* 52:319-323, 1981.

181. Tilders F.J.H., Berkenbosch F., Smelik P.G. Control of secretion of peptides related to adrenocorticotropin, melanocyte-stimulating hormone and endorphin. Front Hormone Res 14:161-196, Karger, Basel, 1985.

182. Tomatis M.E., Taleisnik S. Pituitary melanocyte-stimulating hormone and its hypothalamic factors during the estrous cycle. *Acta Physiol Latinoamer* 208:293-296, 1968.

183. Varga J.M., DiPasquale A., Pawelek J., McGuire J.S., Lerner A.B. Regulation of melanocyte-stimulating hormone at the receptor level: discontinuous binding of hormone to synchronised mouse melanoma cells during the cell cycle. *Proc Natl Acad Sci USA* 71(5):1590-1593, 1974.

184. Varga J.M., Moellmann G., Fritsch P., Godawska E., Lerner A.B. Association of cell surface receptors for melanotropin with the golgi region in mouse melanoma cells. *Proc Natl Acad Sci USA* 73(2):559-562, 1976.

185. Varga J.M., Saper M.A., Lerner A.B., Fritsch P. Nonrandom distribution of receptors for melanocyte-stimulating hormone on the surface of mouse melanoma cells. *J Supramol Structure* 4:45-49, 1976.

186. Varga J.M., Asato N., Lande S., Lerner A.B. Melanotropin-daunomycin conjugate shows receptor-mediated cytotoxicity in cultured murine melanoma cells. *Nature* 267:56-58, 1977.

187. Varga J.M., Asato N. Hormones as drug carriers. In Goldberg E.P. (ed) Targeted Drugs. pp. 73-88, John Wiley and Sons, New York, 1982.

188. Visser M., Swaab D.F. Life span changes in the presence of α–melanocyte-stimulating-hormone-containing cells in the human pituitary. *J Devel Physiol* 1:161-178, 1979.

189. Walter-van Cauter E., Virasoro E., Leclercq R., Copinschi G. Seasonal, circadian and episodic variations of human immunoreactive β–MSH ACTH and cortisol. *Int J Pept Protein Res* 17:3-13, 1981.

190. Weilbach F.X., Bogdahn U., Poot M., Apfel R., Behl C., Drenkard D., Martin R., Hoehn H., Melanoma-inhibiting activity inhibits cell proliferation by prolongation of the S-phase and arrest of cells in the G2 compartment. *Cancer Res* 50:6981-6986, 1990.

191. Wick M.M. L-dopa methyl ester as a new antitumour agent. *Nature* 269:512-513, 1977.

192. Wick M.M., Byers L., Frei III E. Selective toxicity of L-dopa for melanoma cells. *Science* 197:468-469, 1977.

193. Wick, M.M. Dopamine: a novel antitumour agent active against B-16 melanoma *in vivo*. *J Invest Dermatol* 71(2):163-164, 1978.

194. Wick M.M. An experimental approach to the chemotherapy of melanoma. *J Invest Dermatol* 74:63-65, 1980.

195. Wick M.M. Inhibition of clonogenic growth of melanoma cells by a combination of melanocyte-stimulating hormone and theophylline. *J Invest Dermatol* 77:253-255, 1981.

196. Wied D. de. Pituitary and hypothalamic hormones as precursor molecules of neuropeptides. *Acta Morph Hung* 31:159-180, 1983.

197. Wiesehahn G., Varga J.M., Hearst J.E. Interactions of daunomycin and melanotropin-daunomycin with DNA. *Nature* 292:467-469, 1981.

198. Wilkins L.M., Szabo G., Connell L., Gilchrest B.A., Maciag T. Growth of enriched human melanocyte cultures. In Sata O., Pardee A., Sirbasku D. (eds) Cold Spring Harbour Conferences on Cell Proliferation, Growth of Cells in Hormonally Defined Media. pp. 929-936, Cold Spring Harbour, New York, 1982.

199. Wimersma Greidanus T.B. van, Thody A.J., Verspaget H., de Rotte A.A., Goedemans J.H.J., Croiset G., van Ree J.M. Effects of morphine and β-endorphin on basal and elevated plasma levels of α-MSH and vasopressin. *Life Sci* 24:579-586, 1978.

200. Winder A.J., Harris H. New assays for the tyrosine hydroxylase and dopa oxidase activities of tyrosine. *New Eur J Biochem* 198:317-326, 1991.

201. Wraight E.P., Bard D.R., Maughn T.S., Knight O.G., Pagethomas D.P. The use of a chelating derivative of α-melanotic assays for the tyrosine hydroxylase and dopa oxidase activities of tyrosine. Melanocyte-stimulating hormone for the clinical imaging of malignant-melanoma. *Brit J Rad* 65(770):112-118, 1992.

202. Wunderlin R., Minakakis P., Sharma S.D., Schwyzer R. Melanotropin receptors II. synthesis and biological activity of α-melanotropin/tobacco mosaic virus disulphide conjugates. *Hel Chim Acta* 68(1):12-22, 1985.

203. Yamanishi D.T., Graham M., Buckmeier J.A., Meyskens F.L. Jr. The differential expression of protein kinase C genes in normal human neonatal melanocytes and metastatic melanomas. *Carcinogen* 12(1):105-109, 1991.

204. Yip C. Cell-membrane hormone receptors: some perspectives on their structure and function relationship. *Biochem Cell Biol* 66:549-556, 1988.

205. Zeljko B., Pavelic K., Vuk-Pavlovic S. Growth self-incitement in murine melanoma B16: a phenomenological model. *Science* 225:930-932, 1984.

APPENDIX

APPENDIX 1. EXPERIMENTAL DATA FOR MATERIALS AND METHODS

PEPTIDE SYNTHESIS

SYNTHESIS OF NLDP

The synthesis of the peptide and its conjugates was performed by Dr. G.W.J Olivier, therefore the protocol for their synthesis will not be described in full. Peptides were prepared by solid-phase synthesis using the Fmoc strategy as developed by Atherton and Sheppard (6). The peptides were prepared as their carboxyamide forms using the AM-linker on Pepsyn K resin. All the amino-acid reagents were used as their pentafluorophenyl esters with the exception of serine in which the 3,4-dihydro-4-oxobenzotriazin-3-yl ester was employed, and Fmoc-DPhe-OH which was treated with DIC and HOBT to form its HOBT active ester *in situ*. Side chains were protected as follows: Argine, methoxytrimethylbenzene-sulphonyl (Mtr); Glutamic acid, t-butoxy (OBut); Histidine, t-butoxy-carbonyl (Boc); Lysine, (Boc); Serine, t-butyl (But); Tyrosine (But). A four-fold molar excess of reagents was used in all instances.

Deprotection and cleavage was performed using 2% ethanedithiol, 2% anisole and 1% water in TFA for 8 hours at room temperature. Peptide was purified using semi-preparative HPLC employing a gradient elution of 0.1% TFA in water and 0.1% TFA in

acetonitrile : water (70 : 30) at a flow rate of 3 ml/minute or a preparative HPLC using the same solvent system at 10 ml/min. The elutent was continuously monitored by UV spectrophotometry at 217 nm. Fractions were collected every 5 minutes in 1.5 or 5 ml aliquots and each fraction was tested by analytical scale HPLC. Fractions were bulked according to their chromatographic profiles and freeze-dried. Identity was confirmed by FAB-MS and for NLDP, co-chromatography with authentic peptide (Sigma Chemical Co.). Prior to experiments the peptide was prepared at a stock concentration of 1 mg/ml in sterile 0.1 mM HCl and stored at 4°C.

SYNTHESIS OF NLDP CONJUGATES

Peptide conjugates were prepared by the addition of DTAF, MTX (using DIC/HOBT activation), or Biotin-NHS in DMF to 300 mg of the protein resin after deprotection of the N-terminus. The target peptides were obtained after deprotection and cleavage of the peptidyl resin and HPLC purification using the same conditions as for the NLDP-MSH analogue. Identity was confirmed by FAB-MS.

Peptides containing the ATB photoaffinity label were prepared according to the procedure described by Ahmed *et al* (1). An HOBT active ester of ATB was preformed with DIC and HOBT in DMF (activation time of 45 minutes to 1 hour) and allowed to react with purified NLDP or its biotinylated derivative Bi-NLDP, in solution in DMF (100 μl) for 1 hour. The reaction solution was then diluted 50-fold with water/acetonitrile (19:1, v/v) and purified directly by semi-preparative HPLC without UV monitoring. Fractions were subsequently analysed for purity by HPLC. The entire procedure was carried out in a dark room, under red safety light.

187
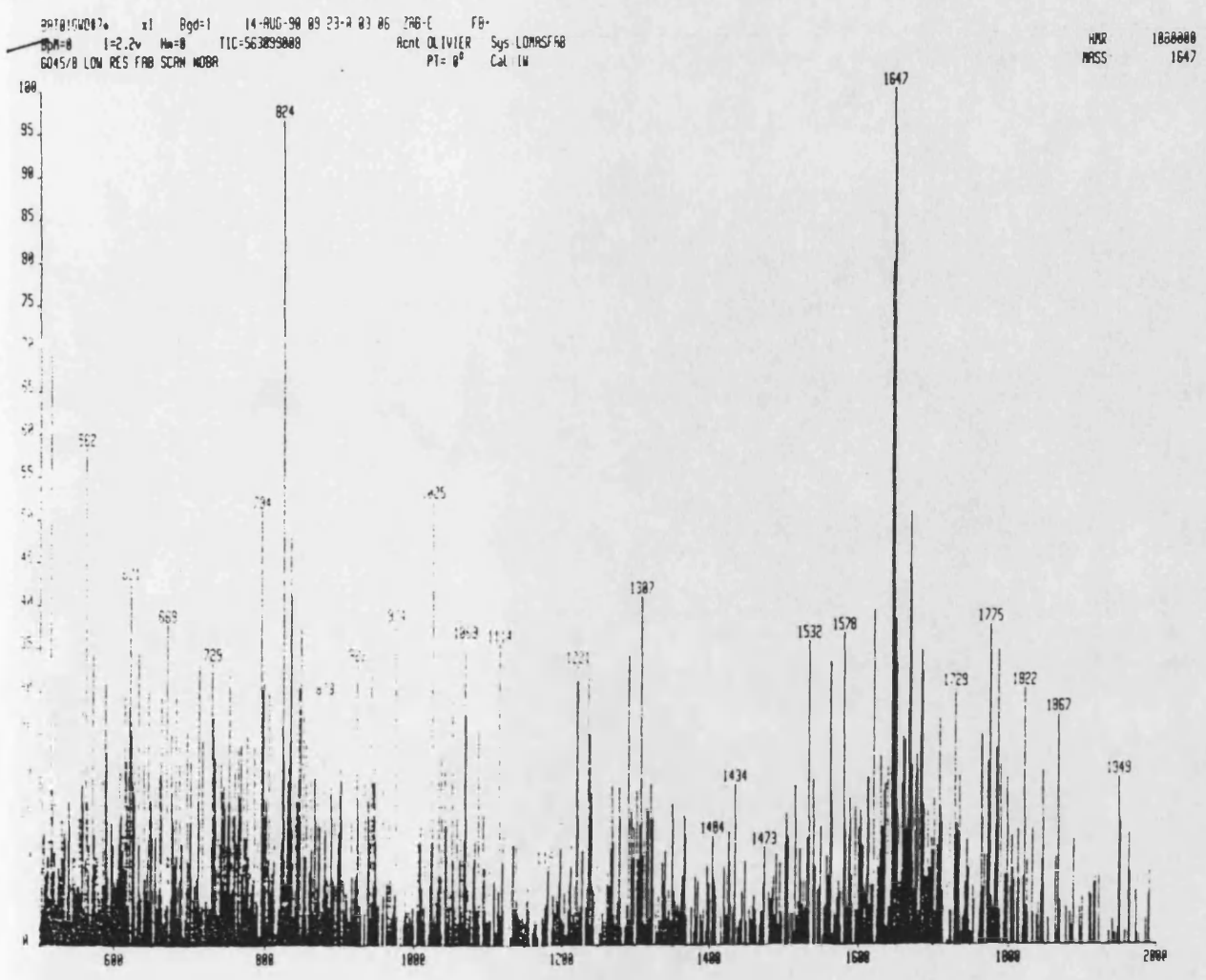
Figure A1.1. The FAB mass spectrometry of NLDP.

188
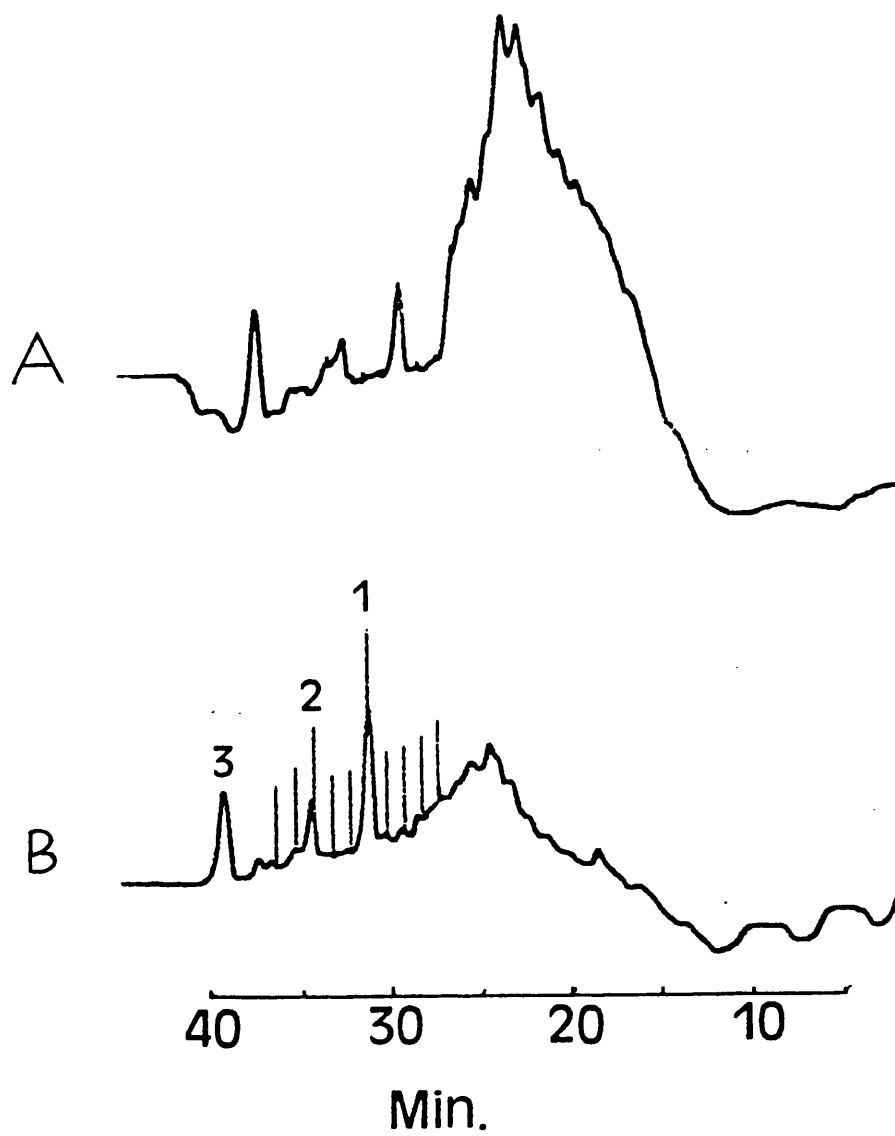
Figure A1.2. HPLC purification of the reaction products from the iodination of NLDP as measured by UV adsorption at 217 nm (B) and 277 nm (A). Peaks 1, 2 and 3 are thought to represent non-labelled, mono-iodinated and di-iodinated peptide respectively.
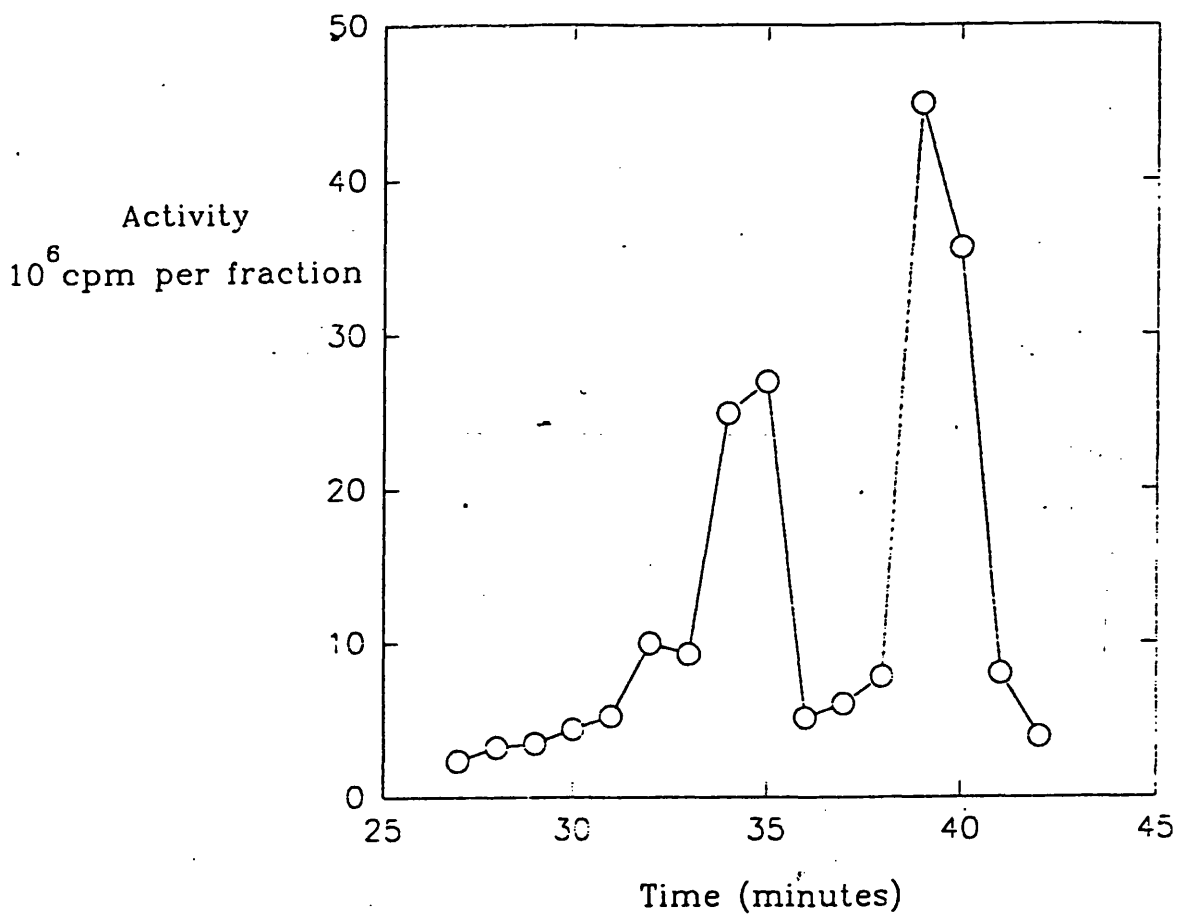
Figure A1.3. Activity per fraction from the HPLC purification of radio-iodinated NLDP from 27 minutes after the injection sample at a flow rate of 1 ml/minute.
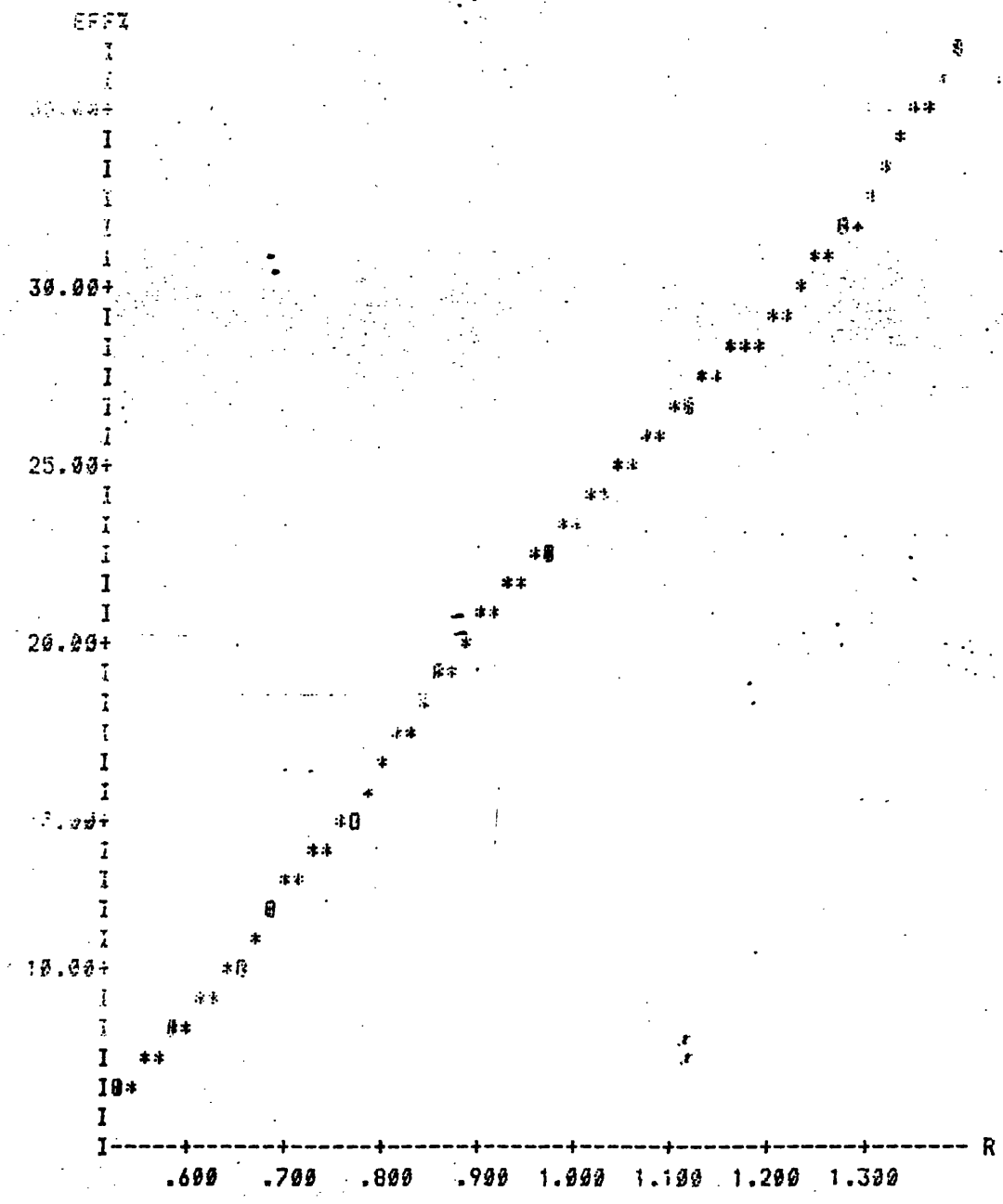
Figure A1.4. Quench curve for ^3H_2O plotted as the counting efficiency of the beta-counter vrs the ratio of the cpm/efficiency of the beta-counter.

APPENDIX 2. EXPERIMENTAL DATA FOR RESULTS

Table A2.3.1. Standard curves for α–MSH radio-immunoassay in bound ^{125}I-α–MSH

(Figure 3.1.)

PMOL α–MSH	SERUM	NO SERUM	SAMPLES
0	3061	3022.5	3010
3.125	3092.5	3059.5	3074
6.25	3100.5	3141	2975.5
12.5	3312.5	3235	2766.5
25	3423	3333.5	3011
50	3527.5	3545.5	2961
100	3698	3734.5	2214
200	3906	3895	2582.5
400	3946.5	3881	2964
			2979.5

Table A2.3.2.1. ^{125}I-NLDP bound at 37°C with different number of rinses (Figure 3.2.1.)

HRS	RINSE 1	RINSE 2	RINSE 3	RINSE 4
0.02	8964.2	4418	3403.1	3054.4
0.5	21214	16268	12910	17260
1	22620	19235	17801	17841
2	16815	16361	14145	12909
4	18153	11483	10038	9031.2

Table A2.3.2.2. ^{125}I-NLDP bound at 37°C in different buffers; total and non-specific to the wells (Figure 3.2.2.)

HRS	RPMI+BSA	RPMI	PBS+BSA	PBS
0.02	401.5	316.13	610.25	429.25
0.5	1456.8	1462.3	1346.8	1432
1	1732.4	1794	1190.5	1005
2	1244	1341.6	1022.7	1049.3
4	1640.4	1159.2	1155.2	626.35
NS 1	112.4	59	348.8	72.1
NS 2	137.5	125.9	221.6	159.7

Table A2.3.2.3. ^{125}I-NLDP bound at 37°C in RPMI or MEM media; total, non-specific

to the cells, and specific (Figure 3.2.3.)

HRS	RHOT	RHC	RSP	MHOT	MHC	MSP
0.02	740.08	382.7	357.38	983.6	443.05	540.55
0.5	1943.8	551.45	1392.4	1887.8	698.83	1188.9
1	2206.2	574.87	1631.4	2270.1	757.7	1512.4
2	1695.7	596.05	1099.7	1816.8	669.62	1147.2
4	1393.8	769.37	624.4	1862	724.2	1137.8

Table A2.3.2.4. ^{125}I-NLDP bound at 37°C with and without, 0.3 mM 1,10-

phenanthroline (Figure 3.2.4.)

HRS	1,10 PHEN	NO 1,10 PHEN
0.02	364.4	706.15
0.25	1101.2	2193.6
0.5	2667.9	4090.7
1	4018.2	5811.5
2	4493.4	4878.5

Table A2.3.2.5. ^{125}I-NLDP bound at 37°C; total, non-specific and acid stripped (Figure

3.2.5.)

HRS	HOT	HC	ACID
0.02	1793.5	469.58	85.65
0.5	20635	608.1	3268.9
1	36953	912.85	9612.7
2	27657	699.18	9182.7
4	28684	1126.5	7539.2

Table A2.3.2.6. ^{125}I-NLDP bound at 15°C; total, non-specific, specific, and acid stripped

(Figure 3.2.6.)

HRS	HOT	HC	SP	ACID
0.02	591.75	101.65	490.1	57.225
0.5	3092.2	179	2913.2	252.37
1	5350.7	231.7	5119	517
2	9902.2	303.07	9599.2	1804.4
4	13103	335.5	12767	2666.4
6	15274	307.87	14967	3969.2
29	21936	535.22	21401	9239

Table 2A.3.2.7. ^{125}I-NLDP bound at 4°C; total, non-specific and acid stripped (Figure

3.2.7.)

HRS	HOT	HC	ACID
0.02	420	333	89
0.5	741	270	86
1	1100	255	112
2	1754	291	154
4	2538	408	194
6	3274	398	202
25	5293	248	384

Table A2.3.2.8. ^{125}I-NLDP bound at 4°C, 0.5 and 2 hours vrs cell density; total and non-specific (Figures 3.2.8. and 3.2.9.)

C/W	0.5 HR HOT	0.5 HR HC	2 HR HOT	2 HR HC
5 00000	2252.4	313.92	4610.5	478.12
400000	1602	436.7	3242	417.62
300000	1011	299	2160	324.92
200000	822.18	301.52	1349	457.22
100000	401.62	315.92	585.13	294.45

Table A2.3.2.9. ^{125}I-NLDP bound at 4°C with and without, 0.3 mM 1,10-phenanthroline (Figure 3.2.10.)

HRS	1,10 PHEN	NO 1,10 PHEN
0.5	769.65	703.88
2	1064	969.38
4	1458.7	1199
8	1820.9	1881.7
12	2359.8	2272.1
16	2391.6	2224.1

Table A2.3.2.10. ^{125}I-NLDP bound at 4°C with and without, various concentrations of collagenase inhibitor (Figure 3.2.11.)

HRS	10-5 MOLE	10-6 MOLE	10-7 MOLE	NO CI
1	3377	3360.5	4321.1	4408.3
2	5139.7	5613.5	4620.4	6284.3
4	7174.9	7312.9	6783.3	6728.7
8	6728.3	7404.7	7284.8	7966.5

Table A2.3.2.11. ^{125}I-NLDP bound at 4°C at different tracer concentrations; total and non-specific (Figure 3.2.12)

HRS	H 1.08	HC 1.08	H 0.27	HC 0.27
0.02	245.75	164.75	117.25	98.25
0.5	656.25	287	198.5	111.5
1	1032.2	411.25	274	101.5
2	1460	322.75	382.25	107.25
4	1981.5	340.75	506.75	130
6	2423	438.5	721.75	136
22	3547.7	453.75	1118.7	131.25

Table A2.3.2.12. ^{125}I-NLDP specifically bound at 4°C at different tracer concentrations (Figure 3.2.13.)

HRS	SP 0.59	SP 0.838	SP 0.27	SP 1.08
0.02	238.58	77	19	81
0.5	1678.2	471	87	369.25
1	2704.5	844	172.5	620.95
2	5148.8	1463	275	1137.3
4	6815.1	2130	376.75	1640.8
6	8265.2	2886	585.75	1984.5
8	10159	*	*	*
14	11779	*	*	*
24	*	5045	987.45	3093.9

Table A2.3.2.13. Binding isotherms of ^{125}I-NLDP; total bound and non-specific (Table 3.2.1.). Isotherm 2* is plotted in Figures 3.2.14. and 3.2.15.

CPM I-NLDP/W	HOT NLDP	HC NLDP

ISOTHERM 1		
1000	108	7
10000	985	66
20000	1752	119
40000	3315	210
70000	5599	433
100000	8203	483
200000	15581	977
500000	33533	1965
1000000	44575	3388
2000000	61143	5566
ISOTHERM 2*		
930	46	5.2
9310	280.68	45.375
38654	1197.9	60.35
68198	1864.5	103.8
100320	2497.1	117
141990	3875.5	206.75
199150	4980.4	275.23
342000	7496.3	351.87
486860	10405	507.18
736930	12564	848.48
979300	16146	1354.5
1952300	20726	2396.4
ISOTHERM 3		
756	47	16
8724	175	23
35275	707	95
63095	1128	163
95386	1527	217
131370	2017	331
194310	3165	374
335290	5377	715
460390	6754	1451
710020	10362	1822
888980	11808	2192
1865400	14228	4387

ISOTHERM 4		
893	156	3
42100	6229	167
73640	8227	244
109420	12546	315
154160	17759	392
190300	18883	557
357510	31791	931
486030	47208	1063
987210	63644	2386
2206200	77556	4532
ISOTHERM 5		
52730	1619	78
73151	2422	142
111780	4572	211
143910	5724	289
192420	5914	325
345930	8774	581
522510	14534	852
1018100	20318	1681
2115400	24034	3381

Table A2.3.2.14. Binding of tracer in competition with dilution series of unlabelled

agonist. Assay 1 for each analogue is plotted in Section 3.2. (Figures 3.2.16-3.2.25.)

NLDP 1 LOG MOLE	CPM TRACER = 0.126 nM	NLDP 2 LOG MOLE	CPM TRACER = 0.126 nM	NLDP 3 LOG MOLE	CPM TRACER = 0.126 nM
-7	688	-7	628.75	-7	663.45
-8	1261.1	-8	1507.3	-8	1493.3
-8.301	1810.5	-8.301	2104.2	-8.301	2196.6
-8699	3179.9	-8.699	3743.8	-8.699	3503
-9	4678.5	-9	5789.9	-9	5848.5

-9.301	6712.5	-9.301	7593.1	-9.301	7667.9
-9.4559	7937.4	-9.4559	8695.8	-9.699	10507
-9.699	9564.4	-9.699	10400	-10	12195
-10	10517	-10	11468	-10.301	12869
-10.301	11398	-10.301	12084	-10.699	13437
-10.699	11989	-10.699	12276	-11	13473
-11	12138	-11	12374	0	12688
NLDP 4 LOG MOLE	CPM TRACER = 0.120 nM	NLDP 5 LOG MOLE	CPM TRACER = 0.124 nM	NLDP 6 LOG MOLE	CPM TRACER = 0.655 nM
-7	736.38	-6	1309.1	-7	1267.8
-8	699.12	-8	1369.9	-7.301	1496.9
-8.4559	695.12	-9	4118.7	-8	2907.9
-9	793.8	-10	9255.3	-8.301	4902.7
-9.301	1373.1	-11	8373.9	-8.6021	7066.9
-9.4559	2170.5	0	10386	-9	11401
-9.699	3323			-9.1249	12360
-10	3756.3			-10	24876
33-10.456	4001.9			-10.301	27877
-11	4281.1			-11	29378
-12	4274.5			-12	31245
0	4229.7			0	30468
NLDP 7 LOG MOLE	CPM TRACER = 0.134 nM	NLDP 8 LOG MOLE	CPM TRACER = 0.136 nM	NLDP 9 LOG MOLE	CPM TRACER = 0.136 nM
-6	470.3	-7	609.85	-7	632.33
-7	534.2	-8	1555.2	-8	1510.4
-8	988.63	-9	7709.7	-9	7167
-8.301	1360	-10	15041	-10	14063
-9	3531.8	-11	17172	-11	15914
-9.301	6529.9	-12	16351	-12	16375
-10	7843.7				
-11	8239.9				
-12	8734.1				

NLDP 10 LOG MOLE	CPM TRACER = 0.139 nM	α–MSH 1 LOG MOLE	CPM TRACER = 0.142 nM	α–MSH 2 LOG MOLE	CPM TRACER = 0.655 nM
-6	404.52	-6	425.02	-5.301	1089.9
-7	403.12	-7	565.8	-6	1470.9
-8	812.13	-8	1391.3	-7	3003.6
-9	4086.8	-8.301	1867.1	-7.301	4328.9
-10	8555.5	-8.699	2846.5	-8	10399
-10.301	8784.7	-9	3288.8	-8.301	15808
-11	9841.6	-9.301	3774.4	-8.6021	17890
-12	9563.7	-9.699	4201.6	-9	22259
		-10	4386.9	-9.1249	25137
		-11	4576.5	-10	29047
		-12	4229.3	-10.301	30259
		0	4125.2	-11.301	31584

α–MSH 3 LOG MOLE	CPM TRACER = 0.125 nM	α–MSH 4 LOG MOLE	CPM TRACER = 1.73 nM	CTAF 1 LOG MOLE	CPM TRACER = 0.128 nM
-7	1157.5	-7	5553.2	-5	507.3
-7.4559	1812.9	-7.301	9457.3	-6	597.82
-8	3598.3	-8	22237	-7	1295.5
-8.301	5817.6	-8.301	30879	-7.301	1978.3
-8.4559	6290.9	-8.6021	31476	-7.699	3537.4
-8.699	7552	-9	39338	-8	5614.3
-9	10234	-9.1249	38961	-8.301	8046.3
-9.301	12286	-10	41316	-8.699	11090
-9.4559	11869	-12	45235	-9	12796
-9.699	12708	0	43390	-9.4559	13752
-10	13040			-10	13865
-11	13664			-11	13329

CTAF 2 LOG MOLE	CPM TRACER = 0.152 nM	CTAF 3 LOG MOLE	CPM TRACER = 1.47 nM	MTX 1 LOG MOLE	CPM TRACER = 0.126 nM
-6	555.3	-4.301	3491.9	-6	404.65
-7	1832.1	-5.301	3801.2	-7	535.58

-8	7527.2	-6.301	9073.7	-7.301	560
-9	10785	-7.301	17902	-8	844.5
-10	10334	-8.301	18098	-8.301	1129.8
-11	9837.3	-9.301	21935	-9	3150.3
		-10.301	23001	-9.301	4918.6
		-11.301	26337	-10	8790.9
		-12.301	22527	-11	11087
		0	24674	-12	10937
				0	11076
MTX 2 LOG MOLE	CPM TRACER = 0.142 nM	MTX 3 LOG MOLE	CPM TRACER = 0.142 nM	BI 1 LOG MOLE	CPM TRACER = 0.120 nM
-6	585.35	-6	490.92	-7	340.25
-7	568.68	-7	542.9	-8	428.67
-8	809.38	-8	1012.7	-8.4559	544.37
-9	2208.2	-9	2908.6	-9	864.3
-10	4634.7	-10	6883.4	-9.301	1213.8
				-9.4559	1486.1
				-9.699	2070.6
				-10	2351.5
				-10.456	2775.3
				-11	2768.9
				-12	2741.2
				0	2795.7
BI 2 LOG MOLE	CPM TRACER = 0.124 nM	BI 3 LOG MOLE	CPM TRACER = 0.108 nM	BI 4 LOG MOLE	CPM TRACER = 0.116 nM
-6	1309.3	-7	815.73	-7	1244.9
-7	1346.3	-8	1029.1	-8	1125.9
-8	1522.3	-8.301	1036.6	-8.301	3256.6
-9	3014.7	-8.4559	1006.2	-8.699	3289.8
-10	7300.3	-8.699	1227.4	-9	1292.5
-11	9117	-9	1102	-9.301	1804.4
-12	8188.2	-9.301	1263.9	-9.699	1614
-13	8560.5	-9.4559	1173.6	-10	2268
0	9399	-9.699	1662	-10.456	3311.3
		-10	1893.8	-11	3570.6

		-10.456	2471.9	-12	2654.2
		-11	2369.6	0	2694.9
		0	2270		
BI 5 LOG MOLE	CPM TRACER = 0.123 nM	BII 1 LOG MOLE	CPM TRACER = 0.134 nM	BII 2 LOG MOLE	CPM TRACER = 0.473 nM
-7	280.27	-7	431.75	-7	1249.4
-8	347.52	-8	574.77	-8	1277.2
-8.301	339.77	-8.301	723.52	-8.4559	1643.8
-8.699	521.1	-8.699	*	-9	2393.8
-9	642.88	-9	1340.8	-9.4559	3326
-9.301	573.38	-9.301	1952.1	-10	4140.7
-9.699	588.52	-9.699	*	-10.456	4078.1
-10	808.23	-10	3021.6	-11	4370.3
-10.456	1135.2	-10.301	3253.7	-11.456	4389.4
-11	1365.2	-10.699	3729.4	-12	4490.3
-12	1331.8	-11	3736.7	-13	4435.7
0	1432	-12	3520.3	0	4401.9
BII 3 LOG MOLE	CPM TRACER = 0.137 nM	BIIATB 1 LOG MOLE	CPM TRACER = 0.143 nM	BIIATB 2 LOG MOLE	CPM TRACER = 0.337 nM
-7	1337.7	-4	9740	-6	11270
-8	1694.7	-5	9996	-7	10995
-9	2730	-6	11547	-8	12378
-10	4331.4	-7	11910	-9	18180
-11	4726.8	-8	15050	-10	33360
-12	4644.2	-9	25062	-11	41985
		-10	48900	-12	51317
		-12	56740		
		0	58207		
IATB 1 LOG MOLE	CPM TRACER = 0.137 nM	IATB 2 LOG MOLE	CPM TRACER = 0.126 nM	IATB 3 LOG MOLE	CPM TRACER = 0.070 nM
-6	2039.7	-6	1602.3	-7	1590.5
-7	2350.9	-7	2287	-8	1862.2

-7.4559	2547.3	-7.4559	2311.5	-8.4559	1954.4
-8.301	3149	-8	2469	-9	2101.8
-8.699	3613.3	-8.4559	2682.1	-9.4559	2270.6
-9	3935.8	-9	3628.2	-10	2178.1
-9.301	4201.4	-9.4559	4197.8	-10.456	2546
-9.699	4496.1	-10	5214.6	-11	2500.3
-10	4569.8	-10.456	5441	-11.456	2621
-11	5100.7	-11	5602.3	-12	2507
-12	4677.3	-12	5463.9	-13	2494.6
0	4762.3	0	6574.9	0	2895.4
(SA)BII 1 LOG MOLE	CPM TRACER = 0.150 nM	(SA)BII 2 LOG MOLE	CPM TRACER = 0.148 nM	(SA)BII 3 LOG MOLE	CPM TRACER = 0.0616 nM
-6	1387.2	-7	1444	-7	1633.2
-7	1826.8	-8	1678.2	-8	1803.1
-8	2145.8	-8.301	2158.1	-9	2191.7
-8.301	2441.1	-8.699	2520.4	-10	2933.2
-8.699	2826.3	-9	3136.6	-11	3092.7
-9	3396.6	-9.301	3837.9	-12	2808.5
-9.301	4439.3	-9.699	5302.1		
-9.699	5123.8	-10	5596.1		
-10	5599.6	-10.301	6128.7		
-10.301	6071.7	-10.699	6246.3		
-11	6127.6	-11	6164.1		
0	6109	-12	6133.7		
(SA-AU)BII 1 LOG MOLE	CPM TRACER = 0.134 nM				
-8	2022.9				
-9	2099.8				
-9.4559	2255.6				
-10	2472.5				
-9.4559	2563.3				
-11	2554.3				
-11.456	2147.6				
-12	2183.5				
-12.456	2346.9				

-13	2531.5				
-14	2490.2				
0	2207.5				

Table A2.3.3.1. Tyrosinase assay with for 24 hours using 5x10^5 and 10^5 cells/well (Figure 3.3.1.)

LOG MOLE NLDP	DPM 5x10^5 C/W	DPM 10^5 C/W
-7	71670	71763
-8	72392	82612
-9	74827	83130
-10	74777	85823
-11	75344	68329
-12	65505	66518
-14	64888	67861

Table A2.3.3.2. Tyrosinase assay for 24 hours using 10^5, 2.5x10^5 and 5x10^5 cells/well (Figure 3.3.2.)

LOG MOLE NLDP	DPM 10^5 C/W	DPM 2.5x10^5 C/W	DPM 5x10^5 C/W
-8	100280	99735	71459
-9	113180	96353	*
-10	106480	97204	77079
-11	101400	120500	*
-12	90677	105350	78163
0	83469	104340	79708

Table A2.3.3.3. Tyrosinase assay for different times at different cell densities (Figure 3.3.3.)

LOG MOLE NLDP	DPM 10^5 C/W 27 HRS	DPM 3×10^4 C/W 48 HRS	DPM 3×10^4 C/W 72 HRS
-6	*	*	91287
-7	93542	193560	113400
-8	88229	200510	116010
-9	94548	208790	124630
-10	93750	196790	114320
-10.456	83814	182740	*
-11	87533	190720	95100
-11.456	84835	184600	*
-12	82447	195480	68496
-13	77338	195050	76458
-14	81533	182470	84716
-15	100850	174340	77310
-16	*	*	70746
-17	*	*	*
0	86413	183690	68893

Table A2.3.3.4. Tyrosinase assays for all analogues tested. Assay 1 of each analogue is

plotted in Section 3.3. (Figures 3.3.4-3.3.8.)

NLDP 1 LOG MOLE	DPM	NLDP 2 LOG MOLE	DPM	NLDP 3 LOG MOLE	DPM
-6	91496	-6	130690	-7	105640
-7	94542	-7	129750	-8	149240
-8	113720	-8	133660	-8.301	143250
-9	128090	-9	142520	-8.699	145650
-10	114910	-10	125360	-9	158930
-11	80928	-10.301	123260	-9.031	153250
-12	60308	-11	103570	-9.699	146890
-13	64112	-11.301	118400	-10	144540
-14	68846	-12	110660	-10.301	146690
-15	68592	-13	104800	-10.699	131520
-16	64778	-14	98529	-11	166410
0	55651	0	119590	0	144870

NLDP 4 LOG MOLE	DPM	NLDP 5 LOG MOLE	DPM	NLDP 6 LOG MOLE	DPM
-6	200730	-9	110430	-6	91287
-7	210620	-10	115380	-7	113400
-8	206380	-10.222	126950	-8	116010
-9	208660	-10.456	108030	-9	124630
-10	208510	-10.699	104620	-10	114320
-11	195920	-11	90168	-11	95100
-12	177990	-11.222	53596	-12	68496
-13	174540	-11.456	66588	-13	76458
0	184680	-11.699	76474	-14	84716
		-12	85605	-15	77310
		-13	89356	-16	70746
				0	68893

NLDP 7 LOG MOLE	DPM	NLDP 8 LOG MOLE	DPM	NLDP 9 LOG MOLE	DPM
-8	81810	-7	111390	-8	69423
-9	83345	-8	98071	-9	73371
-9.4559	83158	-8.4559	108720	-9.301	77673
-10	84245	-9	105020	-9.699	66161
-10.301	78270	-9.301	91990	-10	70740
-10.456	73785	-9.699	91449	-10.301	71787
-10.699	72022	-10	94197	-10.456	55137
-11	57778	-10.456	95992	-10.699	48782
-11.301	52214	-11	77750	-11	41838
-11.699	52834	-12	55736	-11.456	37296
-12	46803	-13	52640	-12	30600
-13	45602	0	57811	0	28790

NLDP 10 LOG MOLE	DPM	α–MSH 1 LOG MOLE	DPM	α–MSH 2 LOG MOLE	DPM
-8	112150	-7	72614	-6	91287
-8.4559	116890	-8	73969	-7	11340
-9	118630	-8.4559	72267	-8	116010
-9.301	115490	-9	60806	-9	124630

-9.699	113410	-9.301	60837	-10	114320
-10	113680	-9.699	50094	-11	95100
-10.301	114380	-10	48628	-12	68496
-10.699	10840	-10.301	42872	-13	76458
-11	101630	-10.699	38427	-14	84716
-11.456	85537	-11	37886	-15	77310
-12	84653	-12	36831	-16	70746
0	84425	0	35519	0	68893
α–MSH 3 LOG MOLE	DPM	α–MSH 4 LOG MOLE	DPM	CTAF 1 LOG MOLE	DPM
-6	111930	-6	75338	-7	131840
-7	140200	-7	95591	-8	137700
-8	141420	-8	98358	-8.4559	15378
-9	141800	-9	88739	-9	132350
-10	119990	-10	69577	-10	115820
-11	91919	-11	57624	-11	78898
-12	94079	-12	54196		
-13	104860	-13	57312		
-14	100420	0	45901		
-15	119620				
0	101010				
CTAF 2 LOG MOLE	DPM	CTAF 3 LOG MOLE	DPM	CTAF 4 LOG MOLE	DPM
-6	203400	-6	143590	-6	127600
-7	212610	-7	166550	-7	125970
-7.4559	209870	-8	161920	-7.4559	144620
-8	215830	-9	131400	-8	137940
-8.4559	211240	-10	125030	-8.4559	134680
-9	203390	-11	125370	-9	119380
-9.455	217320	-12	115560	-9.4559	132510
-10	208610	-13	119820	-10	136270
-10.456	202700	-14	125970	-10.456	142750
-11	207790	0	114920	-11	125960
-12	192890			-12	139100
0	191960			0	195920

MTX 1 LOG MOLE	DPM	MTX 2 LOG MOLE	DPM	MTX 3 LOG MOLE	DPM
-8	87802	-6	195470	-6	.186550
-9	88915	-7	205380	-7	203210
-9.4559	88217	-8	202200	-8	201450
-10	83548	-9	205390	-9	204390
-10.301	76584	-10	199000	-10	189230
-10.456	70673	-11	187240	-11	180290
-10.699	68147	-12	175740	-12	156000
-11	63702	-13	170040	-13	176030
-11.301	57786	-14	177120	-14	177600
-11.699	52042				
-12	39713				
0	41573				

BI 1 LOG MOLE	DPM	BI 2 LOG MOLE	DPM		
-7	184090	-6	153420		
-8	188680	-7	162300		
-8.4559	200930	-8	144390		
-9	209660	-9	155350		
-9.301	199260	-10	143770		
-9.699	188550	-11	131240		
-10	193040	-12	134760		
-10.456	185080	-13	146600		
-11	166390	-14	111430		
-12	159790	0	114920		
-13	162900				
0	166700				

Table A2.3.4.1. Effect of chronic 10^{-9} M NLDP and α–MSH on cell growth (Figure 3.4.2.)

HRS	NO NLDP C/W	NLDP C/W	MSH C/W

0	50000	50000	50000
22	115000	112000	111000
47	392000	296000	310000
70	797000	664000	760000
94	1430000	900000	1080000
115	1190000	318000	844000
142	1370000	810000	920000

Table A2.3.4.2. Effect of chronic or 0.5 hour pulse/day 10^{-9} M NLDP on cell growth

(Figure 3.4.1.)

HRS	NO NLDP C/W	CHRONIC NLDP C/W	PULSE NLDP C/W
0	5×10^4	5×10^4	5×10^4
24	83750	72250	75000
48	214500	215000	234750
72	496000	351500	535000
97	1051000	653500	1016500

Table A2.3.4.3. Effect of chronic 10^{-9} M NLDP on cell growth at different cell densities

(Figures 3.4.3-3.4.9.)

FIGURE	HRS	NO NLDP C/W	NLDP C/W
3.4.3.	0	10000	10000
	22	17000	16600
	47	60000	48000
	70	162000	138000
	94	484000	338000
	115	753000	540000
	142	1130000	770000
3.4.4.	0	25000	25000
	24	148500	120000

	48	280000	265500
	72	641000	584000
	96	1120000	746000
	120	1500000	825000
	144	1760000	960000
3.4.5.	0	50000	50000
	24	270000	270000
	48	560000	520000
	72	940000	822000
	96	1420000	1020000
	120	1500000	825000
	144	1760000	960000
3.4.6.	0	75000	75000
	24	376000	430000
	48	710000	690000
	72	1200000	966000
	96	1380000	860000
	120	1600000	1050000
	144	1940000	1140000
3.4.7	0	100000	100000
	24	430000	500000
	48	830000	720000
	72	1160000	1020000
	96	1340000	940000
	120	1760000	1180000
3.4.8.	0	250000	250000
	24	770000	620000
	48	960000	1000000
	72	1690000	1150000
	96	1500000	770000
	120	1760000	1000000
3.4.9.	0	500000	500000
	24	920000	900000
	48	1240000	1000000
	72	1480000	960000
	96	1250000	690000
	120	1660000	1080000

Table A2.3.4.4. The effect of different concentrations of NLDP on cell growth (Figure
3.4.10.)

LOG MOLE NLDP	0 HRS C/W	24 HRS C/W	48 HRS C/W	72 HRS C/W	96 HRS C/W	120 HRS C/W
-7	70000	213000	450000	651000	619000	773000
-8	70000	213750	409000	585000	830000	867000
-9	70000	207500	404500	657000	825000	784000
-11	70000	222750	428000	733500	926000	1252000
0	70000	204750	448500	569250	1186000	1307000